UNIVERSITY OF OKLAHOMA

GRADUATE COLLEGE

THE ROLE OF SOLAR-POWERED FLOAT-MIX AERATORS ON IRON RETENTION IN PASSIVE TREATMENT OXIDATION PONDS

A THESIS

SUBMITTED TO THE CEES GRADUATE FACULTY

in partial fulfillment of the requirements for the degree of

MASTER OF SCIENCE IN ENVIRONMENTAL ENGINEERING

By

DAYTON M'KENZIE DORMAN

Norman, Oklahoma

2019

THE ROLE OF SOLAR-POWERED FLOAT-MIX AERATORS ON IRON RETENTION IN PASSIVE TREATMENT OXIDATION PONDS

A THESIS APPROVED FOR THE
SCHOOL OF CIVIL ENGINEERING AND ENVIRONMENTAL SCIENCE

BY THE COMMITTEE CONSISTING OF

Dr. Robert W. Nairn, Chair

Dr. Elizabeth C. Butler

Dr. Robert C. Knox

To all the first-generation students who faced countless obstacles but continued to persist.

You can do it.

Acknowledgments

This research would not have been possible without the support of my friends, family, colleagues, and advisors. I would like to thank the Department of Environmental Quality who funded this research. I would also like to think my fellow CREW research members, Juan Arango, Brandon Holzbauer-Schweitzer, Carlton Folz, JD Ingendorf and Maggie Tang who all helped me collect samples (either in a freezing cold or blazing hot canoe in the middle of an oxidation pond), provided useful feedback regarding my research, and watched my dog at some point while I was in the field. Also, a special thanks to Nick Shepherd, who, although let me fall into the oxidation pond, was otherwise pretty helpful and always willing to help me. I would like to think my committee members, Dr. Butler and Dr. Knox for their advice and support and my advisor Dr. Nairn who introduced me to the fun and rewarding work of ecological engineering. I could always count on Dr. Nairn to provide support, advice, and a never-ending supply of sarcasm. To Tri Pham who enabled my coffee addiction and who I owe so many coffee drinks, thank you and I promise I will address my problem.

Lastly, I would like to give a special thanks to my family especially my grandparents Barbara and Roy Walters, my mother, Kim Walters, and my sister, Madison Dorman who all provided love and support throughout my education. I would like to especially thank my mom who is the most important person in my life. She has always supported me in all my endeavors and taught me that with hard work anything is possible. She is the reason I am where I am today.

Table of Contents

List of Figures

List of Tables

Abstract

In passive treatment of net-alkaline mine drainage, oxidation ponds are typically the primary process unit designed to promote iron oxidation, hydrolysis, and precipitation. Iron oxidation kinetics can be accelerated by supplemental aeration. Aeration in passive treatment of mine drainage is commonly achieved by the dissipation of energy from hydraulic head. However, this type of aeration is not feasible for sites located in regions with limited topographic relief. This study investigated the effectiveness of custom-designed float-mix aerators (FMAs) to increase dissolved oxygen (DO) concentrations, degas carbon dioxide(CO_2) and promote iron (Fe) retention from multiple perspectives: (1) with respect to depth in the water column, (2) spatially with respect to the aerator, and (3) spatially within the oxidation pond including the overall effect of aeration on the performance of the oxidation pond. This study was conducted in the oxidation pond of the Southeast Commerce Passive Treatment System at the Tar Creek Superfund Site, the Oklahoma portion of the Tri-State Lead-Zinc Mining District. The study found: (1) The FMAs statistically increased DO saturation and raised pH at depths of 0.4 meters below the surface and shallower. No statistical difference was seen in pCO_2 at any depth with active aeration. The increase in DO and pH promoted Fe oxidation. When the aerators were on, lower total Fe concentrations were found in the shallower reaches of the water column and higher total Fe concentrations were found at depth compared to the FMAs off. Similarly, a larger fraction of the Fe present was in the particulate form indicating that more Fe was oxidized and precipitated and began to settle at increasing depths. (2) The FMAs were able to increase DO saturation up to 9 m downstream compared to solely passive

aeration. The FMAs, however, had a more limited radius of influence with regard to degassing CO_2 and raising pH at approximately 3 m from the FMAs. The increased DO and pH provided by the FMAs allowed for more Fe to be oxidized resulting in lower total Fe concentrations downstream of the FMAs compared to when the FMAs were off. (3) Data comparing influent water quality data to effluent water quality of the oxidation pond shows that the oxidation pond, when the FMAs are on, increases DO saturation over 100%, degasses CO_2, and removes an average 93% of the Fe loading before the water enters the surface flow wetland. Active aeration increased the Fe removal rate of the oxidation pond by 17% from 22 g m^{-2} d^{-1} without the FMAs to 26 g m^{-2} d^{-1} with the FMAs on. This study shows that FMAs are a viable aeration technology for sites where gravitational energy-driven aeration is not feasible due to topographic limitations. The results of this study can help optimize the design and placement of the FMAs to further improve the performance of oxidation units.

Chapter 1: Project Introduction and Literature Review

1.1 Introduction

Mine drainage is a risk to the environment and to the communities of legacy mining districts due to the discharge of ecotoxic metals and its effect on water quality (Limerick 2005; Taylor 2005). A variety of strategies exist to treat mine drainage and the most applicable treatment option depends on the initial water quality, water quantity, available land and surrounding land use (Johnson and Hallberg 2005; Younger et al. 2002). These treatment options are typically characterized as either active treatment or passive treatment. Active treatment systems (ATS) require a continuous input of resources such as chemicals and energy to complete the treatment process (Johnson and Hallberg 2005). On the other hand, passive treatment systems (PTS) require little to no input of resources to complete the treatment process (Johnson and Hallberg 2005; Skousen et al. 2017). Passive treatment is an often-favorable treatment strategy for remote sites with enough land area because they are lower cost in the long-term due to the absence of the need for inputs of chemicals or electricity and lower operator costs (Johnson and Hallberg 2005; Taylor 2005). PTS often consist of a combination of natural treatment technologies that can be designed to neutralize acid, remove and retain metals and generate alkalinity. PTS can include, but are not limited to, oxic or anoxic limestone drains, oxidation and settling ponds, aerobic or anaerobic wetlands, vertical flow bioreactors (also known as biochemical reactors), horizontal flow limestone beds, and permeable reactive barriers (Hedin et al. 1994; Nairn et al. 2009; Taylor et al. 2005).

This research focuses on one of the more common process units of many passive treatment systems, the oxidation pond. Oxidation ponds are implemented to aerobically oxidize and retain iron (Fe). Mine drainage is aerated through water-air surface interactions, or by physical aeration techniques in order to facilitate metals oxidation, hydrolysis and precipitation (Nairn et al. 2009; Nairn et al. 2018; Skousen et al. 2017; Taylor et al. 2005; Younger et al. 2002). Aeration is a critical component of passive treatment because it is needed to address elevated metals concentrations via oxidation, hydrolysis and precipitation removal mechanisms. In many mining regions, enough topographical variability is present to utilize cascade aeration to entrain oxygen into the water (Geroni et al. 2012, Oh et al. 2016). However, mining locations located in relatively flat topographies do not have sufficient hydraulic head to utilize cascade aeration and thus rely on mechanical aeration technologies to add oxygen into the water.

1.2 Problem Statement and Purpose

This study investigated the effectiveness of a mechanical aeration technique not commonly used in treatment of mine drainage to increase dissolved oxygen (DO) concentrations and carbon dioxide (CO_2) exsolution and promote Fe retention in mine drainage at a site with little topographic relief. For this study, mechanical aeration is defined as the use of mechanical energy to mix air and water to increase gas exchange. Determining the effectiveness of mechanical aeration was accomplished by collecting weather-related data and physical and chemical water quality parameters. Total and dissolved metals concentrations

were compared with the float-mix aerators on and off with respect to water depth, spatial distance from the float-mix aerators, and to estimate the overall Fe retention performance of the pond.

1.3 Literature Review

1.3.1 Mine Drainage

Mine drainage is a significant environmental problem that has lasting effects on aquatic ecosystems and organisms (Younger et al. 2002). Mine drainage is produced by chemical weathering processes of sulfide minerals, such as pyrite, by oxygen and water which allows metals to become mobile and bioavailable as shown in Equation 1.1 (Younger et al. 2002).

$$FeS_2\ (s) + \ 3O_2(aq) + 2H_2O \rightarrow Fe^{2+} + 2{SO_4}^{2-} + 4\ H^+ \qquad (1.1)$$

Although this process occurs naturally, it is often exacerbated by the increased surface area of sulfide minerals exposed by the mining and processing of metal ores and coals (Johnson and Hallberg 2005). Mine drainage can form on surfaces in exposed mine tailings or in underground mine workings as the mines fill with groundwater. Groundwater interaction with mine workings may be less problematic in active mines because water tables are often maintained below the mine workings by pumping, limiting the dissolution of acidic salts into the water. However, abandoned underground mines may be more problematic because water tables are not artificially controlled, allowing groundwater contamination to occur as the

groundwater floods the mine workings. The now contaminated groundwater often discharges via artesian head pressures to the surface, negatively impacting the receiving water body (Johnson and Hallberg 2005; Limerick 2005; Taylor et al. 2005; Younger et al. 2002).

Mine drainage can be “net-acidic”, acid mine drainage, or “net-alkaline”, net-alkaline mine drainage, depending on the composition of the water. As metal sulfides in the geologic formation are exposed to oxygen, metals are oxidized, producing dissolved metals, sulfate, and sulfuric acid (Watzlaf et al., 2004) contributing to mineral acidity. Acid mine drainage occurs when the host geologic formation does not have sufficient alkalinity to neutralize the acidity. Determining whether mine drainage is net-acidic or net-alkaline is important in order to implement an effective treatment plan. Treatment of net-acidic mine waters often includes initial processes to generate alkalinity to remove metals at a faster rate than compared to without adequate alkalinity (Hedin et al. 1994; Taylor et al. 2005; Watzlaf et al. 2004; Younger et al. 2002).

1.3.2 Treatment Systems

Mine drainage treatment is broadly classified into two groups, active and passive treatment. ATS rely heavily on chemical addition (e.g., lime, slaked lime, calcium carbonate, hydrogen peroxide and sodium hydroxide) and aeration to both raise the pH and provide enough oxygen to accelerate the rates of metals oxidation and promote the precipitation of metals as hydroxides and carbonates (Johnson and Hallberg 2005; Taylor 2005; Younger 2002). Although ATS can be very efficient and cost-effective for active mining operations and have a

smaller footprint than PTS, they require daily operation and maintenance (O&M), continuous inputs of energy, and often produce high water-content sludges that can be difficult and costly to dispose (Johnson and Hallberg 2005; Watzlaf et al. 2004; Younger et al. 2002). Therefore, active treatment options are not preferred for abandoned mine sites. Passive treatment has been shown as a viable alternative to active treatment in many scenarios and the research to improve and expand passive treatment technologies has been growing (Dempsey et al. 2001; Geroni et al. 2012; Hedin et al. 1994; Hedin 2008; Johnson and Hallberg 2005; Kirby et al. 2007; Leavitt et al. 2011; Nairn et al. 2009; Nairn 2013; Nairn et al. 2018; Oxenford 2016; Schmidt 2004; Skousen et al. 2017; Taylor et al. 2005; Watzlaf et al. 2004; Younger et al. 2002).

PTS are ecologically engineered to utilize a combination of geochemical, biological, and physical processes and renewable energy sources in order to treat mine drainage (Johnson and Hallberg 2005; Nairn et al. 2009; Skousen et al. 2017; Watzlaf et al. 2004; Younger et al. 2002). PTS often consist of a series of treatment process units that individually address a particular characteristic of the mine drainage (Johnson and Hallberg 2005; Nairn et al. 2009; Skousen et al. 2017; Watzlaf et al. 2004; Younger et al. 2002). Unlike active treatment options, PTS do not require daily operation and maintenance and can be used long-term in remote and abandoned sites. Although PTS may be land-intensive due to the deceased treatment efficiencies, the reliance on natural processes allows the systems to operate for years with limited O&M and PTS can provide ancillary benefits to local wildlife and communities (Taylor et al. 2005; Younger et al. 2002).

1.3.3 Iron Retention in Oxidation Ponds

In the absence of PTS, or if Fe precipitates are mobilized and leave the system, Fe hydroxides and oxyhydroxides can coat stream sediments and streambeds destroying habitat and negatively impacting the ecology (Hogsden and Harding 2012; Jennings 2008; Pratt et al. 2014). Precipitated Fe from mine drainage in receiving streams negatively affects habitat and biota in these streams as shown by decreases in submergent and emergent macrophytic vegetation, macroinvertebrate and fish species richness and diversity (Hogsden and Harding 2012; Jennings 2008; Pratt et al. 2014; Taylor et al. 2005). The Fe particulates in receiving streams can also cause increases in turbidity, limiting the sunlight needed for benthic primary production (Pratt et al. 2014).

Fe retention consists of four main removal mechanisms: oxidation, hydrolysis, precipitation and settling. PTS consist of multiple treatment cells placed in series to treat specific water quality characteristics of mine drainage. Oxidation ponds are a common initial process unit used to treat net-alkaline mine drainage (Hedin et al. 1994; Johnson and Hallberg 2005). These open water ponds and aerobic wetlands are a favorable treatment method because they promote the oxidation of ferrous, Fe (II), iron to ferric, Fe (III), iron (Equation 1.2). Oxidation ponds utilize either passive or active aeration which increases DO concentration. Also, the flux of oxygen into the water column causes a concentration gradient for CO_2 which readily degasses into the atmosphere. In net-alkaline mine water, the degassing of CO_2 raises pH by reducing the amount of carbonic acid in the water which facilitates faster Fe oxidation rates. Under circumneutral pH conditions, the dissolved Fe (III) iron quickly hydrolyzes with

water and precipitates to form various Fe oxide and hydroxide species (Equation 1.3) (Younger et al. 2002). Oxidation ponds are recommended to be the first unit in a PTS for mine drainage with an Fe concentration greater than 50 mg/L so that Fe can settle in the oxidation pond before entering wetland systems that are more difficult to maintain (Younger et al. 2002). For net-alkaline mine water, oxidation ponds are designed using an Fe removal rate of 10 to 20 g Fe m^{-2} day^{-1}, with a retention time based on the initial Fe concentration and acid load (Nairn et al. 2009; Nairn et al. 2018; Skousen et al. 2017; Watzlaf et al. 2004; Younger et al. 2002).

$$4Fe^{2+} + O_2 + 4H^+ \rightarrow 4Fe^{3+} + 2H_2O \quad (1.2)$$

$$Fe^{3+} + 3H_2O \rightarrow Fe(OH)_3\,(s) + 3H^+ \quad (1.3)$$

At pH values between 3 and 9, Fe (III) hydrolysis is rapid and Fe (II) oxidation is the limiting chemical step (Dempsey et al. 2001; Singer and Stumm 1970). Many factors can affect the efficiency of oxidation ponds and Fe oxidation rates. Abiotic Fe (II) oxidation can occur by homogeneous and heterogeneous mechanisms. Homogeneous oxidation is controlled by the dissolved reactants including dissolved Fe (II) and DO. Heterogeneous oxidation occurs at the solid-water interface and is controlled by dissolved Fe (II), DO, and solid Fe (III) precipitate (Dietz and Dempsey 2017).

Nairn et al. (2002) performed a field microcosm experiment with ferruginous net-alkaline mine drainagecollected from the Tar Creek Superfund Site. The study investigated the

roles of CO_2 degassing to raise pH and Fe solids addition to promote heterogeneous oxidation on Fe removal rates. Five treatment scenarios were tested in triplicate (closed, open, open + Fe, open + aeration, open + aeration + Fe). The study found that active aeration and the addition of Fe solids can promote pH increase and that heterogeneous oxidation increases Fe retention (Nairn et al. 2002).

Dempsey et al. (2001) performed a field study comparing two field sites where one site had a series of oxidation ponds treating acid mine drainage water and the other site had shallow channels treating net-alkaline mine drainage. The study showed that the second site, with shallow channels, had faster oxygen and CO_2 mass transfer coefficients and thus a larger annual Fe removal rate. Dempsey et al. (2001) attributed this to a higher water velocity which allows for more oxygen entrainment into the water from the atmosphere. However, while channels may allow more oxygen to be added to the water column, the increased velocity can keep the particulate Fe in suspension and limit settling.

Biological factors affecting Fe oxidation rates can include Fe-oxidizing bacteria such as *Acidithiobacillus* spp. which are acidophiles preferring an optimum growth pH < 3 and neutrophilic filamentous organisms such as *Gallionella* spp., *Leptothrix* spp., *Metallogenium* and *Sphaerotilus* spp. which typically occur at groundwater seeps containing Fe (II) iron (Kirby et al. 1999; Watzlaf et al. 2004). A Stella II™ model using initial Fe (II) iron concentration, pH, temperature, *Acidithiobacillus ferrooxidans* concentration, DO concentration, flow rate, and pond volume from seventeen field sites was used to predict Fe (II) oxidation rates and concentrations by Kirby et al. (1999). This study showed that increasing the *Acidithiobacillus*

ferrooxidans concentration only had effects on Fe oxidation rates at pH less than 5 and that abiotic factors primarily influenced Fe oxidation rates at pH greater than 5.

A common criticism of PTS is that their effectiveness can be negatively impacted by higher flow rates and lower temperatures (Hedin 2008). To help evaluate these concerns, the Marchand PTS treating ferruginous net-alkaline mine drainage in western Pennsylvania was monitored for a year to determine the system's effectiveness (Hedin 2008). The Marchand PTS consists of six serially-connected oxidation ponds followed by a shallow constructed wetland. Although reaction kinetics were directly related to temperature, Hedin (2008) found cold weather had minimal influence on the Marchand system's Fe retention effectiveness. Although colder temperatures slow reaction kinetics, DO solubility is inversely related to temperature. The solubility of DO is 25% higher at 9^{o}C than 19^{o}C which, assuming a proportional oxygen transfer rate into the water, increases the oxidation rate of Fe (II) by 25% (Hedin 2008).

Although Fe oxidation and precipitation are important mechanisms for Fe retention, often the settling rate of Fe particulates is the practical rate limiting step (Dempsey and Jeon 2001; Hedin 2008). The settling time of precipitates is considered when designing PTS in either the same oxidation unit or in following deep-shallow-deep vegetated aerobic wetlands (Hedin 2008; Nairn et al. 2009; Skousen et al. 2017; Watzlaf et al. 2004). Fe particulates have a reported settling rate range of 0.01 to 1.91 cm min^{-1}, with the settling rate increasing with the wet density of the sludge (Dempsey and Jeon 2001). The rate of settling is dependent on floc size and density which is calculated using a modified version of Stokes law to account for non-spherical particles (Chakraborti and Kaur 2014). A modified version of Stokes law is

recommended because natural flocs or aggregates often have an increased porosity and irregular shape that lowers their effective density and thus have a lower settling velocity than predicted by Stokes law for solid spherical particles (Perkins et al. 2007). Equation 1.4 shows how a particle's settling velocity (v_s) is dependent on acceleration due to gravity (g), particle's density (ρ_s), density of the medium, commonly water (ρ_w), viscosity of the medium (μ) and the particle's diameter (d) under laminar flow conditions (Chakraborti and Kaur 2014).

$$v_s = \frac{g}{18}\left(\frac{\rho_s - \rho_w}{\mu}\right)d^2 \qquad (1.4)$$

Floc aggregates are very fragile, and therefore disturbance caused by precipitation events may cause the resuspension of retained Fe particulates (Oxenford 2016). The resuspended Fe particulates can then be mobilized into the subsequent process units, negatively impacting the performance of the downstream units (Skousen et al. 2017; Watzlaf et al. 2004). Fe particles can alter flow dynamics in subsequent treatment cells especially vertical flow bioreactors (Watzlaf et al. 2004). To prevent Fe from leaving the oxidation pond, oxidation ponds are designed with sufficient storage volume for accumulated solids so that volume displacement by solids does not impair the unit's performance over time (Watzlaf et al. 2004).

1.3.4 Role of Gas Transfer

CO_2 may play a unique role in some mine drainage by raising pH upon exsolution and thus promoting Fe oxidation (Hedin 2008). Alkalinity in net-alkaline mine drainage waters is

typically produced from the dissolution of limestone or dolomite in which bicarbonate ions are produced, as shown in Equation 1.5 (Younger et al. 2002).

$$CaCO_3 + H_2CO_3 \rightarrow Ca^{2+} + 2HCO_3^- \quad (1.5)$$

Equation 1.6 shows that the bicarbonate alkalinity commonly found in mine drainage reacts with water to form carbonic acid where $H_2CO_3^*$ represents both $H_2CO_{3\,(aq)}$ and $CO_{2\,(aq)}$ species (Kirby et al. 2007; Younger et al. 2002).

$$HCO_3^- + H_2O \rightarrow H_2CO_3^* + OH^- \quad (1.6)$$

Once the mine drainage is exposed to air, the dissolved CO_2 will follow Henry's law and readily degas to the vapor phase in order to reach equilibrium with the atmosphere (Equation 1.7) (Kirby et al. 2007; Younger et al. 2002).

$$H_2CO_3^* \rightarrow H_2O + CO_2\,(g) \quad (1.7)$$

As more CO_2 is degassed, more protons are consumed therefore increasing the pH of water as is more clearly shown in Equation 1.8 (Kirby et al. 2007).

$$HCO_3^- + H^+ \rightarrow H_2O + CO_{2\,(g)} \quad (1.8)$$

In the Kirby et al. (1999) study, biological and abiotic factors were considered to create a more comprehensive rate law. Based on a Stella II™ model using field data from PTS treating acid mine drainage, Kirby et al. (1999) found that a change in pH was critical in Fe oxidation rates as shown in Equation 1.9.

$$\frac{d\,[Fe\,(II)]}{dt} = \frac{k\,[Fe\,(II)][O_2]}{[H^+]^2} \tag{1.9}$$

At a pH greater than 5, Fe oxidation rates were affected mostly by pH, then by temperature and influent Fe (II) concentration, and lastly by pond volume and DO concentration (Kirby et al. 1999). At a pH greater than 5, Fe (II) iron oxidation rates showed a positive relationship with temperature, DO concentration, pH and pond volume (which affects surface area for oxygen transfer) and a negative relationship with influent Fe (II) concentration (Kirby et al. 1999). Hedin (2008) found that pH was inversely related to temperature at the Marchand passive treatment system. This result may be because, as previously discussed, the solubility of DO increases with a decrease in temperature. As more oxygen is dissolved into the water, CO_2 is degassed causing an increase in pH. This phenomenon occurs because the driving force of gas transfer is the gradient of partial pressures between the air-liquid interface. The CO_2 gradient is much higher than for atmospheric oxygen and thus aeration technologies that provide enough oxygen are also useful for CO_2 removal (Eschar et al. 2003). Hedin (2008) predicted that a pH increase of 0.3 units could increase the oxidation rate by 1.9 times the rate

at lower pH under heterogeneous Fe oxidation conditions. However, without the pH increase caused by degassing CO_2 in net-alkaline mine drainage, temperature change may have a larger effect as described by Kirby et al. (1999).

An extensive review of mine drainage literature shows that CO_2 concentrations are commonly presented in terms of their partial pressure (Hedin 2008; Kirby et al. 2007; Kirby et al. 2009; Nairn 2013; Nairn et al. 2018). Therefore, this study utilizes the partial pressure of CO_2 to represent the CO_2 fraction in the aqueous phase. The partial pressure of CO_2 in water can be calculated using the Henderson- Hasselbalch equation for the carbonate species and the Arrhenius equation to correct the first and second carbonic acid dissociation constants (K_1, K_2) and Henry's gas constant (K_H) for temperature (T, in Kelvin) (Jensen, 2003). Equation 1.10 is the Arrhenius equation that utilizes the enthalpy of the reaction at standard conditions ($\Delta H°_{rxn}$) and the universal gas constant (R) equal to 8.314 J/mole-K. Equations 1.11-1.15 show how the partial pressure of carbon dioxide (P_{CO2}) can be calculated from the total alkalinity (Alk), pH in the form of hydrogen ion molar concentration ($[H^+]$), hydroxide ion molar concentration ($[OH^-]$), ionization fraction of CO_2* (α_0), ionization fraction of HCO_3^- (α_1)and the ionization fraction of CO_3^{2-} (α_2) (Jensen 2003; Moran 2010a).

$$K_T = K_{25°} \, exp\left[\left(\frac{-\Delta H°_{rxn}}{R}\right)\left(\frac{1}{T_{25°}} - \frac{1}{T}\right)\right] \tag{1.10}$$

$$P_{CO_2} = \left[\frac{Alk - [OH^-] + [H^+]}{(\alpha_1 + 2\alpha_2)}\right]\left(\frac{\alpha_0}{K_H}\right) \tag{1.11}$$

where

$$E = [H^+]^2 + [H^+]K_1 + K_1K_2 \quad (1.12)$$

$$\alpha_0 = \frac{[H^+]^2}{E} \quad (1.13)$$

$$\alpha_1 = \frac{[H^+]K_1}{E} \quad (1.14)$$

$$\alpha_2 = \frac{K_1K_2}{E} \quad (1.15)$$

1.3.5 Aeration Techniques

Although oxygen is readily available in the atmosphere, greater Fe oxidation rates can be achieved by actively introducing oxygen into the water column (Geroni et al. 2012; Hedin 2008; Kirby et al 2007; Leavitt 2011; Nairn et al. 2009; Oh et al. 2015; Schmidt 2004). A variety of aeration techniques exist, including simple energy dissipation devices and mechanical aeration technologies such as air sparging, fine bubble diffusers, the Maelstrom Oxidizer and floating surface aerators (Geroni et al. 2012; Hedin 2008; Kirby et al 2007; Leavitt 2011; Nairn et al. 2009; Nairn et al. 2018; Oh et al. 2015; Parker and Suttle 1987; Schmidt 2004; Shammas 2007; Zhang et al. 2000). Cascade aeration is a common energy dissipating practice used in PTS. Oh et al. (2015) performed an experiment comparing changes in water quality caused by air diffuser and cascade aeration of mine drainagebefore the water entered an oxidation pond. The air diffuser experiment showed that the main mechanisms limiting Fe oxidation was gas exchange of oxygen and CO_2 (Oh et al. 2015). The aeration efficiency of cascade aerators is dependent on drop height rather than mine drainage water quality or plunge pool depth. Both

experiments showed that the implementation of aeration technologies fosters more efficient Fe oxidation and precipitation compared to relying on surface diffusion (Oh et al. 2015).

The rate of gas transfer is directly dependent on the surface area of the air-water interface (Zhang et al. 2000). Geroni et al. (2012) compared the efficiency of degassing of CO_2 and the corresponding effects on Fe (II) removal between cascade aeration and mechanical aeration techniques including a submersible self-venting pump. The study found that cascade aeration degasses CO_2 at a greater rate than forced mechanical aeration due to the cascade's ability to expand the air-water interface. Falling water creates eddies that entrain many air bubbles into the water which encourages the formation of small droplets increasing exposed surface area of the air-water interface (Geroni et al. 2012). However, while cascade aeration creates more air-water interface, it is limited because it requires a site with enough relief to provide sufficient hydraulic head (Geroni et al. 2012). A further limitation of using cascade aeration for ferruginous mine water is that Fe particulates can accumulate on the steps of the cascade, decreasing the drop height of the mine drainage and ultimately reducing the oxygen transfer efficiency of the cascade aerator (Younger et al. 2002). Geroni et al. (2012) also found that although cascade aeration degasses CO_2 in less time, mechanical aeration techniques remove more CO_2 overall due to their longer residence times.

Although cascade aeration is typically used in PTS, mechanical aeration techniques are used in many wastewater treatment and aquaculture applications, and in PTS with limited elevation changes. One such mechanical aeration technology is a fine bubble diffuser, which is a diffuser plate placed at the bottom of the pond that pushes air through very fine holes to create

fine bubbles (Schmidt 2004; Shammas 2007). Although fine bubble diffusers have a high oxygen transfer rate due to the fine bubbles increasing water-air interface area, both ceramic and membrane diffusers have proven to be susceptible to fouling (Schmidt 2004; Shammas 2007). Fine bubble diffusers are often used in water and wastewater treatment applications and can be susceptible to Type I (clogging by metal hydroxides or carbonates) or Type II (biofilm layer) fouling (Shammas 2007). Therefore, while fine bubble diffusers provide greater oxygen transfer rates resulting in greater CO_2 exsolution rates, they are not favorable for treating ferruginous mine drainage due to fouling of the membranes (Schmidt 2004; Shammas 2007).

Another aeration technology being explored for passive treatment of mine drainageis a trompe. A trompe is a device that uses falling water to compress air by allowing water to flow down a pipe at a high enough velocity to entrain air and then enter a chamber below the discharge elevation that separates the compressed air from water for use for aeration (Danehy et al. 2016; Leavitt 2011). This technology, developed in the 17th century, has been applied at the Curley PTS site in Pennsylvania to treat net-alkaline mine drainage with alkalinity ranging from 425-450 mg/L $CaCO_3$ and an average Fe concentration of 23 mg/L (Leavitt, 2011). The study found that the trompe added over 3 mg/L of DO which was enough oxygen to oxidize 82-97% of the Fe in the raw water. While trompes increase DO concentrations, they do rely on sufficient head differences to aerate the water and thus are not suitable in sites with limited topographical relief.

Another type of mechanical aeration technology is the use of floating mix aerators, also commonly referred to as airlift aerators, lifterators or float-mix aerators. Airlift aerators operate

by introducing diffused air into the water through a riser where the air-water mixture becomes less dense and more buoyant and travels up the riser and out to the atmosphere (Burris et al. 2002; Parker and Suttle 1987). Upon reaching the surface, some of the oxygen is lost to the atmosphere while the remainder becomes entrained in the water (Burris et al. 2002). Airlift aerators have different designs with water either spilling across a plate on the surface or traveling through vertical pipes that discharge the oxygenated water at specific depths (Burris et al. 2002; Parker and Suttle 1987).

Although airlift aerators are less susceptible to fouling, they are not as efficient at transferring oxygen into the water column (Burris et al. 2002; Moran 2010b; Parker and Suttle 1987). Moran (2010a, b) investigated the efficiency of cascade aeration and airlift aerators to add oxygen into and degas CO_2 from water. This process is important in aquaculture applications since increased fish production can cause an increase in respired CO_2 in fish units and creation of oxygen demand (Moran 2010a). The Moran 2010 studies showed that airlift aerators were not affected by salinity of the water but overall had poorer CO_2 mass transfer performance compared to cascade aeration (Moran 2010a, b). Similarly, airlift aerators require significant power input (Burris et al. 2002; Parker and Suttle 1987). The carbon footprint of power input needed for aeration can be reduced by using renewable energy sources such as solar and wind energy. In addition, the use of a renewable energy source allows the technology to be implemented in remote locations without access to grid energy.

Loyless and Malone (1998) performed a bench-scale study evaluating the water delivery, oxygen transfer, and CO_2 degasification performance of airlift aerators in order to

determine their usefulness in aquaculture applications. Their study showed that delivering air directly into open water systems via air stones or tubing had a higher standard oxygen transfer rate (SOTR) than delivering air via an airlift with either air stones or tubing. At a constant air injection rate of 56.64 L min^{-1}, open water delivery had SOTRs between 0.02-0.04 kg O_2 hr^{-1}, while airlift delivery only had SOTRs between 0.015-0.0175 kg O_2 hr^{-1}. This result is because, in an open water system, bubbles tend to disperse and thus are less likely to coalesce and lose their surface area. However, bubbles in an airlift riser are crowded together and coalesce forming bigger bubbles with less surface area available for oxygen transfer. Airlifts also typically discharge water near the surface which is closer to oxygen saturation decreasing the driving force for gas transfer. Loyless and Malone's (1998) study also showed that steady-state DO concentrations were strictly a function of total air injection rate, while steady-state CO_2 concentrations varied with the total air injection rate and the total number of airlift aerators used. CO_2 stripping improved slightly with less air delivered per airlift aerator. Overall, Loyless and Malone (1998) determined that airlift aerators transfer oxygen at only 20%-50% of the rate as open water aeration systems and thus are encouraged for water delivery use rather than to promote gas transfer.

While airlift aerators have a lower oxygen transfer rate than cascade aeration or fine bubble diffusers, they still aerate the water and degas CO_2. Airlift aerators are also less prone to fouling like fine bubble diffusers and can be used in sites with limited topographic relief since they do not rely on hydraulic head to operate. More research needs to be performed reviewing

the role airlift aerators, such as float-mix aerators, can play in aerating mine drainage and promoting Fe retention.

1.4 Site Description

This research focused on the Southeast Commerce Passive Treatment System (SECPTS), an ecologically engineered system designed to treat net-alkaline mine drainage from abandoned lead and zinc mining operations at the Tar Creek Superfund Site in Ottawa County, Oklahoma. The Tar Creek Superfund Site covers approximately 100 km^2 located within the larger Tri-State Lead-Zinc Mining District (TSMD) of Kansas, Oklahoma and Missouri. Commercial mining in the region started in the 1830s and continued through the 1970s. During peak production in the 1920s, approximately 120,000 metric tons of lead and 680,000 metric tons of zinc were produced annually in the TSMD (USEPA, 2018). Small scale mining operations continued to extract materials in the Oklahoma portion of the TSMD, known as the Picher Field, until the cessation of mining activities in the 1970s (USEPA,2018). After the mines were abandoned and the pumps in the underground mines were all shut off, groundwater began to infiltrate into the mine workings and surface water entered through abandoned shafts, boreholes and collapse features eventually producing artesian flowing mine drainage in 1979 (USEPA 2018). The artesian flowing mine water discharges flowed into Tar Creek and its tributaries, where Fe hydroxides stained the creek orange and negatively impacted downstream aquatic life (USEPA 2018). Due to the degraded environmental conditions caused by the mine drainage, the site was proposed for the U.S. Comprehensive Environmental Response, Compensation and Liability Act (US CERCLA or Superfund) National Priorities List in

1981 and the site was listed as the Tar Creek Superfund Site (TCSS) in 1983 (USEPA 2018). At this time, the Oklahoma Department of Environmental Quality is cited as the cleanup oversite agency under the guidance of the United Sates Environmental Protection Agency (EPA).

The Hazard Ranking System is a score applied by the EPA to classify the risks associated with the severity and diversity of exposures and is determined by an assessment of physical and chemical properties and abiotic exposure pathways. The TCSS maintained a score of 51.85 through 2003 due to the complexity and scope of the contamination found during preliminary assessments (USEPA 2018). The EPA has designated five operable units (OU) to address contamination at the TCSS as shown in Table 1.1 (USEPA 2018). The record of decision (ROD) for OU 1 at Tar Creek, which focuses on surface and groundwater contamination, was released in 1984 (USEPA 1984). Following the release of the ROD for OU 1, the state of Oklahoma and EPA agreed that the poor water quality of surface waters was due to “irreversible man-made conditions” (USEPA 1994).

Table 1.1 Summary of US EPA's Operable Units at the Tar Creek Superfund Site (USEPA, 2017)

Operable Unit	Issue	Status
OU 1	Surface water quality degradation due to the discharge of acid mine drainage and the threat of potential contamination of the Roubidoux Aquifer beneath the site from mine water and abandoned wells.	Abandoned wells have been and continue to be plugged in order to prevent migration of contaminated water into the Roubidoux Aquifer. Groundwater monitoring is ongoing. Berms were placed to divert surface flow into major inflow areas.
OU 2	Contaminated soil in residential areas linked to elevated blood lead levels in children	Soil removal and clean fill dirt replacement on residential and high access areas. Currently over 2,000 properties have been remediated. ODEQ is continuing yard remediation efforts. Ottawa County Health Department has implemented education and outreach programs.
OU 3	Storage and retention of chemicals at the Eagle-Picher office and laboratory complex	One hundred and twenty containers of chemicals were removed in 2000
OU 4	Undeveloped areas where mine and mill residues and smelter wastes have been placed, deposited, stored, disposed or located as a result of mining, milling or smelting operations.	Residential buyout occurred in Picher and Cardin, Oklahoma and Treece, Kansas in 2009. Remediation of a former lead smelter, chat piles and chat bases are ongoing.
OU 5	Characterize sediment and surface water throughout the lower Spring and Neosho River basin to determine potential risk and human exposure	Currently there are insufficient data to determine if there is human health risk related to sediment and surface water exposure. Modeling is ongoing.

However, based on research conducted by the University of Oklahoma Center for Restoration of Ecosystems and Watersheds (CREW), the Mayer Ranch Passive Treatment System and SECPTS were constructed in 2008 and 2017, respectively, to treat artesian-flowing mine waters. Treated effluent from these systems enters an unnamed tributary before entering Tar Creek and making its way to the Neosho River. Figure 1.1 shows the Unnamed Tributary (UT) watershed, a CREW sampling location and the locations of the PTS. The implementation of

both treatment systems has improved water quality and returned fish communities in the Unnamed Tributary watershed. Historical total aqueous metal concentrations at a site named Unnamed Tributary- Downstream (UT-D) which is downstream of both PTS are shown in Figures 1.2 -1.4.

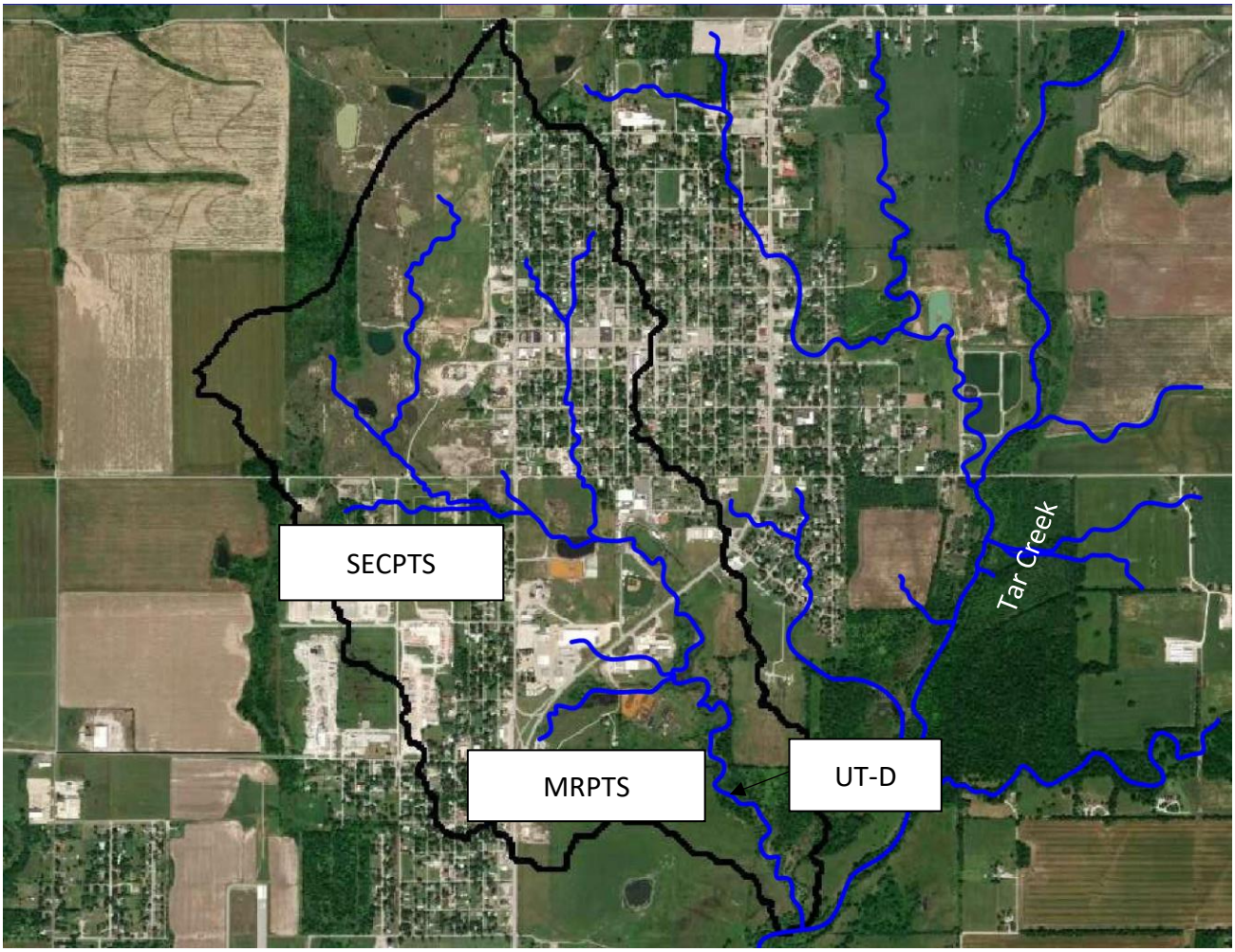

Figure 1.1 Aerial of the Unnamed Tributary watershed with CREW historical sampling location (UT-D) and location of the PTS shown

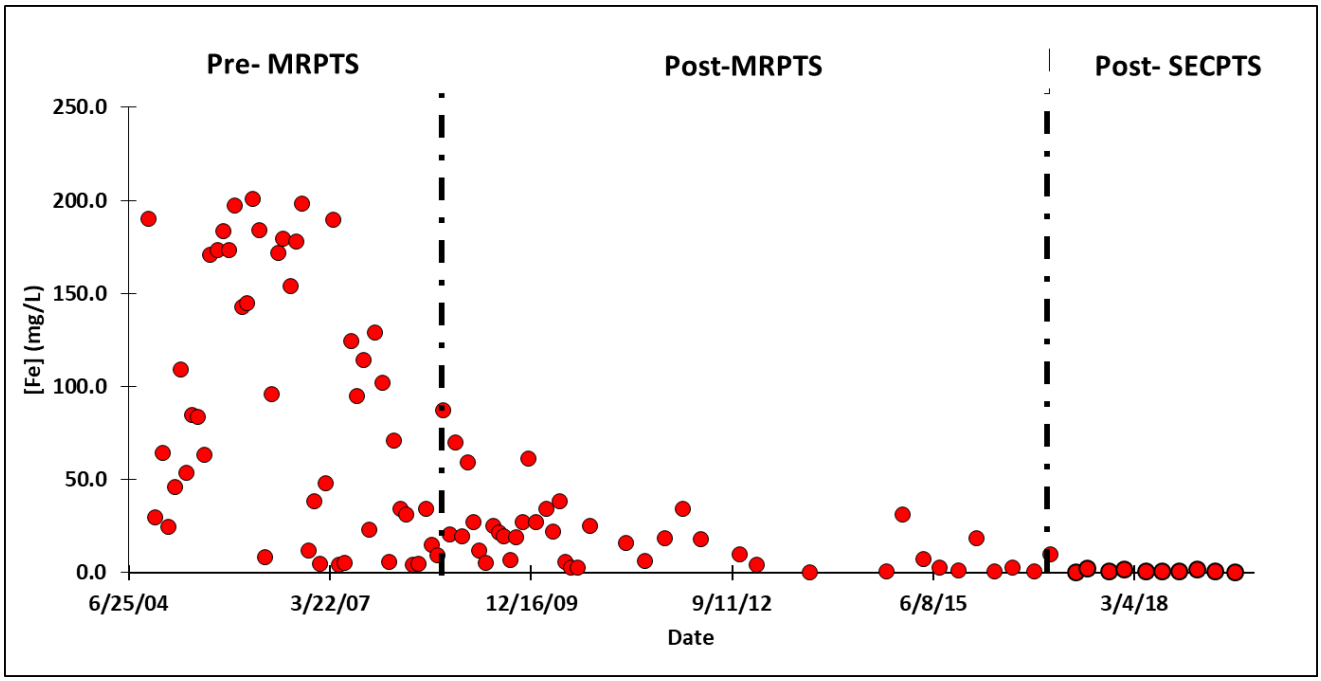

Figure 1.2 Historical total aqueous Fe concentrations at UT-D from 2004 to 2019; vertical lines denote when each system came online.

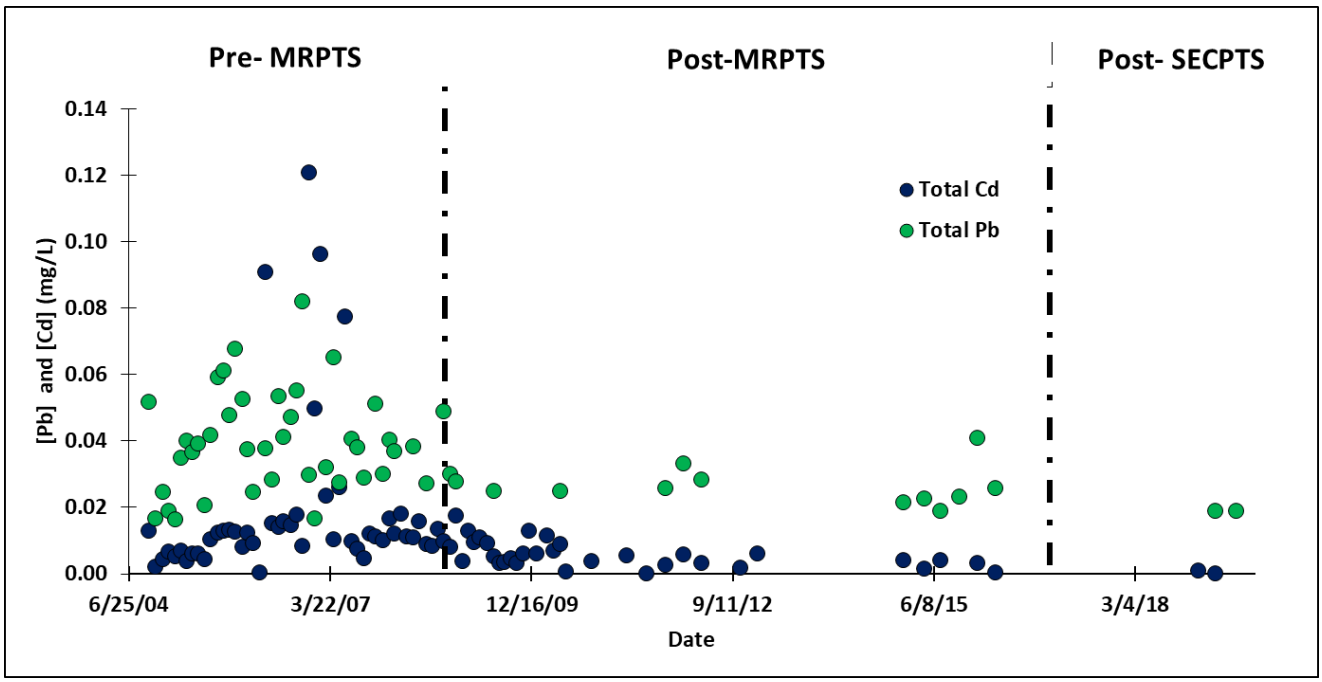

Figure 1.3 Historical total aqueous Pb and Cd concentrations at UT-D from 2004 to 2019; vertical lines denote when each system came online. Concentrations below the PQL are excluded.

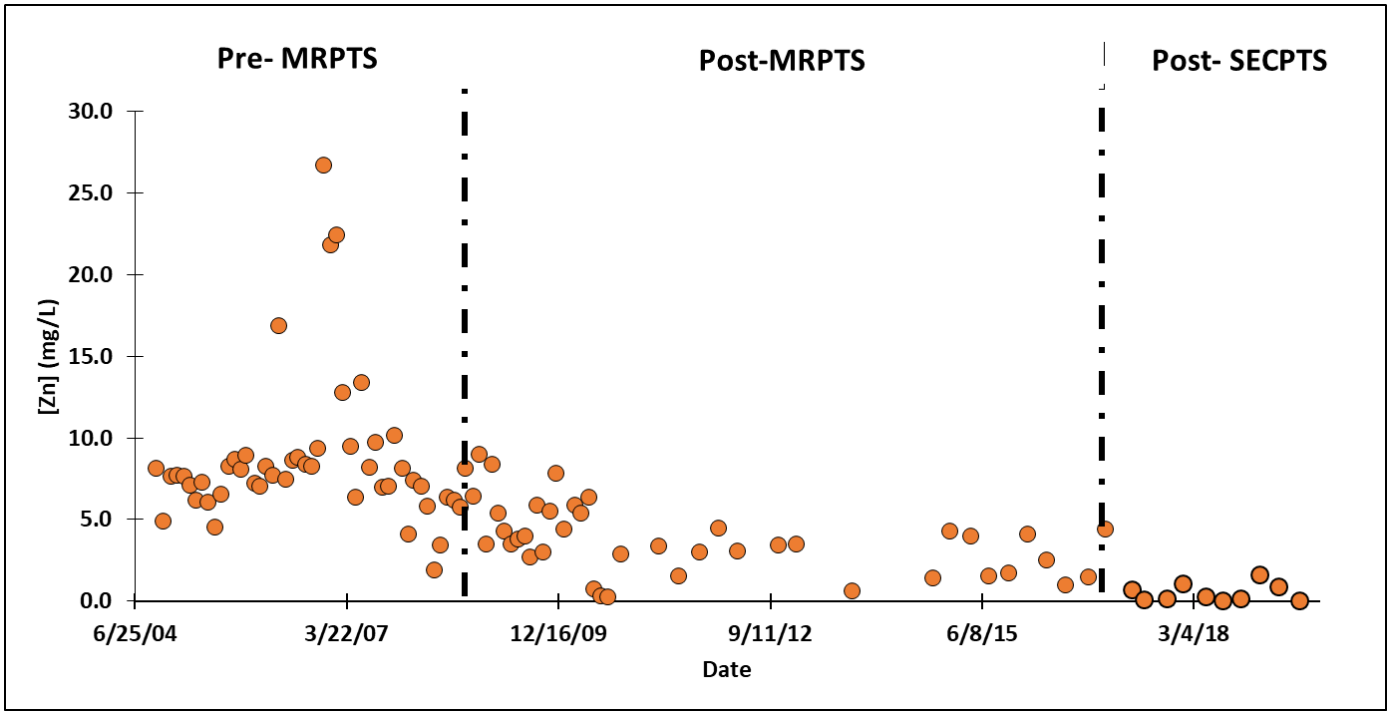

Figure 1.4 Historical total aqueous Zn concentrations at UT-D from 2004 to 2019; vertical lines denote when each system came online.

SECPTS was constructed in 2017 to treat artesian-flowing mine drainage from a collapse feature. Between 2006 and 2007, two collapse features at southeast Commerce were filled and capped and the mine drainage was collected in the subsurface via French drains and discharged into the Unnamed Tributary of Tar Creek. During construction of SECPTS, the French drain was intercepted, creating two inflow locations on the north (N-in) and South (S-in) sides of the oxidation pond (Figure 1.5). Additional mine drainage upwellings were encountered during the construction of the oxidation pond. These upwellings enter at multiple locations in the floor and inside slopes of the oxidation pond, preventing accurate flow rate measurements entering SECPTS. A well was installed in October 2018 that captured water from the upwelling that has

been consistently sampled for water quality parameters. Comparing flows exiting the system and flows from N-IN and S-IN, approximately 80% of the system's flow comes from the upwellings in the bottom of the oxidation pond.

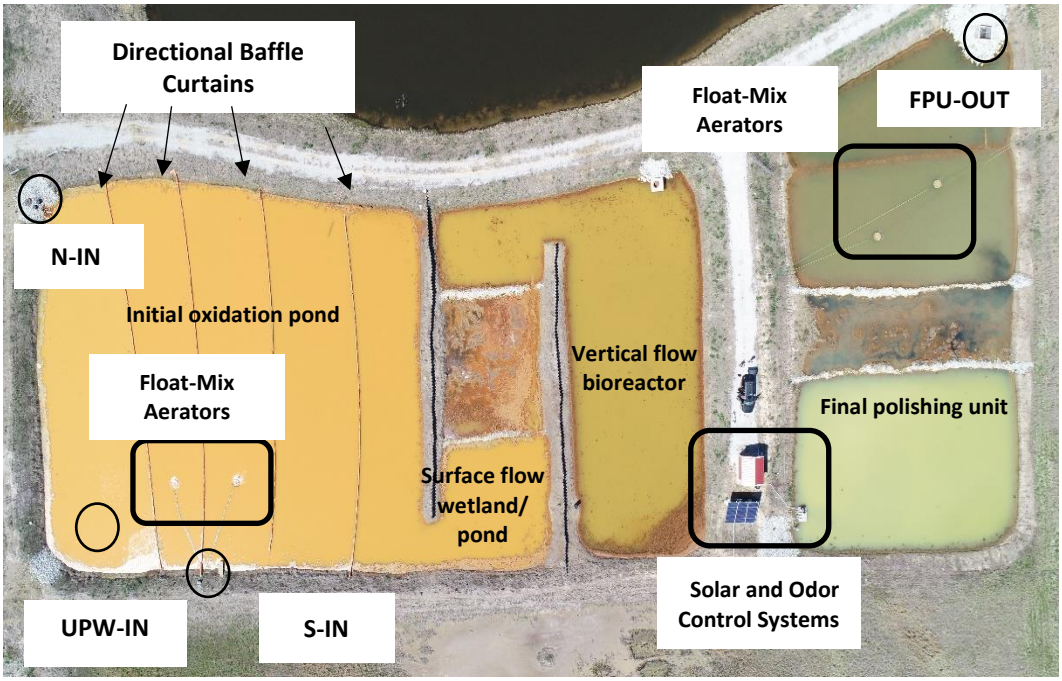

Figure 1.5 Aerial photograph of the SECPTS noting the important process units, inlets and outlets and technology incorporated in each unit

The SECPTS is designed with four treatment units including an oxidation pond, horizontal flow surface wetland, vertical flow bioreactor (VFBR) and a final polishing unit with a central treatment wetland shelf. The oxidation pond has a surface area of approximately 3,315 m^2 and a volume of 4,175 m^3 at a design water elevation of 794.6' above mean sea level. The oxidation pond is approximately 1 m deeper to the west and slopes shallower to the east. This was designed to increase the volume capacity of the oxidation pond to the west but becoming

shallow enough to the east that enough hydraulic head would be present to allow the water to flow into the wetland process unit. The wetland has a surface area of approximately 1,185 m^2 and a total storage volume capacity of approximately 1,465 m^3. The oxidation pond and wetland were designed based on an Fe removal rate of 20 $g/m^2/d$. Directional baffle curtains were added to the oxidation pond to create a serpentine flow path to provide a total hydraulic residence time of nine days for the oxidation pond and wetland. The wetland is designed to provide additional Fe retention and a vegetative filter to remove remaining particulate Fe before the water enters the VFBR. The VFBR consists of a woodchip and spent mushroom compost media that supports sulfate reducing bacteria to form and sequester metal-sulfides. This system is intended to remove Cd, Pb and Zn as metal-sulfides. Discharge pipes from the VFBR enter an odor-control system that uses a vacuum to remove hydrogen sulfide gas from the water and through an activated carbon filter that strips the sulfides to eliminate nuisance-odors. The water then travels into the FPU which consists of a series of pools with a wetland shelf and two float-mix aerators which aerate the highly reduced effluent from the VFBR before it is discharged into the Unnamed Tributary.

Aerators were added to this system because the site lacks enough topographic variability to sustain effective cascade aeration. The float-mix aerators at SECPTS allow air to push water up a riser and spill across a plate on the surface so that fouling becomes less of an issue. Figure 1.6 shows the design of the float-mix aerators used at the SECPTS. The SECPTS includes a 3,180-W photovoltaic array connected to a combiner box, two charge controllers, a 1500 W 24V DC inverter and a 24V battery bank used to power two regenerative pressure

blowers and one regenerative vacuum blower that when combined provide more than 150 m^3/min to four float-mix aerators (two in the oxidation pond and two in the final polishing unit) and to an odor control system receiving gaseous effluent from the VFBR. Table 1.2 shows the overall performance of the SECPTS comparing influent and effluent total aqueous metals concentrations.

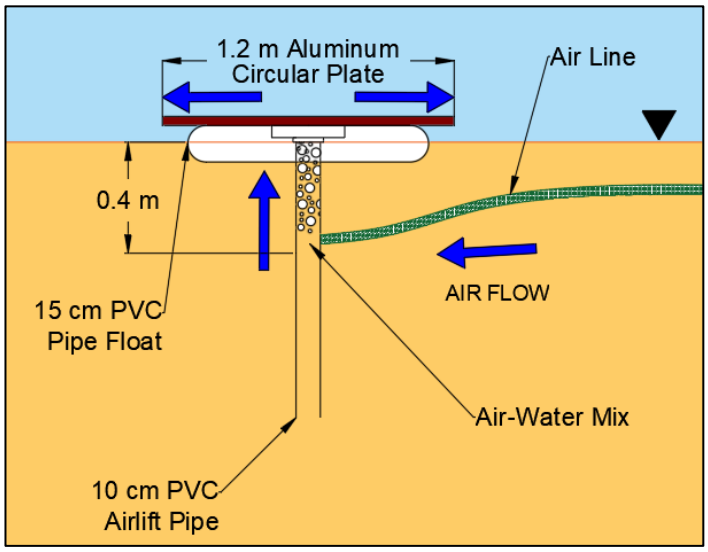

Figure 1.6 Schematic of the float-mix aerator, also known as a lifterator or airlift aerator, used in the PTS.

Table 1.2 Mean total aqueous metal concentrations for the influents and effluent of the SECPTS

Sampling location	Cd (mg/L)	Fe (mg/L)	Pb (mg/L)	Zn (mg/L)
S-IN (n=31, 11/16- 08/19)	0.015 ± 0.008	153.792± 11.968	0.149 ± 0.091	6.920 ± 0.741
N-IN (n=28, 03/17-08-19)	0.014 ± 0.006	133.976 ± 13.347	0.139 ± 0.077	6.746 ± 0.727
UPW-IN (n=8, 10/18-08/19)	0.022 ± 0.005	142.640 ± 28.166	0.274 ± 0.112	7.106 ± 0.642
Effluent (FPU-OUT) (n=31,01/17-08/19)	<PQL*	1.333 ± 0.779	0.024 ± 0.003	0.850 ± 1.897

*26 of 31 samples were below the practical quantification limit (PQL) of 0.00067 mg/L

1.5 Hypotheses

Limited research exists which investigates the effectiveness of airlift aerators to transfer oxygen into and degas CO_2 from the water column especially for passive treatment of mine drainage. Research analyzing the effectiveness of airlift aerators to promote Fe oxidation is necessary to determine if this technology is applicable for PTS in sites with limited topographic relief. The hypotheses that were explored in this study include:

- Aeration provided by solar-powered FMAs will significantly increase DO and decrease dissolved CO_2 concentrations nearer to the water surface than at discrete depths and will promote greater Fe retention.
- Aeration provided by solar-powered FMAs will significantly increase DO and decrease CO_2 concentrations at locations in closer proximity to the aerators at a common given depth resulting in more Fe retention nearer to the aerators.
- Aeration provided by solar-powered FMAs will improve the treatment performance of the oxidation unit by increasing DO concentrations, degassing more CO_2 and retaining more Fe particulates compared to wholly passive aeration.

1.6 Objectives

The objectives of this research were:

- Determine the effectiveness of the float-mix aerators to supply oxygen into the water column and to degas CO_2 in order to promote Fe retention with respect to depth within the water column.

- Determine the spatial effectiveness of the float-mix aerators to supply oxygen into the water column and to degas CO_2 in order to promote Fe retention.
- Determine the overall effectiveness of the float-mix aerators to supply oxygen to the water column and to degas CO_2 to promote Fe retention as the water travels from the inlets to the outlet of the oxidation pond.

This study investigated the effectiveness of novel mechanical aeration techniques to increase the rate of Fe oxidation in mine drainage as a substitute to common head-driven aeration technologies. This thesis is divided into five chapters: 1) Project Introduction and Literature Review, 2) The Effectiveness of Float-Mix Aerators with Respect to Depth, 3) Spatial Analysis of the Effectiveness of Float-Mix Aerators, 4) Analysis of the Effectiveness of Float-Mix Aerators to Promote Iron Oxidation Within an Oxidation Pond and 5) Conclusions and Future Work. Chapter 1 provides an overview of PTS, Fe removal mechanisms, aeration techniques, the role of CO_2 on Fe precipitation and an overview of the Tar Creek Superfund Site and the Southeast Commerce Passive Treatment System. Chapters 2-4 are written with the intention of being submitted to refereed journals and thus will include a short introduction, site description, and methodologies specific to the hypothesis being investigated. Chapter 5 provides a summary of the conclusions made from the three studies and discusses areas for future research.

Chapter 2: The Effectiveness of Float-Mix Aerators for Iron Retention Within Oxidative Units with Respect to Depth

2.1 Introduction

Mine drainage is a risk to the environment and to the communities of legacy mining districts due to the discharge of ecotoxic metals and its effect on water quality (Limerick 2005; Taylor 2005). A variety of strategies exist to treat mine drainage and the most applicable treatment option depends on the initial water quality, water quantity, available land and surrounding land use (Johnson and Hallberg 2005; Younger et al. 2002). One of these approaches is the use of passive treatment systems (PTS). PTS require little to no continual input of resources to complete the treatment process (Johnson and Hallberg 2005). Passive treatment is an often-favorable treatment strategy for remote sites with enough land area because they are lower cost in the long-term due to the absence of regular chemical additions, electricity and operator costs (Johnson and Hallberg 2005; Taylor 2005).

Aeration is a critical process for effective treatment of mine drainage in order to address elevated concentrations of ecotoxic metals, most notably iron (Fe). In PTS treating mine drainage, oxidation ponds are often designed to increase Fe oxidation rates by entraining more oxygen into the water beyond passive diffusion at the air-water interface (Hedin et al. 1994; Nairn et al. 2009, Nairn 2013; Nairn et al. 2018; Skousen et al. 2017). Aeration can have substantial effects on net-alkaline mine drainage as addition of oxygen into the water column

degasses carbon dioxide (CO_2), drives pH upward and enhances Fe oxidation rates (Hedin 2008; Kirby et al. 1999).

Many mine drainage PTS are in mining regions with substantial topographic variability that can be utilized for cascade aeration or other hydraulic head driven technologies (Geroni et al. 2012; Oh et al. 2015). Cascade aeration expands the air-water interface by spreading the water and dropping it over a series of drops to create eddies that entrain many air bubbles into the water which encourages the formation of small droplets that have a larger surface area exposed to the air (Geroni et al. 2012). Although cascade aeration has proven to promote oxygen transfer and CO_2 degassing, it is a technology not viable for sites in flat landscapes where the hydraulic head may be insufficient. Therefore, a need exists for novel aeration techniques that do not rely on hydraulic head for passive treatment systems located in relatively flat landscapes.

Mechanical aeration technologies that do not require hydraulic head to entrain oxygen into the water column are commonly used in aquaculture and water and wastewater treatment operations in order to promote mixing and increase dissolved oxygen (DO) concentrations (Burris et al. 2002; Parker and Suttle 1987; Shammas 2007). Fine bubble diffusers are one such technology that pushes air through tiny holes in a diffuser plate to create fine bubbles that increase the water-air interface (Loyless and Malone 1998; Schmidt 2004; Shammas 2007). Due to the large water-air interface, fine bubble diffusers have a high oxygen transfer rate. However, they are often susceptible to fouling from metal hydroxides or from a biofilm layer

and thus may not be suitable for waters with high suspended solids like a mine drainage oxidation pond (Schmidt 2004; Shammas 2007).

Airlift aerators, also known as float-mix aerators, are another technology commonly used in aquaculture settings. Airlift aerators introduce diffused air through a riser in the water column where the air-water mixture becomes more buoyant and travels up the riser and out to the atmosphere, typically across a plate (Burris et al. 2002; Parker and Suttle 1987). Although airlift aerators are less susceptible to fouling, they are not as efficient at transferring oxygen into the water column (Loyless and Malone 1998; Moran 2010 a, b). Moran (2010 a, b) investigated the efficiency of cascade aeration and airlift aerators to add oxygen into, and degas CO_2 from, water. This process is important in aquaculture applications since increased fish production can cause an increase in respired CO_2 in fish units and create an oxygen demand (Moran 2010a). The studies showed that airlift aerators were not affected by salinity of the water but overall had a poorer CO_2 mass transfer performance compared to cascade aeration (Moran 2010 a, b). Outside of Moran's 2010 work, limited research has been done to review the effectiveness of airlift aerators to degas CO_2.

2.2 Methods

2.2.1 Site Description

The Southeast Commerce Passive Treatment System (SECPTS) was constructed in 2017 to treat artesian-flowing mine drainage at the Tar Creek Superfund Site in Ottawa County, Oklahoma, USA. The Tar Creek Superfund Site covers approximately 100 km^2 located within the

larger Tri-State Lead-Zinc Mining District (TSMD) of Kansas, Oklahoma and Missouri. Between 2006 and 2007, two collapse features at southeast Commerce were filled and capped and the mine drainage was collected subsurface via French drains and discharged into an unnamed tributary of Tar Creek. During construction of SECPTS, the French drain was intercepted, creating two inflow locations on the north (N-in) and South (S-in) sides of the oxidation pond (Figure 2.1). Additional mine drainage upwellings were encountered during the construction of the oxidation pond. These upwellings enter at multiple locations in the floor and inside slopes of the oxidation pond, preventing accurate flow rate measurements entering SECPTS. In October 2018, a well was installed to capture water from the upwellings and water quality data has been collected since. The system consists of an oxidation pond that transitions into a wetland before water flows into a vertical flow bioreactor (VFBR). The water is then piped under a berm and enters a final polishing unit with a central wetland shelf (Figure 2.1). Table 2.1 shows the mean total metals concentrations for the influents and effluent of the SECPTS.

This study focuses on the oxidative unit of the SECPTS. The oxidation pond has floating directional baffle curtains that promote serpentine flow to maximize retention time (Figure 2.1). Supplemental aeration from two solar-powered float-mix aerators is provided to promote more Fe oxidation and retention within the oxidation pond. A 3,180 W solar panel powers a regenerative blower that can provide airflows of more than 50 $m^3 hr^{-1}$. Air is delivered via an airline to the float-mix aerator downtube where the air and water are mixed creating a less dense mixture that rises to the surface and spills across a 1.2-m diameter steel plate (Figure 2.2). The two airlift, or float-mix, aerators are denoted by their position in the oxidation pond:

west float-mix aerator (WFMA) and east float-mix aerator (EFMA). A literature gap exists on the role these novel float-mix aerators (FMAs) can have on increasing DO and Fe retention in oxidation ponds in passive treatment systems. It was hypothesized that the FMAs will increase DO and decrease CO_2 concentrations nearer to the water surface than at depth and that aeration will promote greater Fe retention. This study investigated the effectiveness of the FMAs to increase DO and decrease CO_2 concentrations and to promote iron retention by comparing water quality data when the aerators were off and then when they were on.

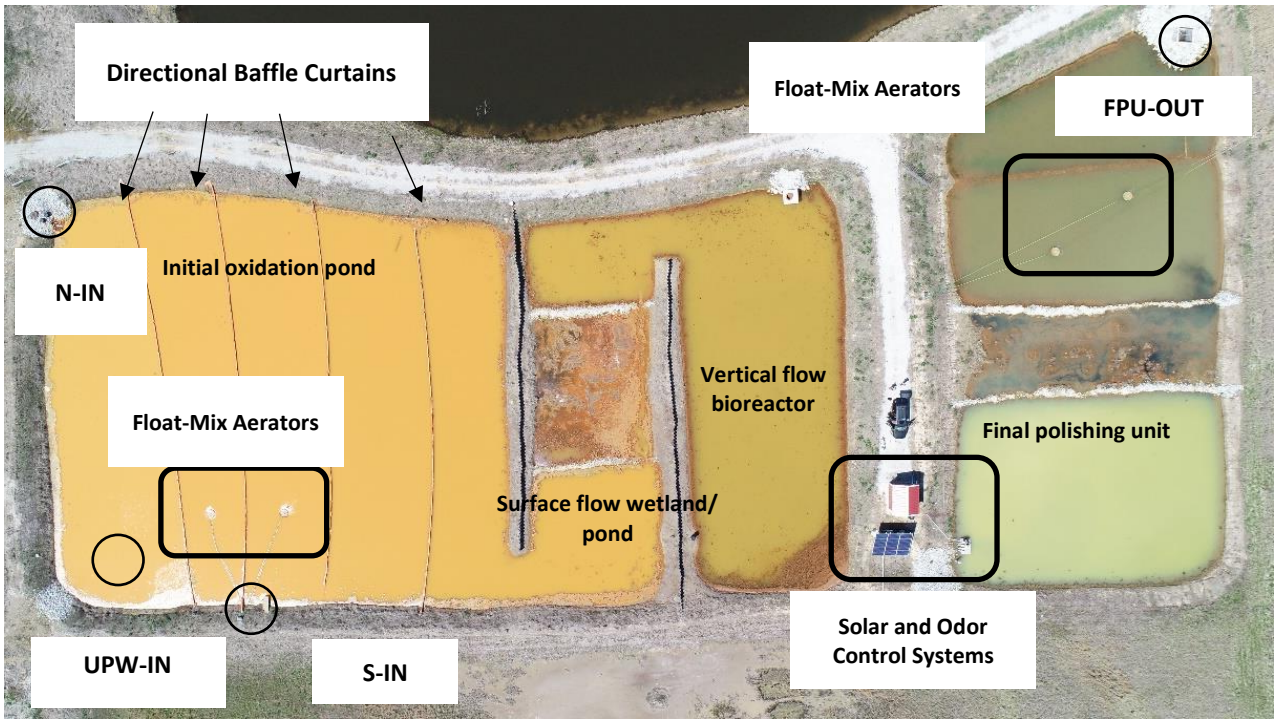

Figure 2.1 Aerial photograph of the SECPTS noting the important process units, inlets and outlets and technology incorporated in each unit

Table 2.1 Mean ± standard deviation total aqueous metal concentrations for the influents and effluent of the Southeast Commerce Passive Treatment System located in Ottawa County, Oklahoma, USA.

Site	Cd (mg/L)	Fe (mg/L)	Pb (mg/L)	Zn (mg/L)
South-IN (n=31, 11/16- 08/19)	0.015 ± 0.008	154± 11.9	0.149 ± 0.091	6.92 ± 0.741
North-IN (n=28, 03/17-08-19)	0.014 ± 0.006	134± 13.347	0.139 ± 0.077	6.75 ± 0.727
Upwelling-IN (n=8, 10/18-08/19)	0.022 ± 0.005	143 ± 28.2	0.274 ± 0.112	7.11 ± 0.642
Effluent (FPU-OUT) (n=31,01/17-08/19)	<PQL*	1.33 ± 0.779	0.024 ± 0.003	0.850 ± 1.90

*26 of 31 samples were below the practical quantification limit (PQL) of 0.00067 mg/L

2.2.2 Water Sample Collection and Analysis

Water samples and in-situ measurements were collected at increasing depths near the west float-mix aerator (WFMA) and east float-mix aerator (EFMA) in the oxidation pond of the SECPTS. Sampling stations were installed near the aerators with a flotation device and a rebar anchor driven into the native soil of the oxidation pond. YSI multiparameter datasondes were deployed at the surface, 0.4 meters, 0.9 meters and 1.4 meters below the water surface and secured to the flotation device located approximately one meter from the aerator. Figure 2.2 shows the sampling location and datasonde deployment setup used at the WFMA and EFMA. The datasondes were programmed to collect in-situ water quality measurements (including pH, temperature, specific conductance and dissolved oxygen) every 15 minutes (Table 2.2).

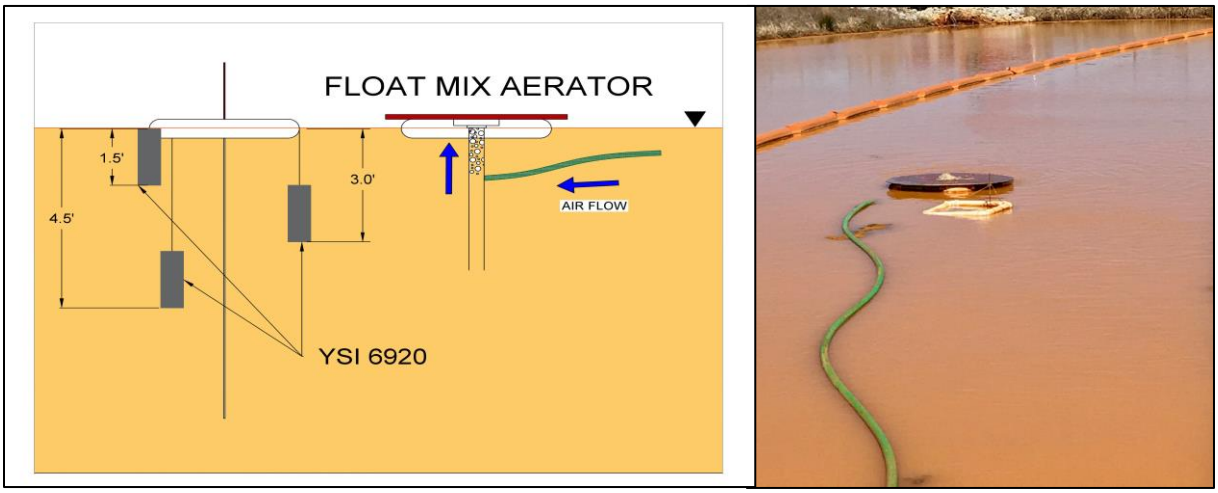

Figure 2.2 (a) Schematic of the experimental setup showing how the YSI datasondes were deployed at increasing depth near each aerator; (b) Image of the experimental setup located next to the aerator with air flowing

Water samples were collected at each site from a canoe using a discrete horizontal sampler commonly used in limnological studies. Grab samples were captured at a given depth in the water column at the same locations where the multiparameter datasondes were deployed: at the surface, 0.5 meters (1.5'), 0.9 meters (3') and 1.4 meters (4.5') below the water surface. Since the oxidation pond is deeper to the west and slopes to the east, the WFMA had YSIs deployed and water samples collected to 1.4 m below the water surface, while the EFMA only had up samples collected to 0.9 m below the water surface. The analyses completed for each grab sample are shown in Table 2.2. Samples were collected starting from the surface, working towards increasingly deeper samples in order to prevent any unnecessary disturbance to the water column. Total alkalinity and turbidity were measured immediately after samples were collected. Total alkalinity was measured via a colorimetric titration (Hach Method 8203)

and therefore turbid samples, where a colorimetric change could not be seen, were filtered with 0.45 μm filters prior to measuring total alkalinity. Turbid samples that fell outside the measuring range of the turbidimeter were diluted with an aliquot of filtered sample in order to lower the turbidity within the measuring range without allowing solids to dissolve into solution.

This sample collection and analysis was performed when the aerators were off (OFF) and then when the aerators were on (ON). The OFF study was performed in 2019 from February 9th to March 17th. During the OFF study, YSI datasondes were not deployed at the surface near the aerators for continuous data collection, and thus the physical parameters were taken only during sampling events. The ON study was performed in 2019 initially from March 18th to April 12th, but was postponed due to sensor fouling and resumed June 18th through July 15th. The hiatus during the ON study was necessary because fouling of the pH and optical DO sensors was noticed, and the sensors had to be replaced. Total suspended solids (TSS) and total and dissolved metal samples were collected during each sampling event for the OFF (February 9th, March 2nd, March 11th, and March 17th) and ON (April 4th, April 12th, June 17th, June 27th, July 2nd and July 15th) studies.

Table 2.2 Water quality parameters, respective units and methods used to assess the performance of the float-mix aerators in the SECPTS in Commerce, OK

	Units	Method/ Instrumentation
Physical Parameters		
Temperature	°C	YSI 6920 V2 Multiparameter Datasonde
Specific Conductance	mS/cm	
Conductivity	µS/cm	
Resistivity	Ohm-cm	
Total Dissolved Solids	g/L	
Salinity	ppt	
DO Saturation (DOsat)	%	
DO Concentration	mg/L	
pH	s.u., mV	
Oxidation Reduction Potential	mV	
Total Suspended Solids	mg/L	USEPA 160.2
Total Metals	mg/L	USEPA 3015a and 6010c
Dissolved Metals	mg/L	USEPA 3015a and 6010c
Alkalinity	mg/L as $CaCO_3$	Hach Method 8203
Turbidity	NTU	Hach 2100P Turbidimeter

2.2.3 Weather Data Collection

In order to determine the possible effect wind can have on oxygen entrainment in the water and therefore the DO concentrations at the surface of the water column, wind data were collected. A HOBO U30 USB Weather Station was deployed near the northwest corner of the SECPTS oxidation pond. This weather station recorded temperature, relative humidity, wind speed and wind direction data every 15 minutes. It should be noted that the weather station was not deployed adjoining the FMAs because the weather station needed to be deployed on level ground and be located far enough away from a wind break. Due to the presence of a building to the southwest of the system and the steep slope of the berm surrounding the oxidation pond, the northwest corner of the oxidation pond berm was determined to be the

best location. Figure 2.3 shows the weather station set up on the northwestern corner of the oxidation pond berm.

Figure 2.3 HOBO U30 USB Weather Station deployed near northwestern corner of oxidation pond to collect wind data

2.2.4 pCO_2 Calculation

Partial pressure of carbon dioxide (pCO_2) was calculated using the Henderson Hasselbalch equation for the carbonate species and the Arrhenius equation to correct the equilibrium constant for temperature (Jensen, 2003). Equations and definitions of all variables can be found in Chapter 1.

For these calculations, DO and pH measurements were represented by continuous data collected every 15 minutes throughout the study. Alkalinity was measured during each sampling event. Since the alkalinity data set was not continuous, the mean alkalinity between two sampling events was used to calculate pCO_2 values. Sampling events were anywhere from one to two weeks apart.

2.3 Results and Discussion

2.3.1 Dissolved Oxygen and Carbon Dioxide

Box and whisker plots representing DO, alkalinity, dissolved CO_2 partial pressure (pCO_2) and pH data collected from deployed YSIs and sampling events are shown in Figures 2.5-2.12. The box and whisker plot setup in shown in Figure 2.4. The lack of continuous data at these locations resulted in a sample size of n=3 each for the water surface (WFMA-S and EFMA-S), which limited the statistical power of these datasets. Due to the fouled sensors, data from the deployed YSI datasondes from March 18th until April 12th were removed from the WFMA-0.4 m and WFMA-0.9 m data set. The pH sensor began to foul during the OFF study for the WFMA-0.9 m deployment resulting in erroneously high pH measurements and low calculated dissolved CO_2 pressures. Therefore, the range of pH values from all the other datasets was used to determine which data to discard. pH values lower than 5.45 and greater than 6.57 were discarded from the WFMA-0.9 OFF dataset and the corresponding pCO_2 calculated from pH values outside of that range were discarded. This was meant to protect the integrity of the

analysis between the aerator off and on studies and ensure that erroneous data did not skew the analysis.

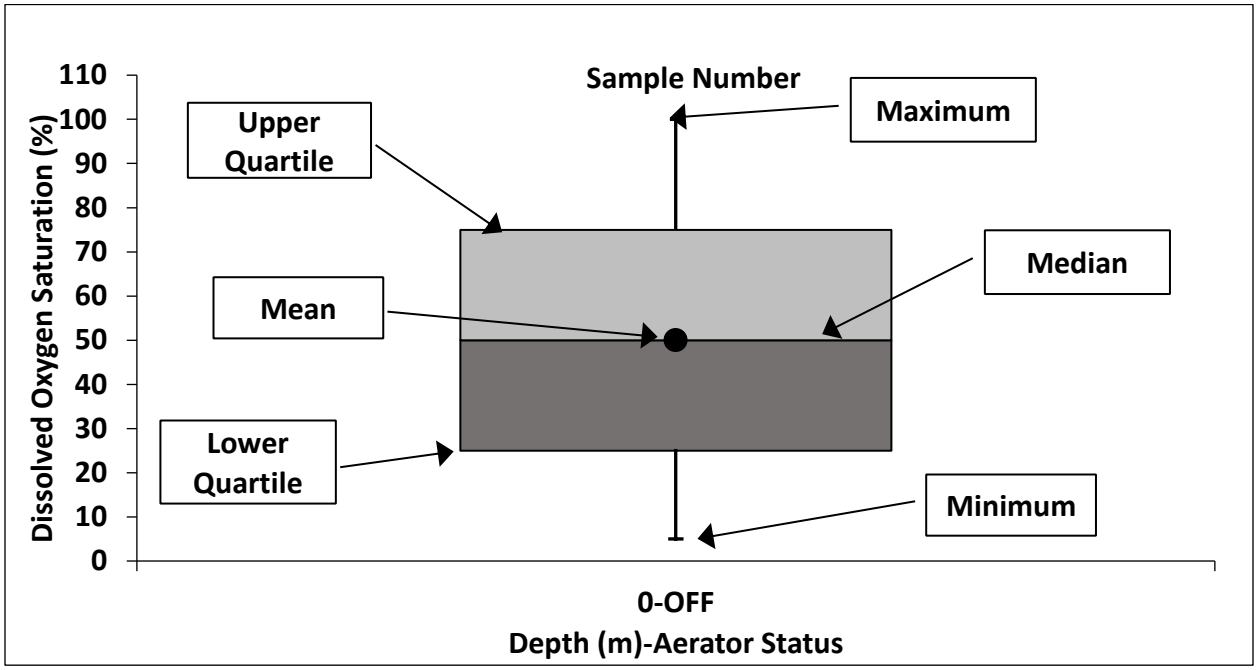

Figure 2.4 Layout of box and whisker plots used to display the data collected during each study.

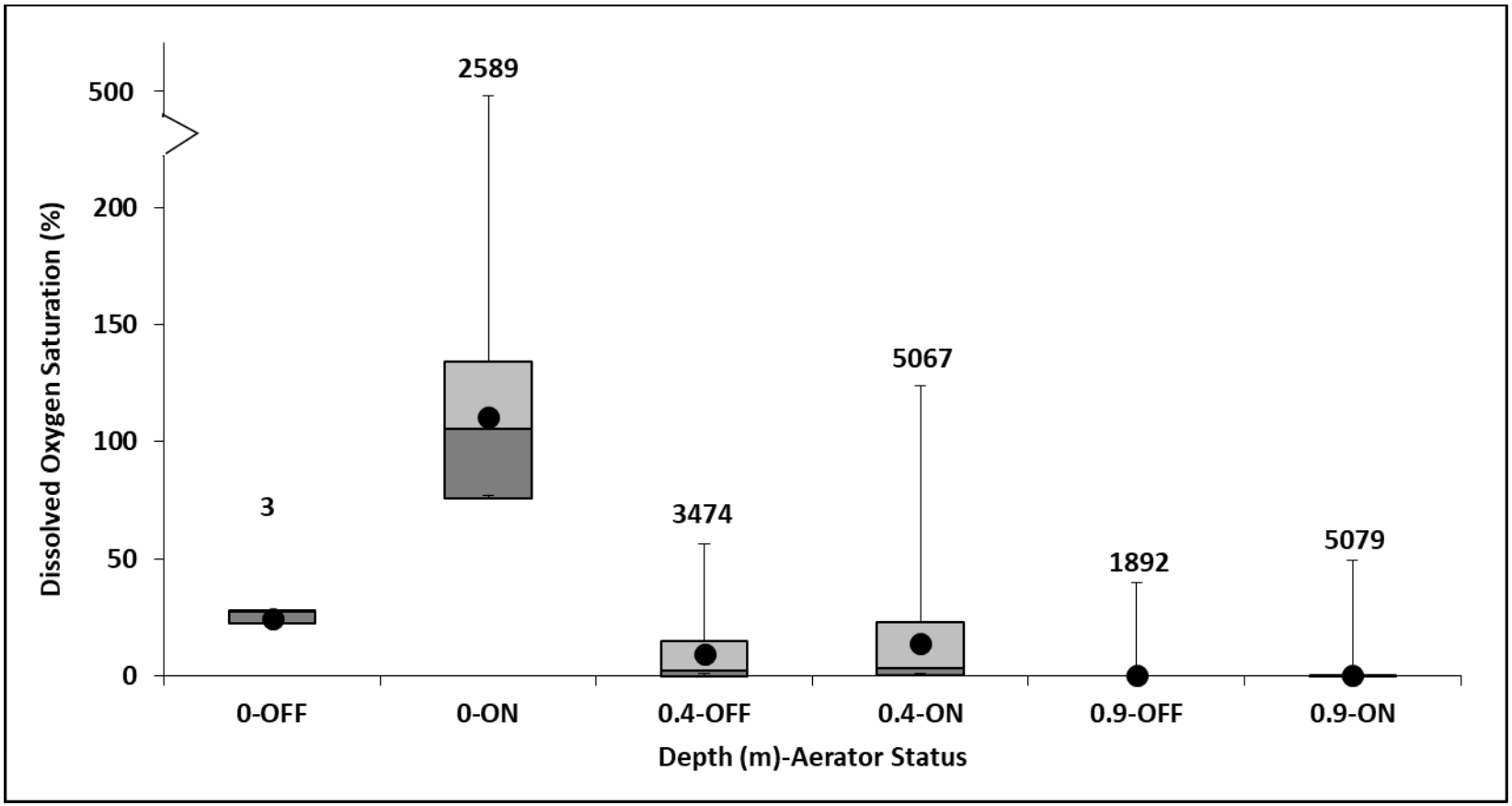

Figure 2.5 Box and whisker plot of dissolved oxygen saturation readings collected at each depth for the ON and OFF studies at the east float-mix aerator (EFMA). The points represent the mean value for each data set and the numbers above the plot represent *n*, the sample size for each data set.

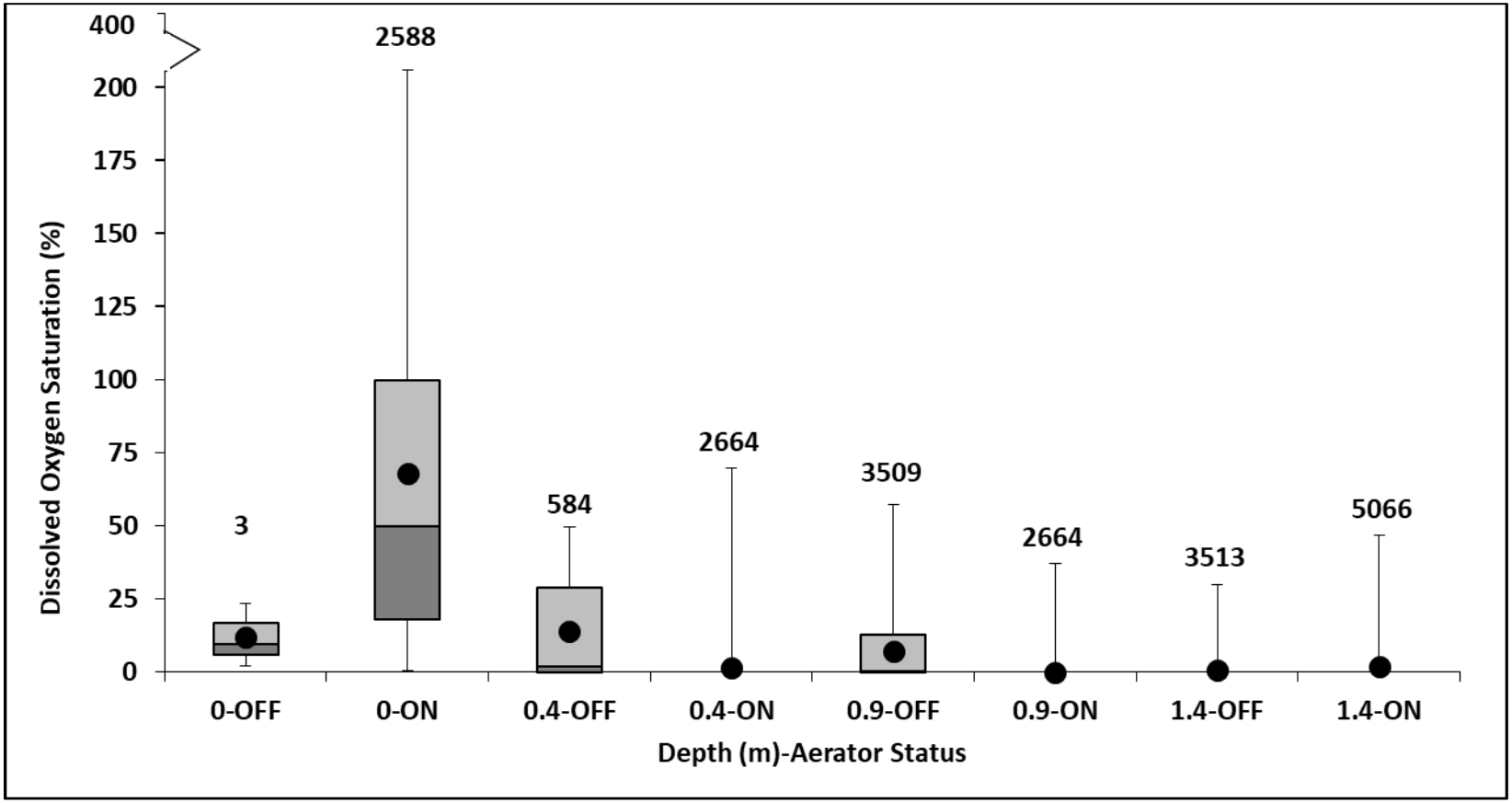

Figure 2.6 Box and whisker plot of dissolved oxygen saturation readings collected at each depth for the ON and OFF studies at the west float-mix aerator (WFMA). The points represent the mean value for each data set and the numbers above the plot represent *n*, the sample size for each data set.

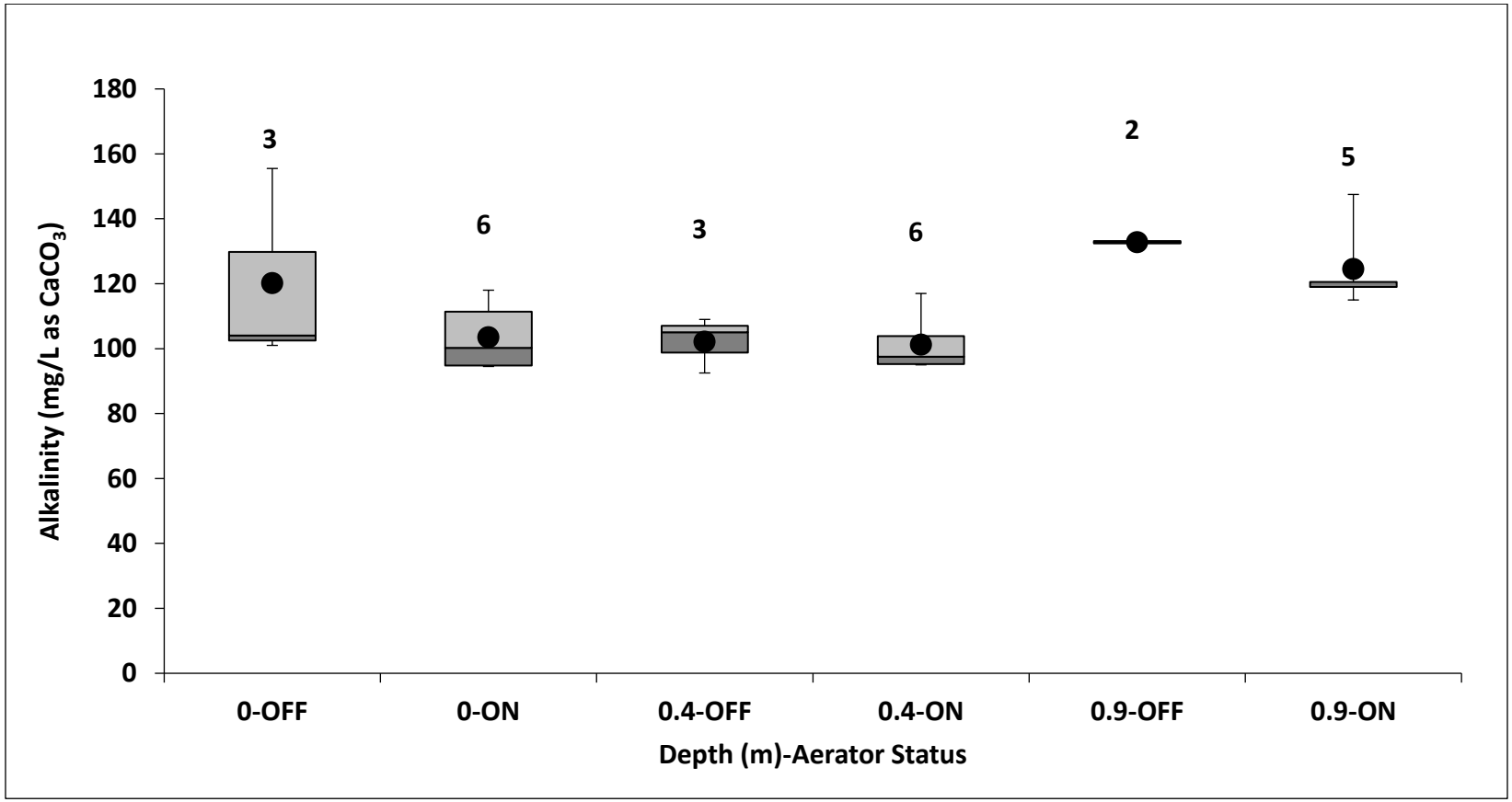

Figure 2.7 Box and whisker plot of total alkalinity measurements collected at each depth for the ON and OFF studies at the east float-mix aerator (EFMA). The points represent the mean value for each data set and the numbers above the plot represent *n*, the sample size for each data set.

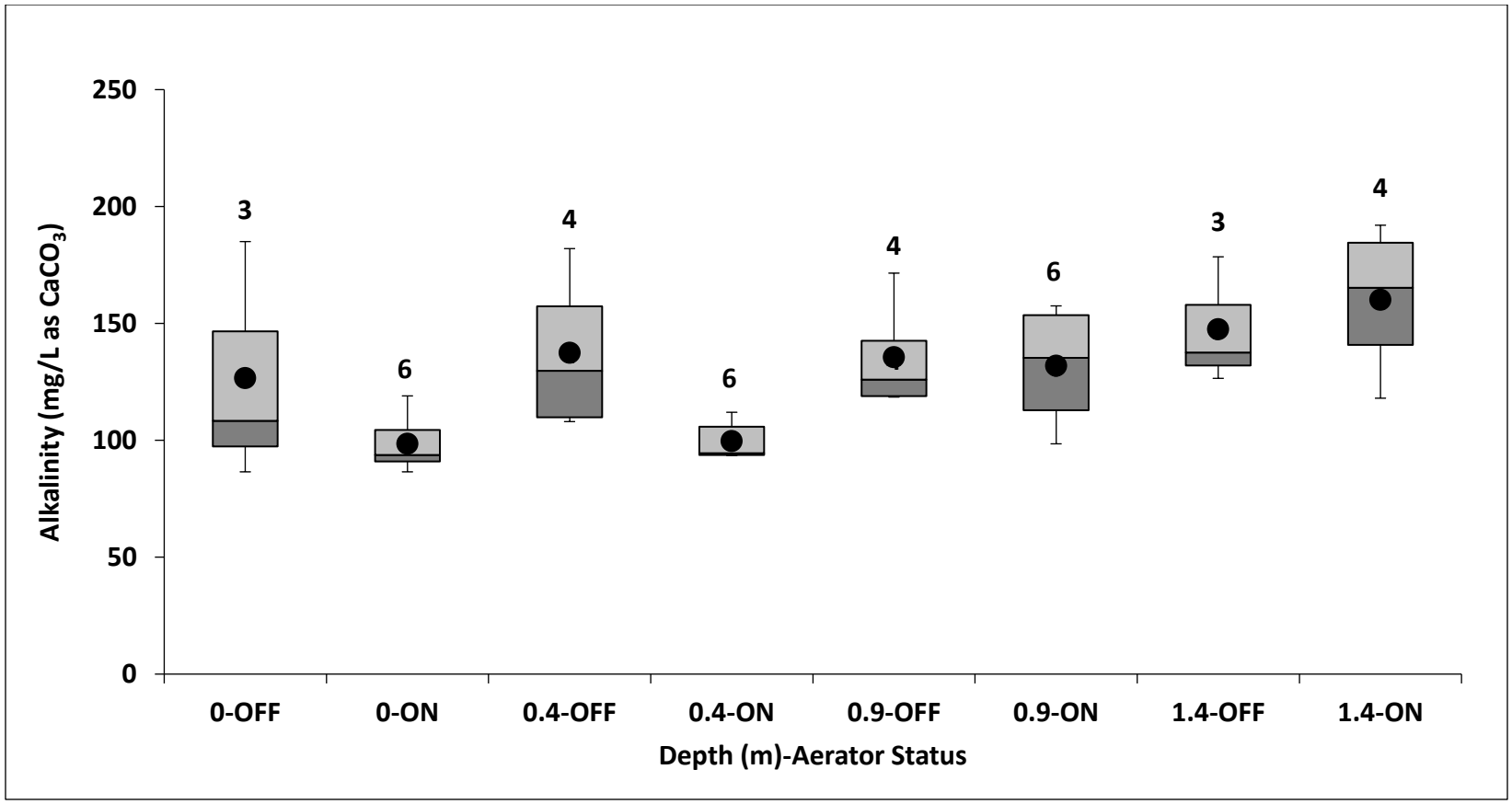

Figure 2.8 Box and whisker plot of total alkalinity measurements collected at each depth for the ON and OFF studies at the west float-mix aerator (WFMA). The points represent the mean value for each data set and the numbers above the plot represent *n*, the sample size for each data set.

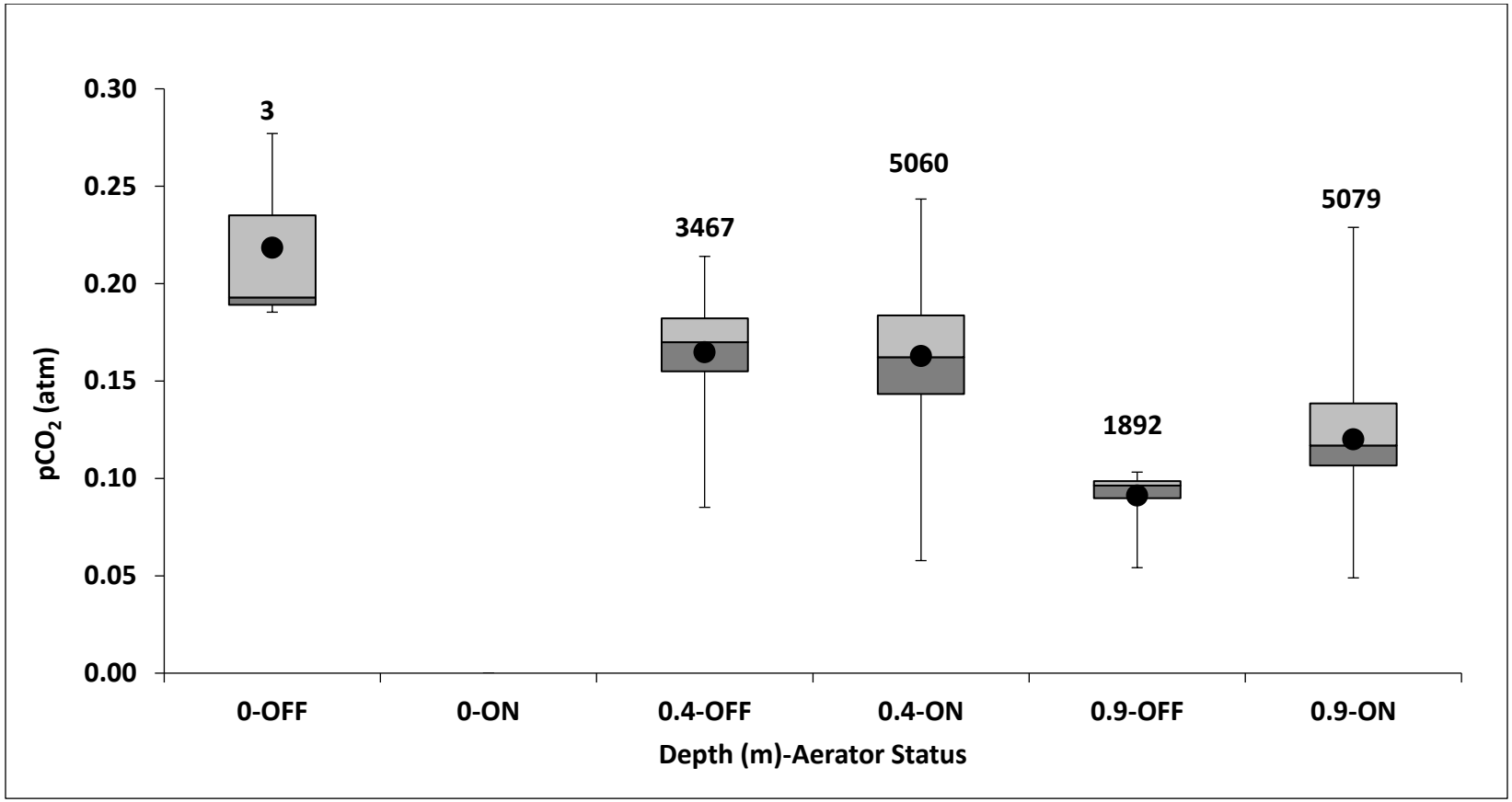

Figure 2.9 Box and whisker plot of calculated dissolved carbon dioxide partial pressures at each depth for the ON and OFF studies at the east float-mix aerator (EFMA). The points represent the mean value for each data set and the numbers above the plot represent *n*, the sample size for each data set. No pH data were collected at the surface EFMA location during the ON study and thus pCO_2 values couldn't be calculated.

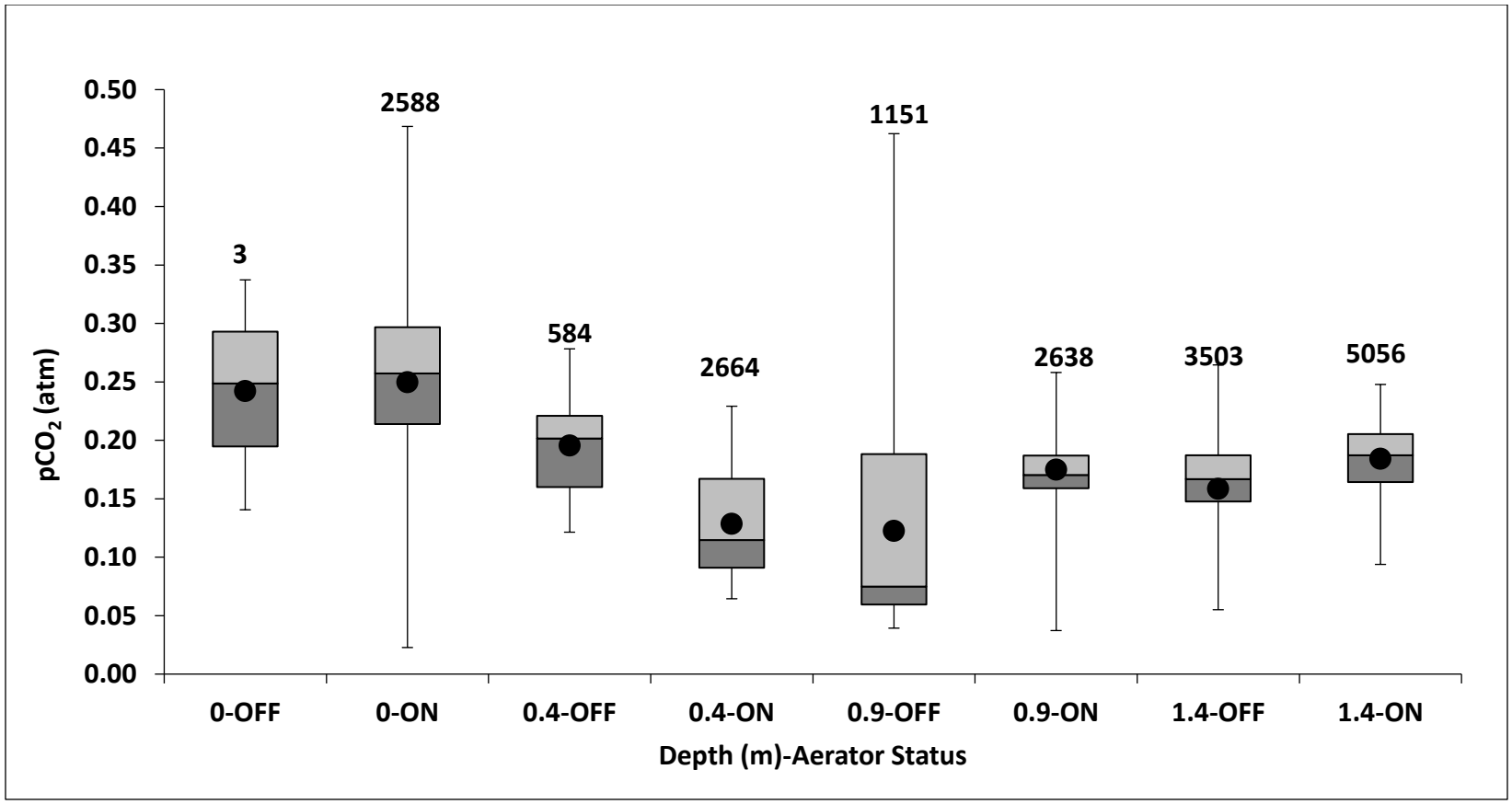

Figure 2.10 Box and whisker plot of calculated dissolved carbon dioxide partial pressures at each depth for the ON and OFF studies at the west float-mix aerator (WFMA). The points represent the mean value for each data set and the numbers above the plot represent *n*, the sample size for each data set.

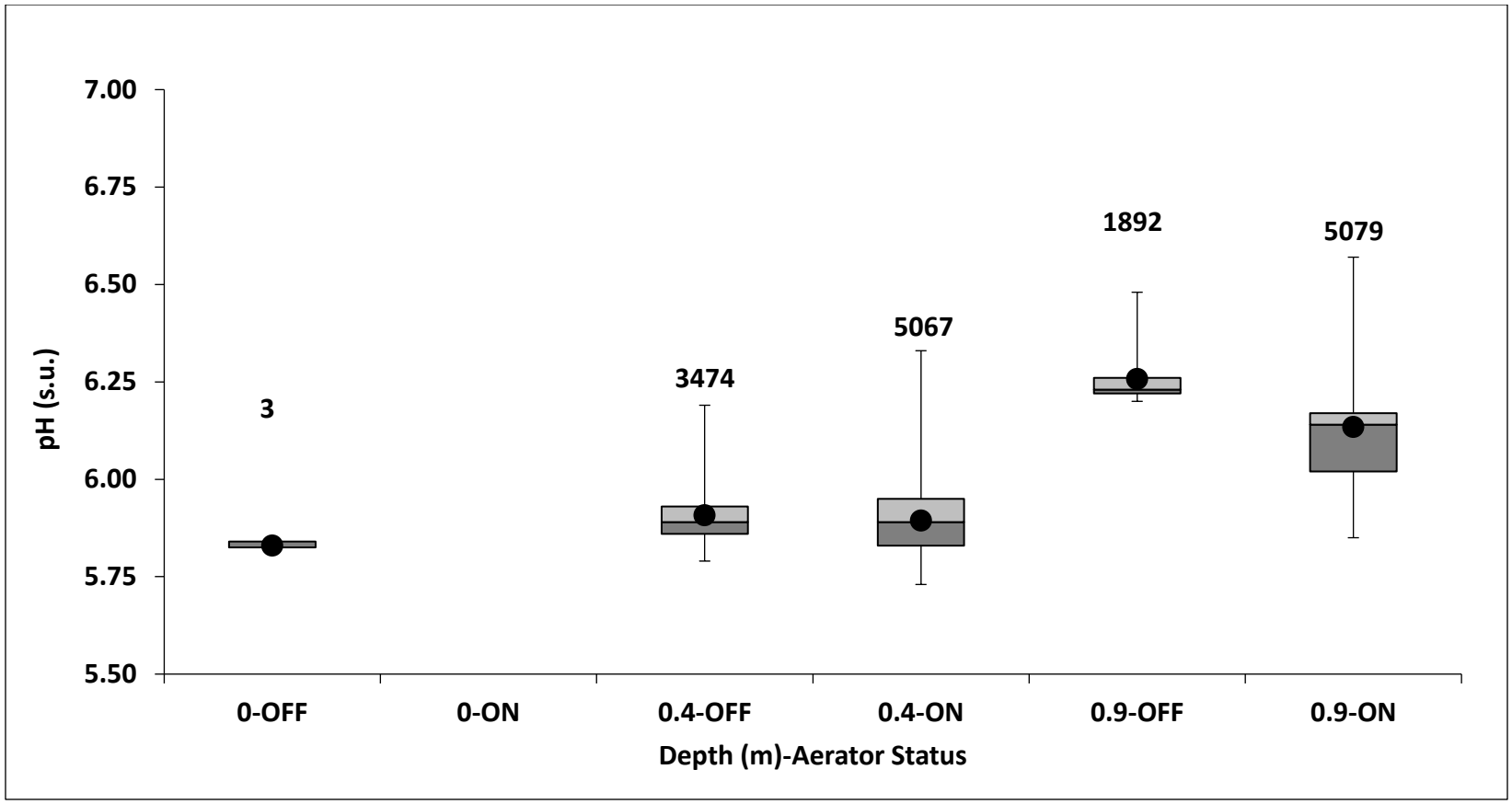

Figure 2.11 Box and whisker plot of pH readings at each depth for the ON and OFF studies at the east float-mix aerator (EFMA). The points represent the mean value for each data set and the numbers above the plot represent *n*, the sample size for each data set. No pH data were collected at the surface EFMA location during the ON study.

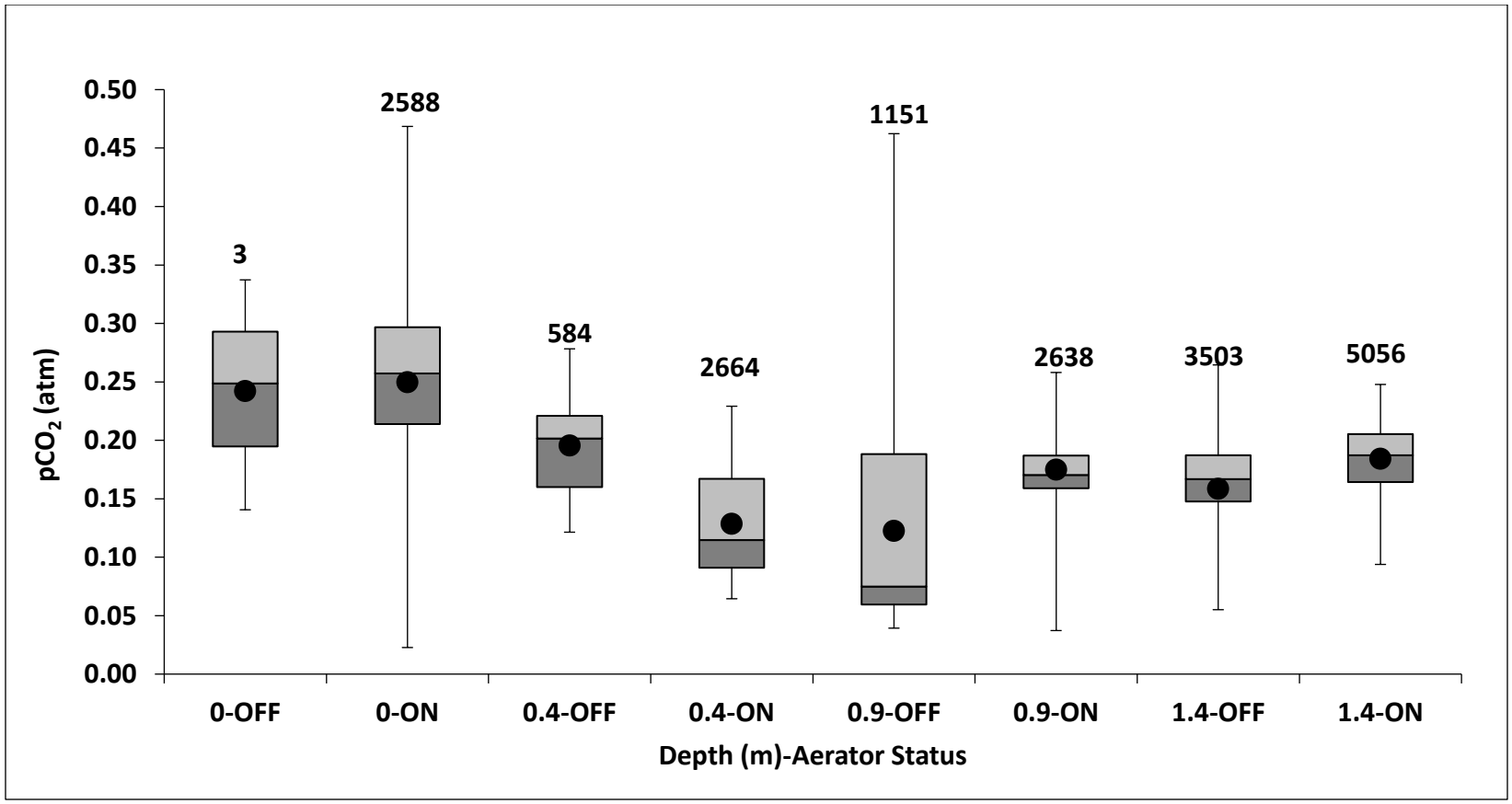

Figure 2.12 Box and whisker plot of pH readings at each depth for the ON and OFF studies at the west float-mix aerator (WFMA). The points represent the mean value for each data set and the numbers above the plot represent *n*, the sample size for each data set.

Analysis of the data showed they were not normally distributed and thus non-parametric statistical analyses were conducted. A Mann Whitney U- test and Mood's median test were performed at each depth to determine if DO saturation, pH and pCO_2 were significantly different when the aerators were on compared to when the aerators were off. The Mann Whitney U-test examines the hypothesis that the samples originate from the same distribution while the Mood's median test examines the null hypothesis that the medians of the populations are the same. A summary of the p-values found from each statistical analysis is shown in Table 2.3 and 2.4. Figures 2.12-2.14 show median values for DO saturation, pCO_2 and pH for each sampling location with the aerators on and off. Based on these analyses, the hypothesis that aerators will increase DO saturation and pH while decreasing pCO_2 concentrations nearer to the water surface than at depth was partially accepted. The performance seen nearer to the surface is likely because the aerators discharge oxygen enriched water at the surface limiting mixing and oxygenation at deeper depths.

Table 2.3 Resulting p-values from a Mann-Whitney U-test comparing dissolved oxygen saturation (DO %Sat), carbon dioxide partial pressure (pCO_2) and pH at each depth when aerators were on and then off.

Independent Samples- Mann Whitney U-Test			
Site	**DO Saturation**	**pCO_2**	**pH**
WFMA-0	0.067	0.982	0.096
WFMA-0.4	<0.001	<0.001	<0.001
WFMA-0.9	<0.001	<0.001	<0.001
WFMA-1.4	<0.001	<0.001	<0.001
EFMA-0	0.003	—[a]	—[a]
EFMA-0.4	<0.001	<0.001	<0.001
EFMA-0.9	<0.001	<0.001	<0.001

[a] Values were not used for statistical tests due to limited data

Table 2.4 Resulting p-values from a Mood's median test comparing dissolved oxygen saturation (DO %Sat), carbon dioxide partial pressure (pCO_2) and pH at each depth when aerators were on and then off.

Independent Samples- Mood's Median Test			
Site	**DO Saturation**	**pCO_2**	**pH**
WFMA-0	0.248	0.999	0.243
WFMA-0.4	<0.001	<0.001	<0.001
WFMA-0.9	<0.001	<0.001	<0.001
WFMA-1.4	<0.001	<0.001	<0.001
EFMA-0	N/A	—[a]	—[a]
EFMA-0.4	0.061	0.002	<0.001
EFMA-0.9	<0.001	<0.001	<0.001

[b] Values were not used for statistical tests due to limited data

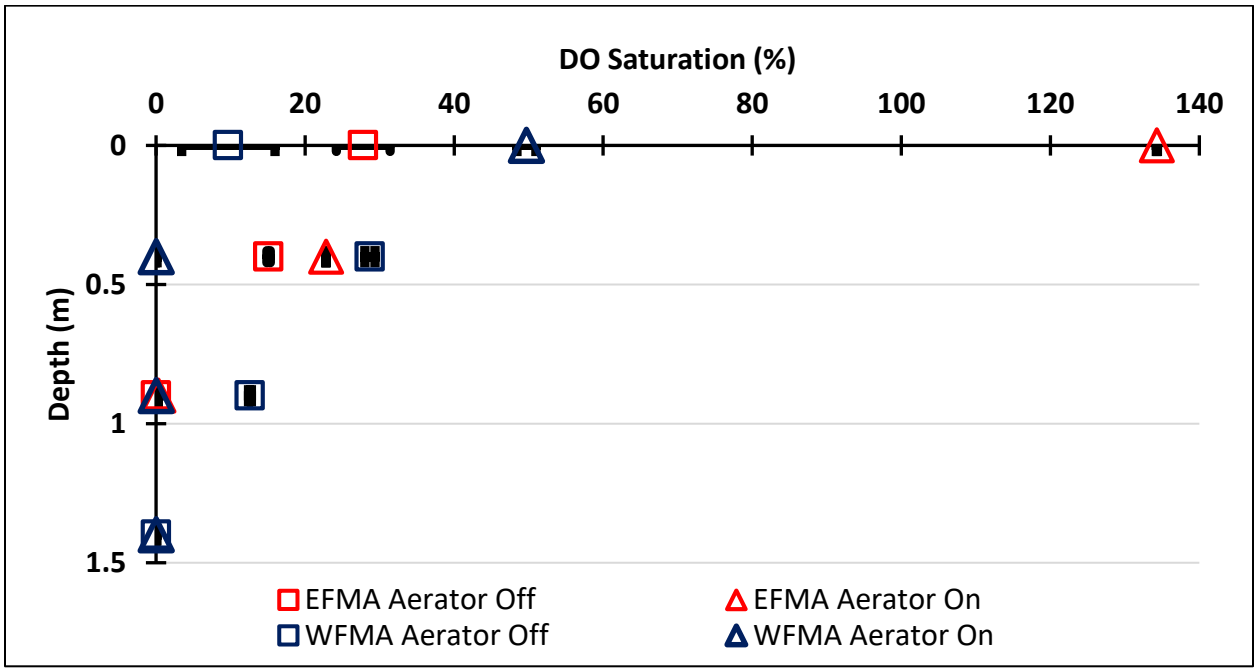

Figure 2.13 Median dissolved oxygen saturation (%) data with standard error bars for each sampling location for the ON and OFF studies. Standard error bars may be smaller than the data point.

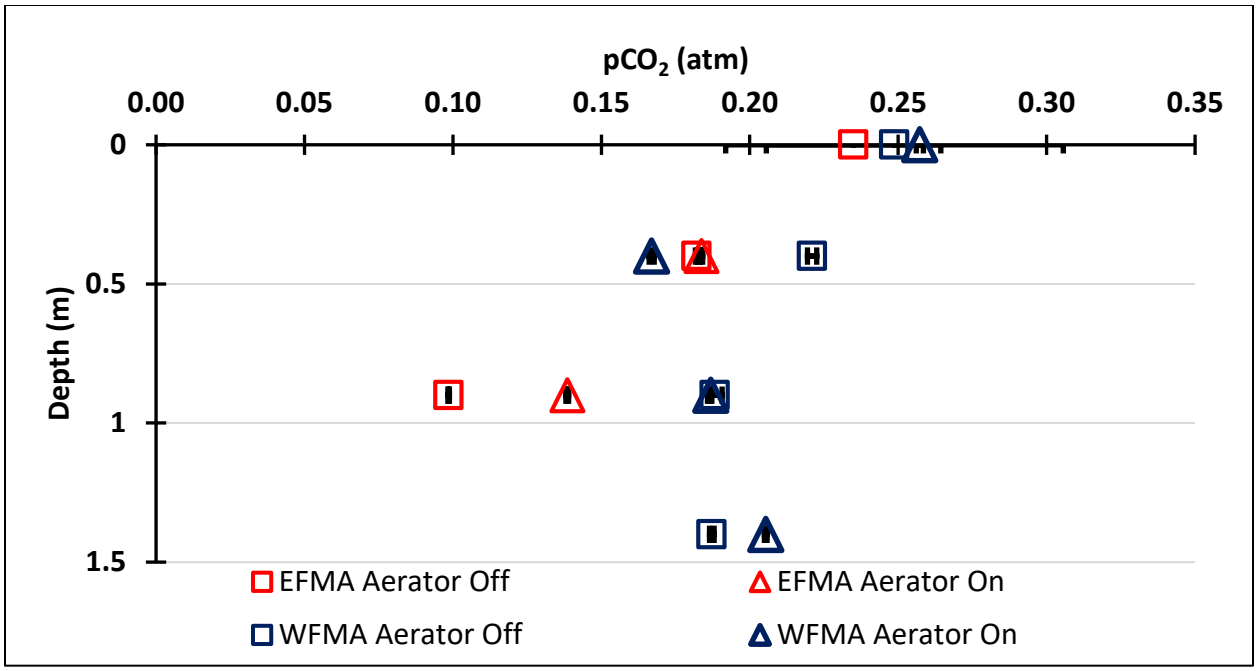

Figure 2.14 Median carbon dioxide partial pressures (pCO_2) data with standard error bars for each sampling location for the ON and OFF studies. Standard error bars may be smaller than the data point.

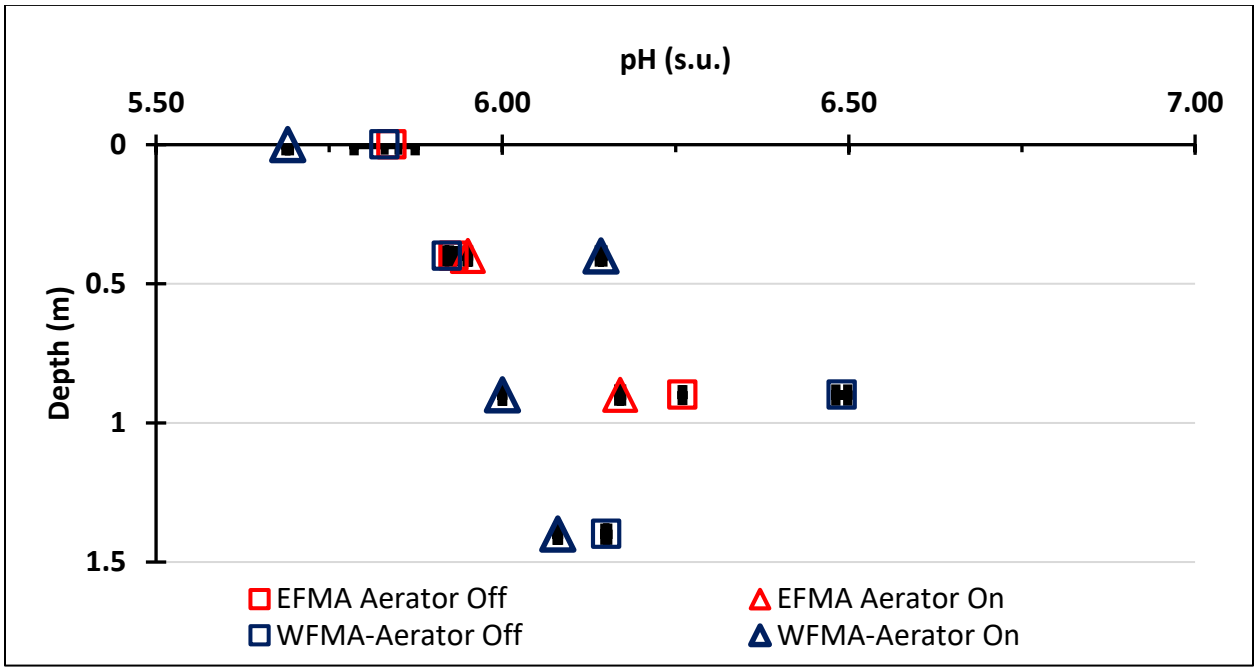

Figure 2.15 Median pH data with standard error bars for each sampling location for the ON and OFF studies. Standard error bars may be smaller than the data point.

DO, pCO_2 and pH data from most of the sampling depths showed a significant difference ($p<0.05$) when the aerators were on compared to when the aerators were off. Wind speed data were compared to DO saturation for both surface datasets for the WFMA and EFMA. Yu et al. (1984) performed field experiments and found that below a threshold wind speed of 2-4 m/s, there was no significant wind effect on the reaeration coefficient. However, there was a significant relationship between wind speeds and the reaeration coefficient at wind speeds faster than 4 m/s (Yu et al. 1984). Therefore, wind speeds greater than 4 m/s were compared to DO saturation measurements measured at the same time step to determine if wind affects surficial DO concentrations (Figure 2.16). The lack of correlation between wind speed and DO saturation at the WFMA-S and EFMA-S locations may be due to the wind break effect of the berm surrounding the oxidation pond. These data show that since there is no correlation between wind speed and DO saturation at the WFMA-S and EFMA-S locations, the difference in DO is due to aeration provided by the aerators and not from the wind.

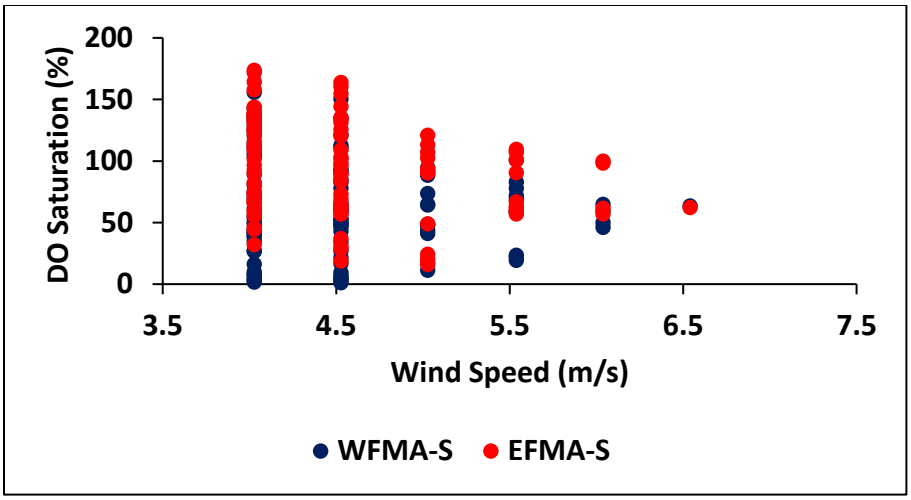

Figure 2.16 Comparison of wind speed (m/s) collected from the deployed HOBO Weather Station to dissolved oxygen (DO) saturation (%) measurements collected at the surface near the west float-mix aerator (WFMA) and the east float-mix aerator (EFMA).

WFMA-0.4m and WFMA-0.9m had a greater median DO saturation when the aerator was off rather than when the aerator was on, opposite of what was predicted. This result may be due to the influence of the nearby upwelling discharging most of the mine drainage that enters the system with a low DO content that negates the added oxygen provided by the aerator. Table 2.5 shows the average water quality data collected from the UPW-IN location since October 2018. The upwellings located in the bottom of the oxidation pond provide approximately 80% of the system's flow, with an average DO saturation of 42%, pH of 5.87 and pCO_2 of 0.532 atm. The low pH and elevated pCO_2 of the upwelling influent may also be why there was not a large decrease in pCO_2 and increase in pH for the WFMA-0.9m and WFMA-1.4m. It should be noted however, that in all cases, the pCO_2 at each depth were lower than the influent pCO_2 of the upwelling. The CO_2 readily degasses as it becomes open to the atmosphere as shown in Figure 2.17.

Table 2.5 Water quality data for the upwelling located in the oxidation pond of the Southeast Commerce Passive Treatment System in Oklahoma, USA.

	Specific Conductivity (mS/cm)	DO Saturation (%)	pH	Total Alkalinity (mg/L CaCO3)	pCO_2 (atm)
n	12	12	11	12	11
Mean	3.264	42.5	5.87	321	0.532
Median	3.311	47.9	5.87	321	0.546
Std. Deviation	0.156	13.1	0.08	8.1	0.095
Minimum	2.916	12.3	5.75	309	0.398
Maximum	3.410	56.6	5.98	333	0.712

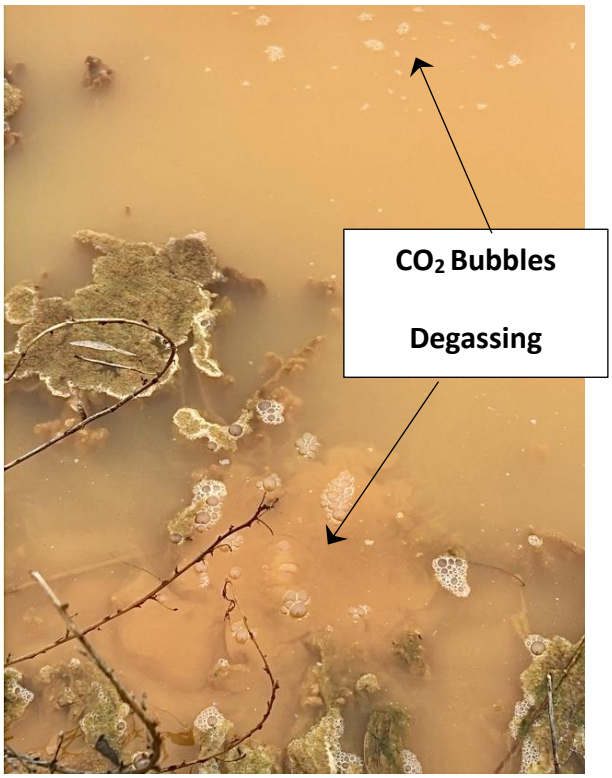

Figure 2.17 Carbon dioxide from the upwelling in the oxidation pond of the Southeast Commerce Passive Treatment system degassing upon exposure to the atmosphere

Comparison of EFMA-0.9m shows that the aerator has limited effect with increasing depth. However, at depths shallower than 0.4 m, the aerators increase DO, degas CO_2 and raise pH. The relationships between DO saturation, pCO_2 and pH are shown in Figures 2.18– 2.20 using data from EFMA-0.4m. The EFMA-0.4m location was chosen to model the relationship because it is minimally affected by surficial interactions and the upwelling. These data show that increasing DO raises the pH (Figure 2.18) because an increase in DO degasses more CO_2 (Figure 2.19) and the degassing of CO_2 raises the pH (Figure 2.20). This correlation further supports the role aeration plays to degas CO_2 and raise pH by shifting the carbonate chemistry.

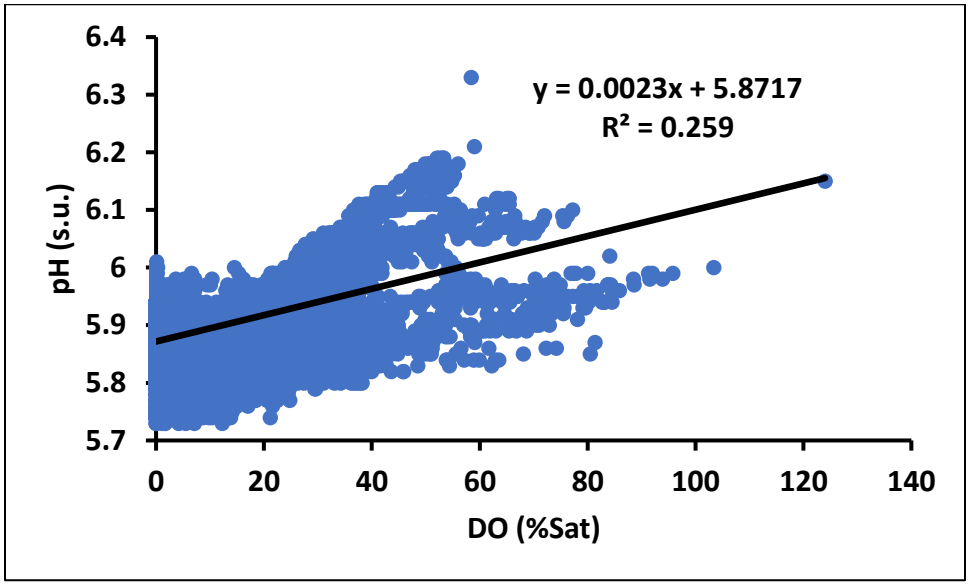

Figure 2.18 Direct positive relationship between dissolved oxygen saturation and pH showcased from data collected at EFMA-0.4m.

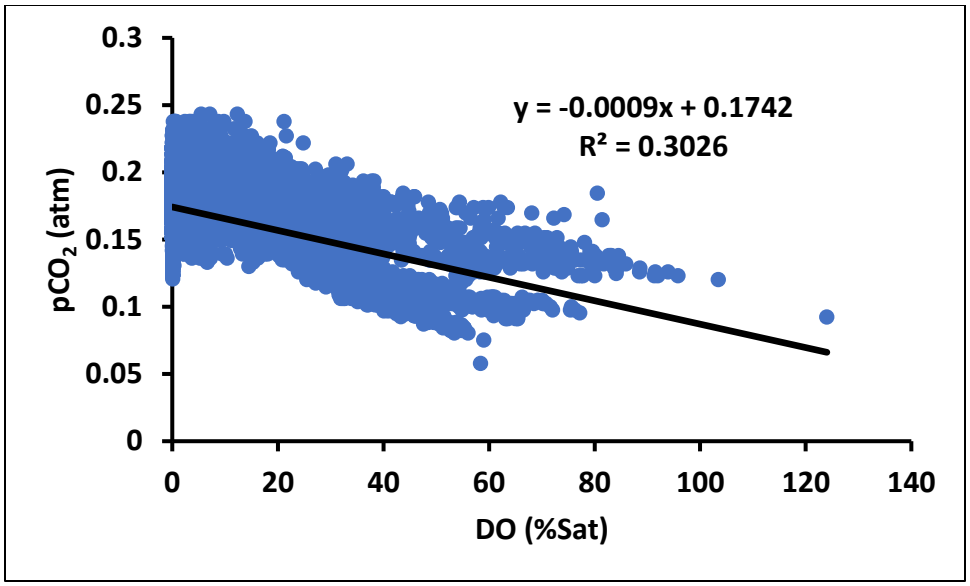

Figure 2.19 Inverse relationship between dissolved oxygen saturation and carbon dioxide partial pressure showcased by data collected at EFMA-0.4m.

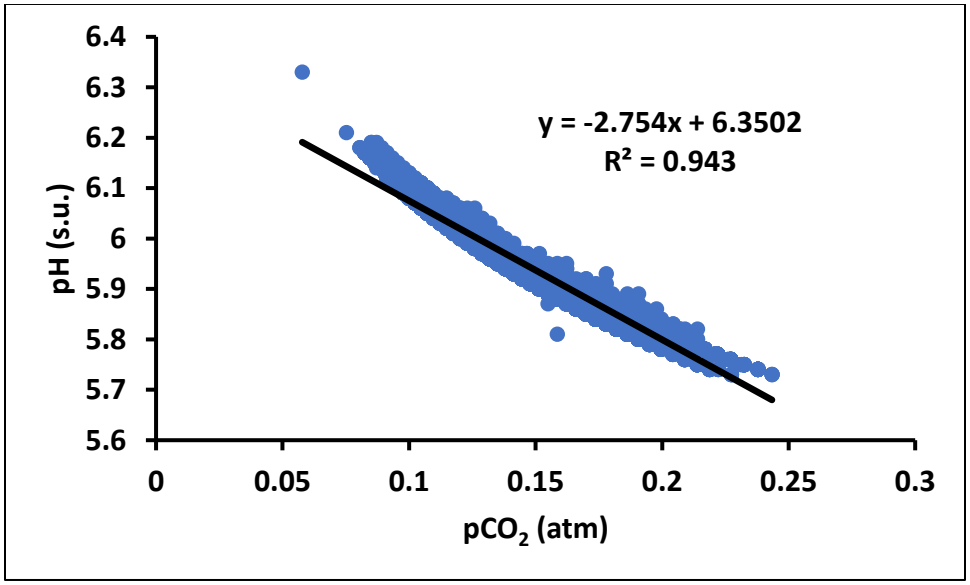

Figure 2.20 Inverse relationship between carbon dioxide partial pressure and pH showcased by data collected at EFMA-0.4m.

2.3.2 Iron Retention

Figures 2.21-2.26 show box and whisker plots representing TSS, total Fe, dissolved Fe and particulate Fe concentration data collected during these sampling events. There was minimal difference in total Fe concentrations at each depth between the OFF and ON studies (Figures 2.21 and 2.22). Similarly, particulate Fe concentrations (estimated as the difference between total and dissolved Fe concentrations) showed minimal difference between ON and OFF studies for each depth (Figures 2.25 and 2.26). To further analyze the relationship between total and particulate Fe, the ratio of particulate Fe to total Fe was calculated as a percent and compared for ON and OFF at each depth (Table 2.6).

There was a substantial difference in percentage of Fe in particulate form at the surface of the west aerator between ON and OFF, and a significant difference at a depth of 0.4 m near the west aerator ($p=0.016$). However, the east aerator showed minimal difference in the percentage of Fe in particulate form between ON and OFF at all depths. It is hypothesized that the inconsistency between the east and west aerators may be because as the water travels from the N-IN and upwelling inlets, the Fe is oxidized by the air provided by the WFMA and passive diffusion and begins to settle by the time the Fe reaches the EFMA location. The EFMA is also located in a shallower part of the pond and thus settling of particulate Fe may be more apparent than in the deeper part of the oxidation pond near where the WFMA is located. The particulate Fe concentrations at the east and west aerator support this hypothesis, where particulate Fe is approximately three times greater for the east aerator than the west aerator at the 0.9 m depth (Figures 2.25 and 2.26). More research needs to be performed analyzing Fe

transport within the pond and the removal mechanisms that dominate in each section of the pond. This could allow the FMAs to be deployed strategically to increase Fe oxidation and maximize time for Fe settling.

There were lesser concentrations of dissolved Fe when the aerators were on compared to when the aerators were off, except for the 0.9 m and 1.4 m depths at the west aerator. This result is likely because more oxygen is added to the water column allowing for more dissolved Fe (II) to be oxidized to Fe (III) and precipitated as Fe oxide and hydroxide species when the aerators are on. The deeper west aerator locations, 0.9 m and 1.4 m below the surface, were affected more by the nearby upwelling, which discharges approximately 82% of the raw mine drainage treated by the PTS with an average Fe loading of 94 kg d^{-1}. The magnitude of mine drainage with low DO and elevated dissolved Fe (II) concentrations that comes from the upwelling seemingly increases the dissolved Fe concentrations at those depths.

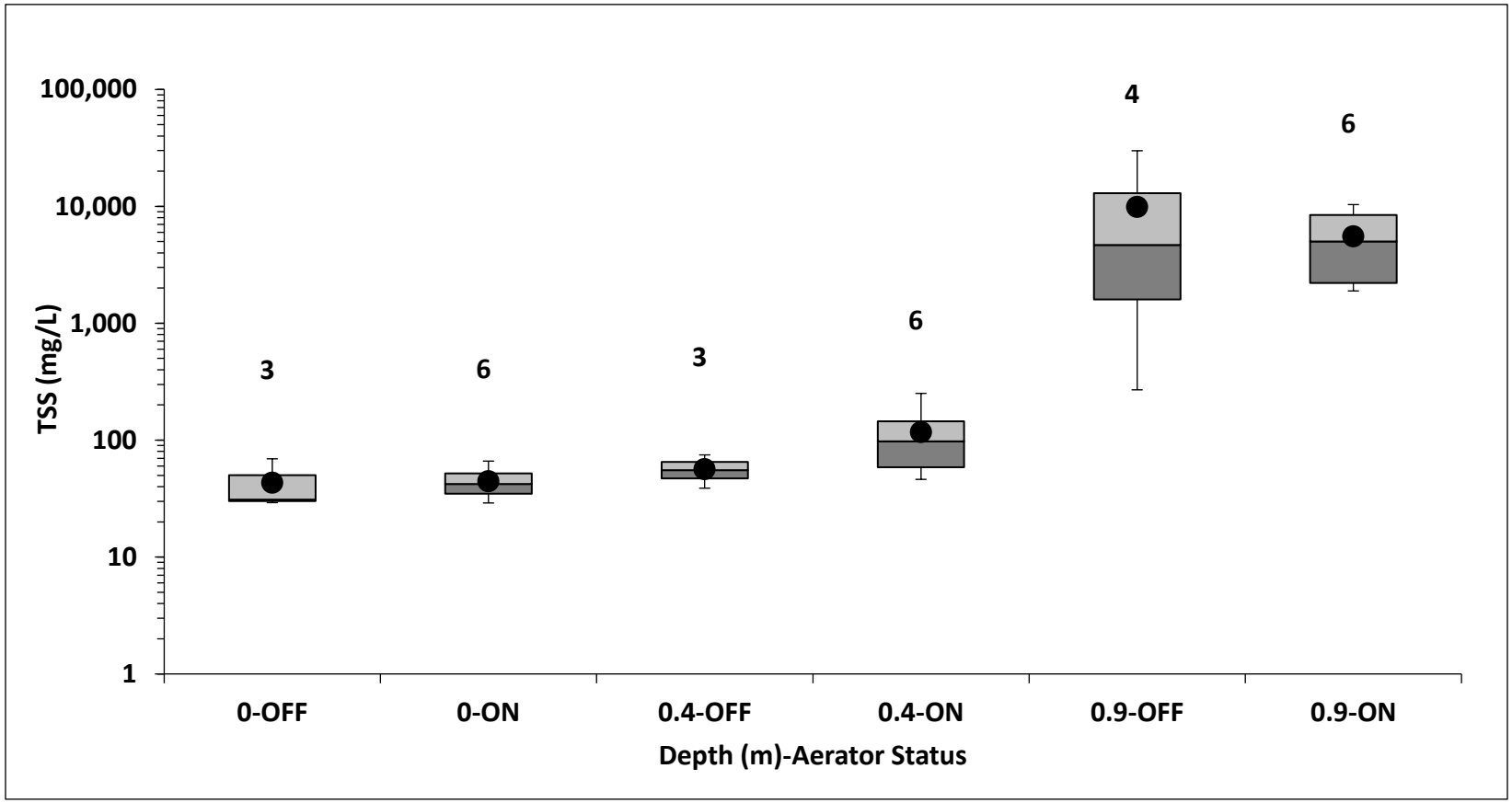

Figure 2.21 Box and whisker plot of TSS concentrations at each depth for the ON and OFF studies at the east float-mix aerator (EFMA). The points represent the mean value for each data set and the numbers above the plot represent *n*, the sample size for each data set. Note that the y-axis is logarithmic.

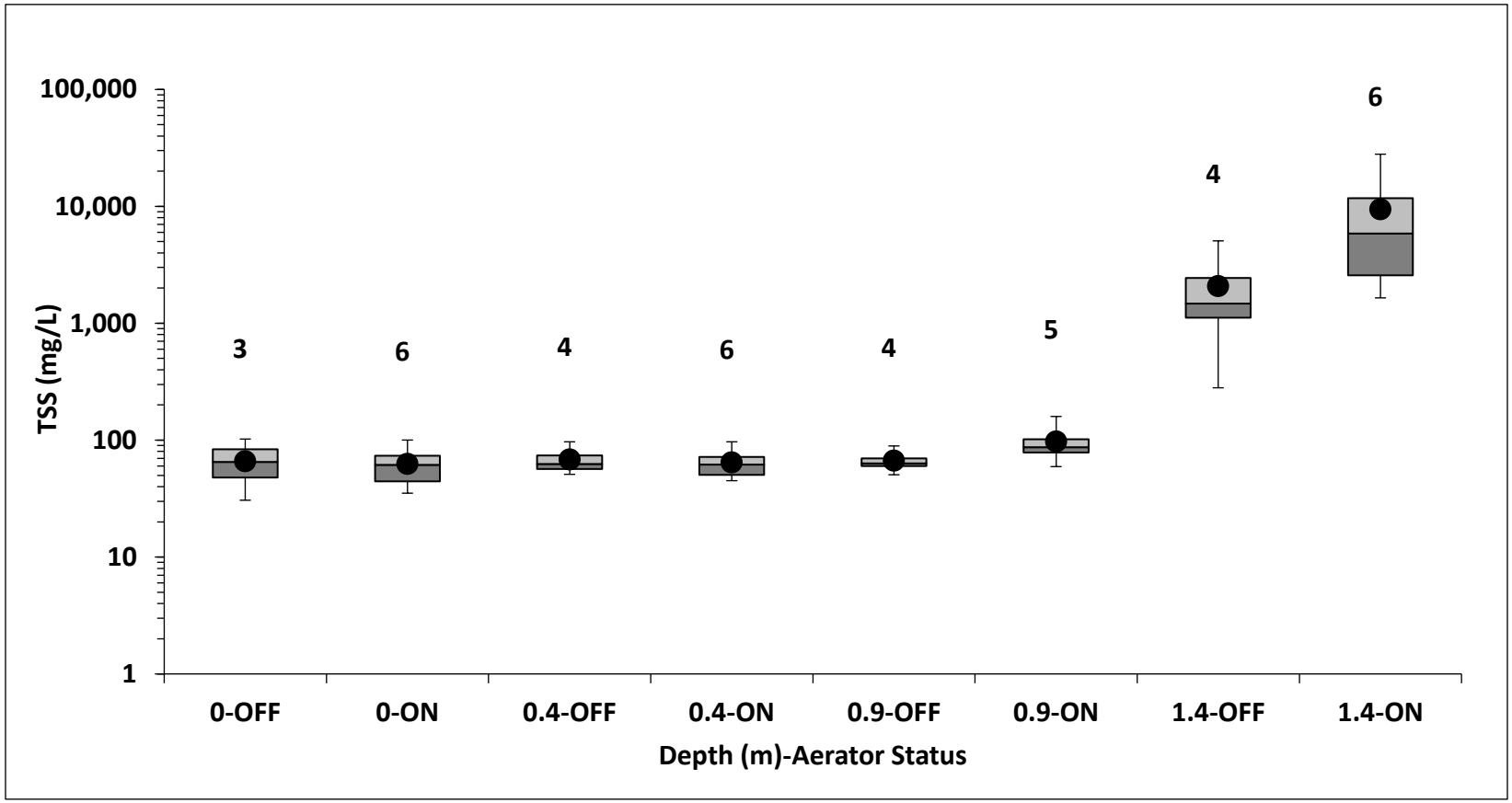

Figure 2.22 Box and whisker plot of TSS concentrations at each depth for the ON and OFF studies at the west float-mix aerator (WFMA). The points represent the mean value for each data set and the numbers above the plot represent *n*, the sample size for each data set. Note that the y-axis is logarithmic.

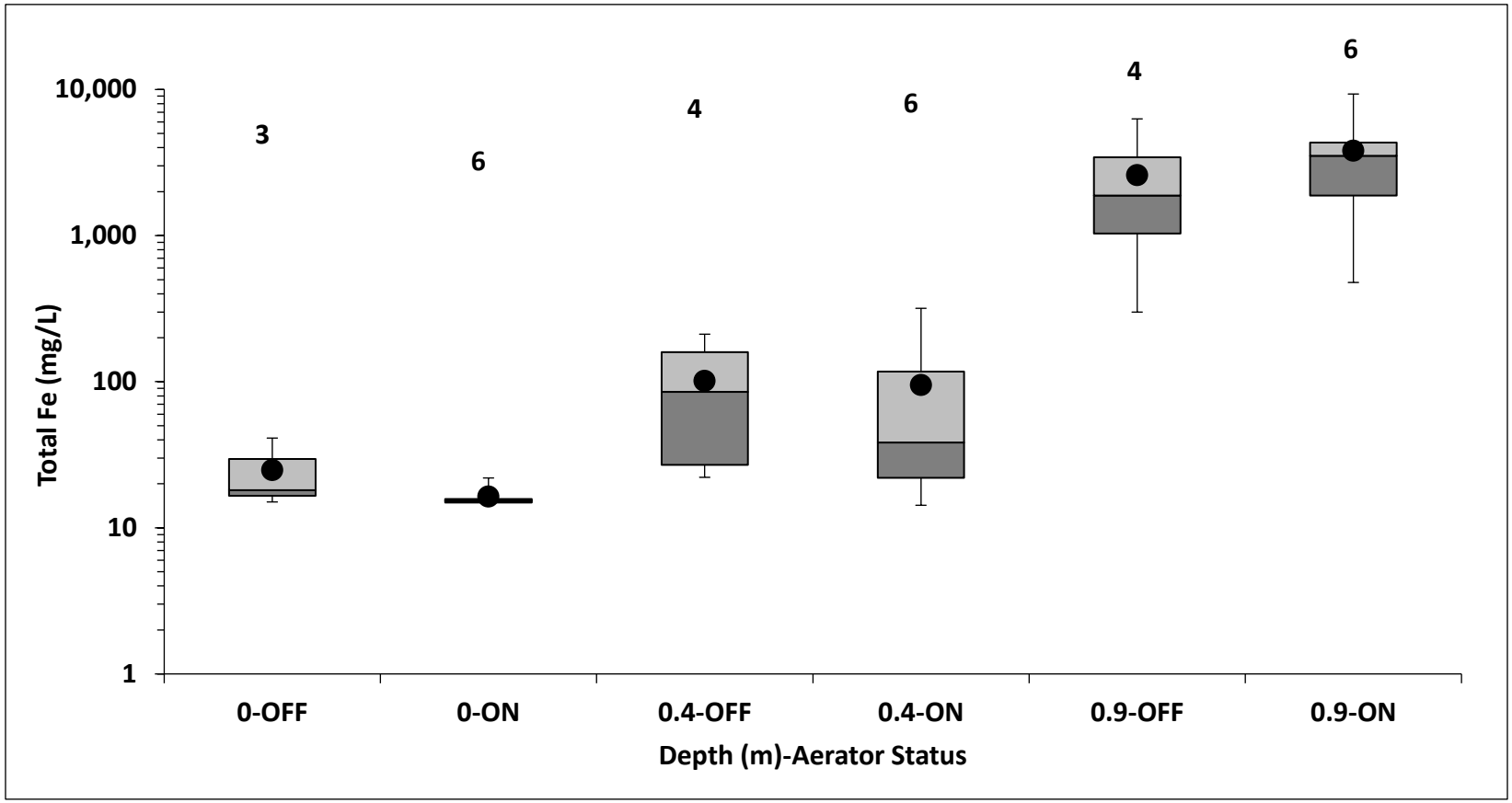

Figure 2.23 Box and whisker plot of total Fe concentrations at each depth for the ON and OFF studies at the east float-mix aerator (EFMA). The points represent the mean value for each data set and the numbers above the plot represent *n*, the sample size for each data set. Note that the y-axis is logarithmic.

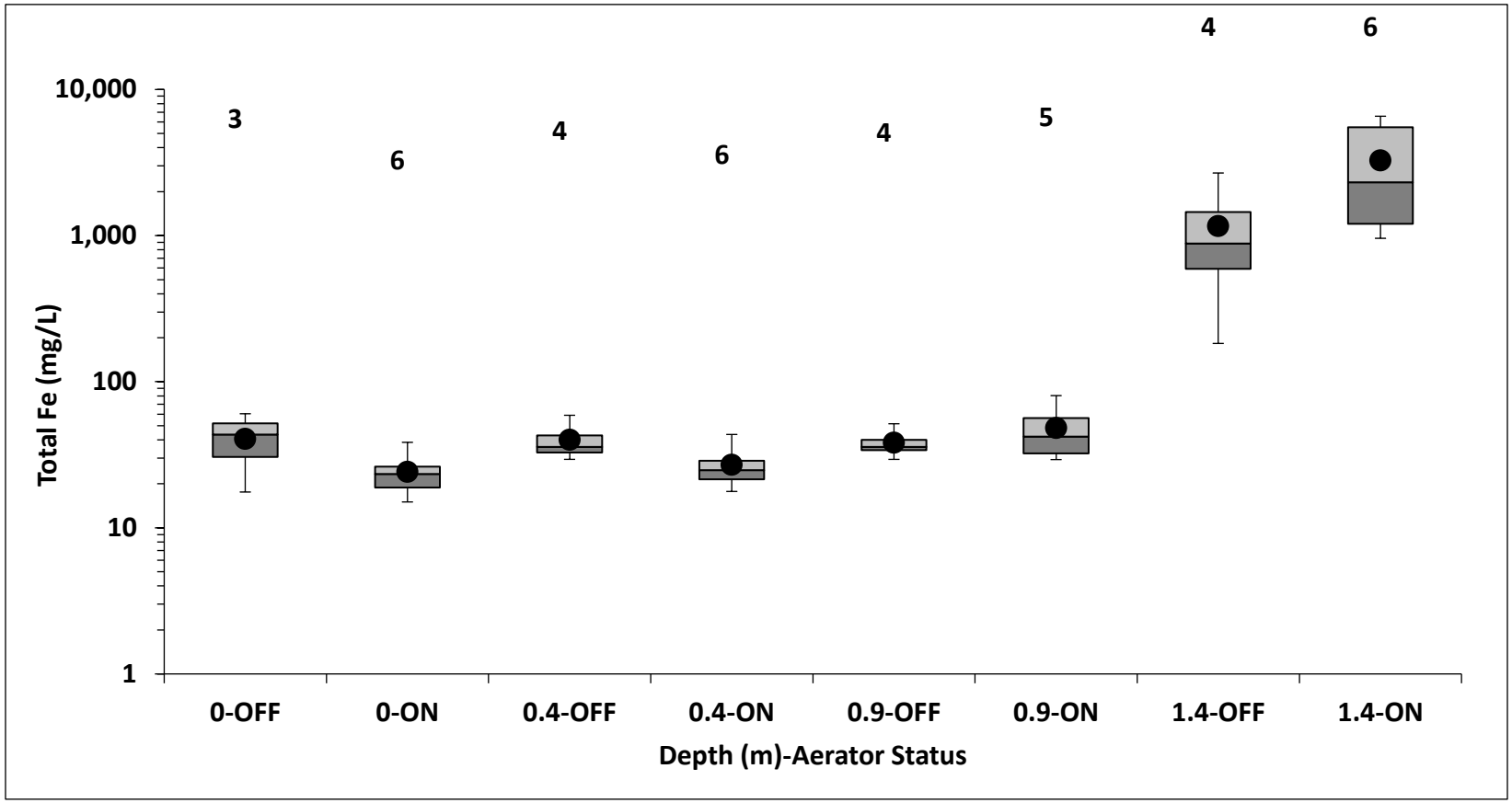

Figure 2.24 Box and whisker plot of total Fe concentrations at each depth for the ON and OFF studies at the west float-mix aerator (WFMA). The points represent the mean value for each data set and the numbers above the plot represent *n*, the sample size for each data set. Note that the y-axis is logarithmic.

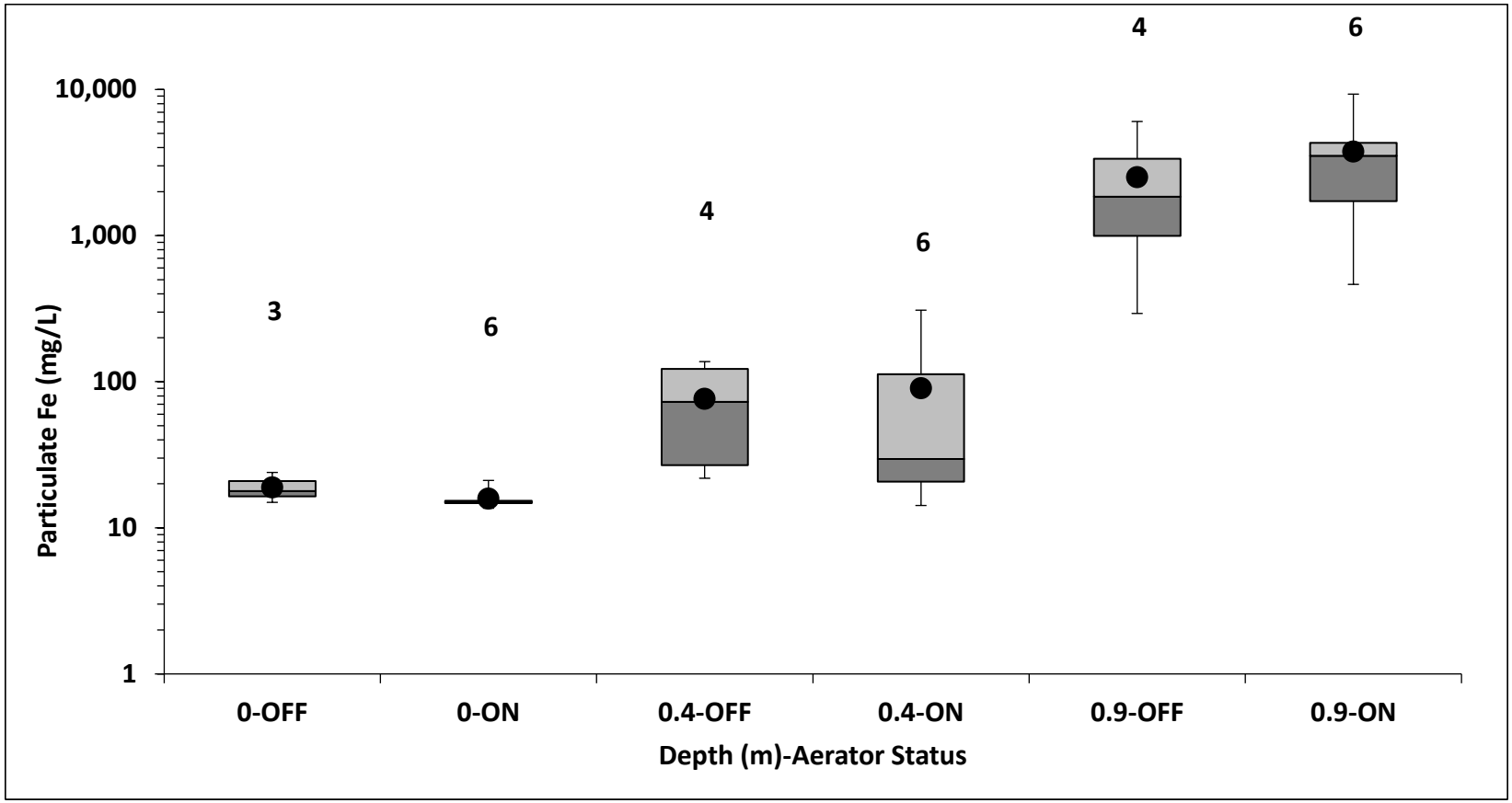

Figure 2.25 Box and whisker plot of particulate Fe concentrations at each depth for the ON and OFF studies at the east float-mix aerator (EFMA). The points represent the mean value for each data set and the numbers above the plot represent n, the sample size for each data set. Note that the y-axis is logarithmic.

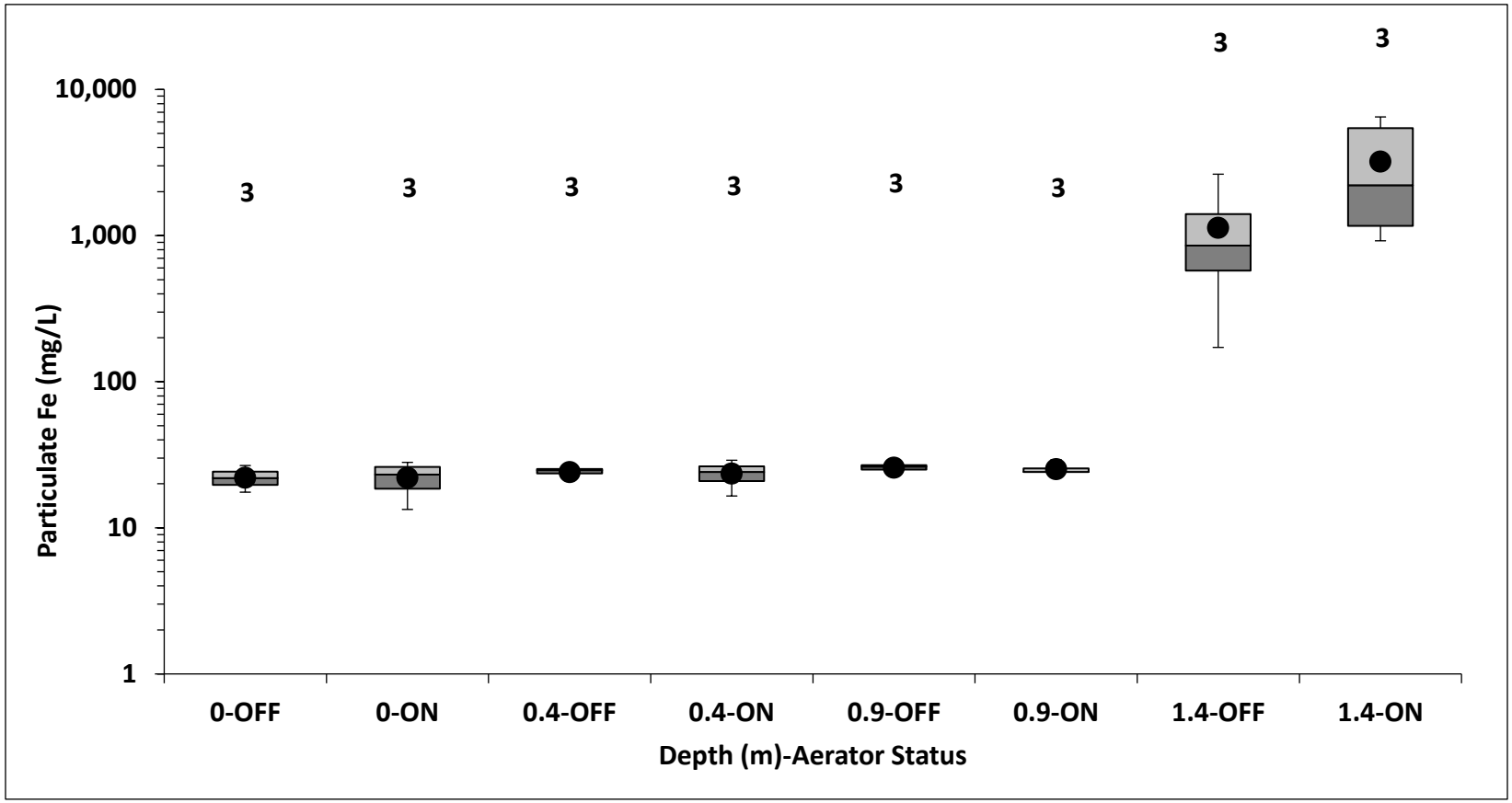

Figure 2.26 Box and whisker plot of particulate Fe concentrations at each depth for the ON and OFF studies at the west float-mix aerator (WFMA). The points represent the mean value for each data set and the numbers above the plot represent n, the sample size for each data set. Note that the y-axis is logarithmic.

Table 2.6 Average percentage (%) of total Fe in particulate form at each depth with the west float-mix aerator (WFMA) and east float-mix aerator (EFMA) off and on and p-values calculated using a Mann-Whitney U-test comparing the fraction of total Fe in particulate form.

Site	OFF	ON	p-value
WFMA-0	64.7%	92.9%	0.219
WFMA-0.4	64.6%	90.8%	**0.016**
WFMA-0.9	69.8%	66.8%	0.415
WFMA-1.4	96.4%	97.2%	0.227
EFMA-0	85.4%	96.8%	0.500
EFMA-0.4	87.6%	91.7%	0.415
EFMA-0.9	97.3%	97.0%	0.333

The lack of statistical difference for particulate Fe concentrations between ON and OFF may be driven by the small sample size and large variability in the data. One of the reasons for the large variability in the data set was because the OFF study occurred during a dryer winter season, while the ON study occurred during an abnormally wet spring and summer season. Rainfall data were retrieved from Oklahoma Mesonet Miami weather station located approximately 5 km southeast of the SECPTS. Table 2.7 shows the maximum daily rainfall accumulation, maximum 5-minute rainfall intensity and number of days in the study when it rained. The ON study had substantially greater rainfall in terms of the amount of rain that fell in a given day and a much greater number of higher intensity storms (Table 2.7). Similarly, while the OFF study had more days with rainfall (38%) compared to the ON study (26%), the ON study had almost 13 times the total rainfall indicating that while the storms were less frequent they were higher intensity. Rainfall can affect water quality by changing the pH of the water, disturbing the settling of Fe particulates and creating a dilution effect that can cause variability in the water quality data.

Table 2.7 Summary of rainfall data collected at the Miami Mesonet station approximately 5 km southeast of the SECPTS

	OFF	ON
Maximum Daily Rainfall (cm)	2.26	13.8
Maximum 5-Minute Rainfall Intensity (cm/hr)	8.84	15.2
Total Rainfall During Study Period (cm)	6.86	95.9
Number of Days in Study with Rainfall	14	12
% Days of Study with Rainfall	38%	26%

2.4 Conclusions

Novel aeration technologies are necessary for PTS located in areas with limited topographic relief, where hydraulic head driven aeration technologies are not feasible. This study investigated the effect FMAs have on increasing DO concentrations and degassing CO_2 in net-alkaline mine waters in order to promote more Fe retention with respect to depth. This study showed that airlift aerators increased DO concentrations and decreased dissolved CO_2 pressures at depths of 0.4 m and shallower. The decrease in CO_2 resulted in higher pH values and more Fe being oxidized and precipitated into Fe hydroxide and oxyhydroxide particulates at these depths. The aerators appeared to have less influence on DO and CO_2 concentrations at depths greater than 0.4 m. The limited change at depths greater than 0.4 m may be because the aerators operate by adding diffused air into a riser that raises the air-water mixture to the surface where it spills across a plate floating on the surface. The oxygen enriched water is discharged at the surface and thus limited mixing and oxygenation occurs at deeper depths. Although the influence of the aerators is limited to shallower depths, the aerators are a feasible technology for sites with limited relief because overall, they increase DO and pH in the water which leads to more Fe being oxidized and precipitated.

Chapter 3: Spatial Analysis of the Effectiveness of Float-Mix Aerators

3.1 Introduction

Mine drainage can contain elevated concentrations of metals and sulfate (SO_4^{2-}) from oxidation of pyrite and other sulfide minerals (Watzlaf et al. 2004; Younger et al. 2002). When mine drainage enters surface waters it causes biotic impairment due to either direct toxicity, habitat destruction by metal precipitates, or other mechanisms (Skousen et al. 2017). Passive treatment systems (PTS) are ecologically engineered systems that utilize a combination of geochemical, biological, and physical processes and renewable energy sources in order to treat mine drainage (Johnson and Hallberg 2005; Nairn et al. 2009; Skousen et al. 2017; Watzlaf et al. 2004; Younger et al. 2002). PTS often consist of a series of treatment process units that each individually address a specific characteristic of the mine drainage (Johnson and Hallberg 2005; Nairn et al. 2009; Skousen et al. 2017; Watzlaf et al. 2004; Younger et al. 2002).

Oxidation ponds are a common initial process unit used to treat net alkaline mine drainage (Hedin et al. 1994; Johnson and Hallberg 2005). These open water ponds and aerobic wetlands are a favorable treatment method because they promote the oxidation of ferrous (Fe (II)) iron to ferric (Fe (III)) iron (Equation 3.1). Oxidation ponds promote either passive or active aeration which increases dissolved oxygen (DO) concentration. Also, the flux of oxygen into the water column causes a concentration gradient for carbon dioxide (CO_2) which readily degasses into the atmosphere. In net-alkaline mine water, the degassing of CO_2 raises pH by reducing the amount of carbonic acid in the water which facilitates faster Fe oxidation rates. Under

circumneutral pH conditions, the dissolved Fe (III) iron quickly hydrolyzes with water and precipitates to form various Fe oxide and hydroxide species (Equation 3.2) (Younger et al. 2002). Oxidation ponds are recommended to be the first unit in a PTS for mine drainage with an Fe concentration greater than 50 mg/L so that Fe can settle in the oxidation pond before entering wetland systems that are more difficult to maintain (Younger et al. 2002). For net-alkaline mine water, oxidation ponds are designed using an Fe removal rate of 10 to 20 g Fe m^{-2} day^{-1}, with a retention time based on the initial Fe concentration and acid load (Nairn et al. 2009; Nairn et al. 2018; Skousen et al. 2017; Watzlaf et al. 2004; Younger et al. 2002).

$$4Fe^{2+} + O_2 + 4H^+ \rightarrow 4Fe^{3+} + 2H_2O \quad (3.1)$$

$$Fe^{3+} + 3H_2O \rightarrow Fe(OH)_3\,(s) + 3H^+ \quad (3.2)$$

Although oxygen is readily available in the atmosphere, greater Fe oxidation rates can be achieved by actively introducing oxygen into the water column (Geroni et al. 2012; Hedin 2008; Kirby et al 2007; Leavitt 2011; Nairn et al. 2009; Nairn et al. 2018; Oh et al. 2015; Schmidt 2004). A variety of aeration techniques exist, including simple energy dissipation devices and mechanical aeration technologies such as air sparging, fine bubble diffusers, the Maelstrom Oxidizer and floating surface aerators (Geroni et al. 2012; Hedin 2008; Kirby et al 2007; Leavitt 2011; Nairn et al. 2009; Nairn et al. 2018; Oh et al. 2015; Parker and Suttle 1987; Schmidt 2004; Shammas 2007; Zhang et al. 2000). Cascade aeration is a common energy dissipating practice used in PTS that effectively aerates the water by increasing the air-water interface. However,

while cascade aeration creates more air-water interface, it is limited because it requires a site with enough relief to create sufficient hydraulic head (Geroni et al. 2012). Therefore, a need exists for novel aeration techniques that do not rely on hydraulic head for PTS located in relatively flat landscapes.

Aeration technologies that do not require hydraulic head to entrain oxygen into the water column are commonly used in aquaculture and wastewater treatment applications and include technologies such as fine bubble diffusers and airlift aerators. Although fine bubble diffusers have a high oxygen transfer rate, they are more prone to fouling and thus are less favorable in PTS from an operation and maintenance standpoint. However, airlift aerators, also known as float-mix aerators (FMAs), are less prone to fouling. Airlift aerators introduce diffused air through a riser in the water column where the air-water mixture becomes more buoyant and travels up the riser and out to the atmosphere, typically across a plate (Burris et al. 2002; Parker and Suttle 1987). A literature gap exists regarding the effectiveness of airlift aerators, or float-mix aerators (FMAs), to oxygenate the water, degas CO_2 and promote Fe retention in initial oxidative units of PTS. Chapter 2 study showed that FMAs increased DO concentrations and decreased dissolved CO_2 partial pressures at depths of 0.4 m and shallower. This study investigated the effect FMAs have at increasing DO, degassing CO_2 and promoting Fe retention at increasing distances from the FMA. It was hypothesized that the FMAs would have limited influence as distances increased from the FMA.

3.2 Methods

3.2.1 Site Description

The Tar Creek Superfund Site is an approximately 100 km^2 site in northeastern Oklahoma located within the Tri-State Mining District which includes Oklahoma, Kansas and Missouri. This site is impacted by net-alkaline mine drainage from abandoned lead and zinc mining operations. Two PTS have been constructed to address artesian discharges of mine drainage: Mayer Ranch Passive Treatment System (MRPTS) in operation since 2008 and Southeast Commerce Passive Treatment System (SECPTS) in operation since 2017. This study focuses on the performance of the initial oxidation pond located in the SECPTS. Table 3.1 shows the process units and the design functions of the SECPTS. The SECPTS treats approximately 500 L/min of mine drainage with elevated Cd (2-33 µg/L), Fe (109-180 mg/L), Pb (30-398 µg/L) and Zn (5.4-8.4 mg/L) concentrations.

Table 3.1 Process units and design functions of the Southeast Commerce Passive Treatment System located in the Tar Creek Superfund Site, Oklahoma, USA

Process Units	Design Function
Initial Oxidation Pond (OX-POND)	Oxidative Fe retention via active aeration Trace metal sorption
Surface Flow Wetland/Pond (WL)	Additional Fe and trace metals retention
Vertical Flow Bioreactor (VFBR)	Metal sulfide retention
Final Polishing Unit (FPU)	Reaeration Stripping of sulfide and oxygen demand

The oxidation pond and final polishing unit each have a set of FMAs that deliver approximately 50 m^3/min of air via a blower. Figure 3.1 shows a schematic of an FMA used in the oxidation pond and FPU. Air is delivered via an airline and enters the airlift pipe

approximately 0.4 m below the water surface. The air-water mixture becomes more buoyant and travels up the airlift pipe and spills across the 1.2 m diameter aluminum plate to allow additional passive diffusion of oxygen. Given the design of the FMAs and their limited mixing of the water column, higher DO concentrations and lower pCO_2 concentrations are expected closer to the FMA rather than at a distance further from the FMA. This study investigated the DO, pH, pCO_2 and Fe concentrations at an increasing distance from the FMAs to determine their influence.

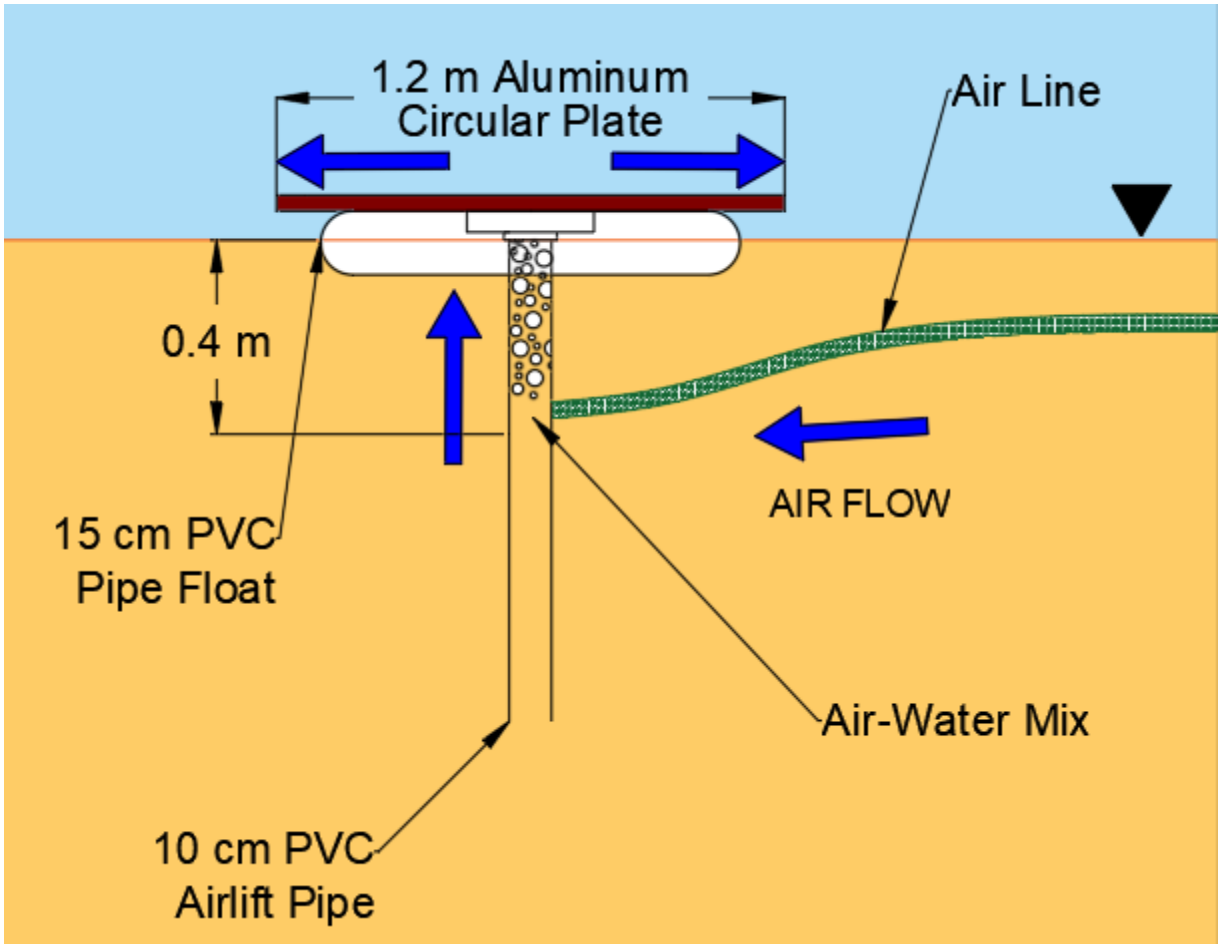

Figure 3.1 Schematic of the float-mix aerator, also known as an airlift aerator, used in the SECPTS.

3.2.2 Water Sample Collection and Analysis

Water samples and in-situ measurements were collected at increasing distances from the west float-mix aerator (WFMA) and east float-mix aerator (EFMA) in the oxidation pond of the SECPTS. Sampling stations were installed near the FMAs with rebar anchor driven into the native soil of the oxidation pond. YSI multiparameter datasondes were deployed 3 m upstream and 3 m, 6 m, and 9 m downstream of the WFMA, as well as 3 m upstream and downstream of the EFMA approximately 0.4 m below the water surface. The datasondes were deployed and samples taken 0.4 m below the water surface to limit effects of surficial interaction yet still show influence from the aerators as determined during the depth study. Figure 3.2 shows the sampling and datasonde deployment locations of the spatial study. The datasondes were programmed to collect in-situ water quality measurements including temperature (°C), specific conductivity (mS/cm), DO saturation (%), DO concentration (mg/L), pH (s.u. and mV) and oxidation-reduction potential (mV) every 15 minutes. DO saturation compares the DO concentration to the saturated DO concentration at the given temperature. This study was performed with the FMAs on (ON) and then when the FMAs were off (OFF). The ON study was performed from July 16th, 2019 to August 20th, 2019 and the OFF study was performed from August 20th, 2019 to September 20th, 2019.

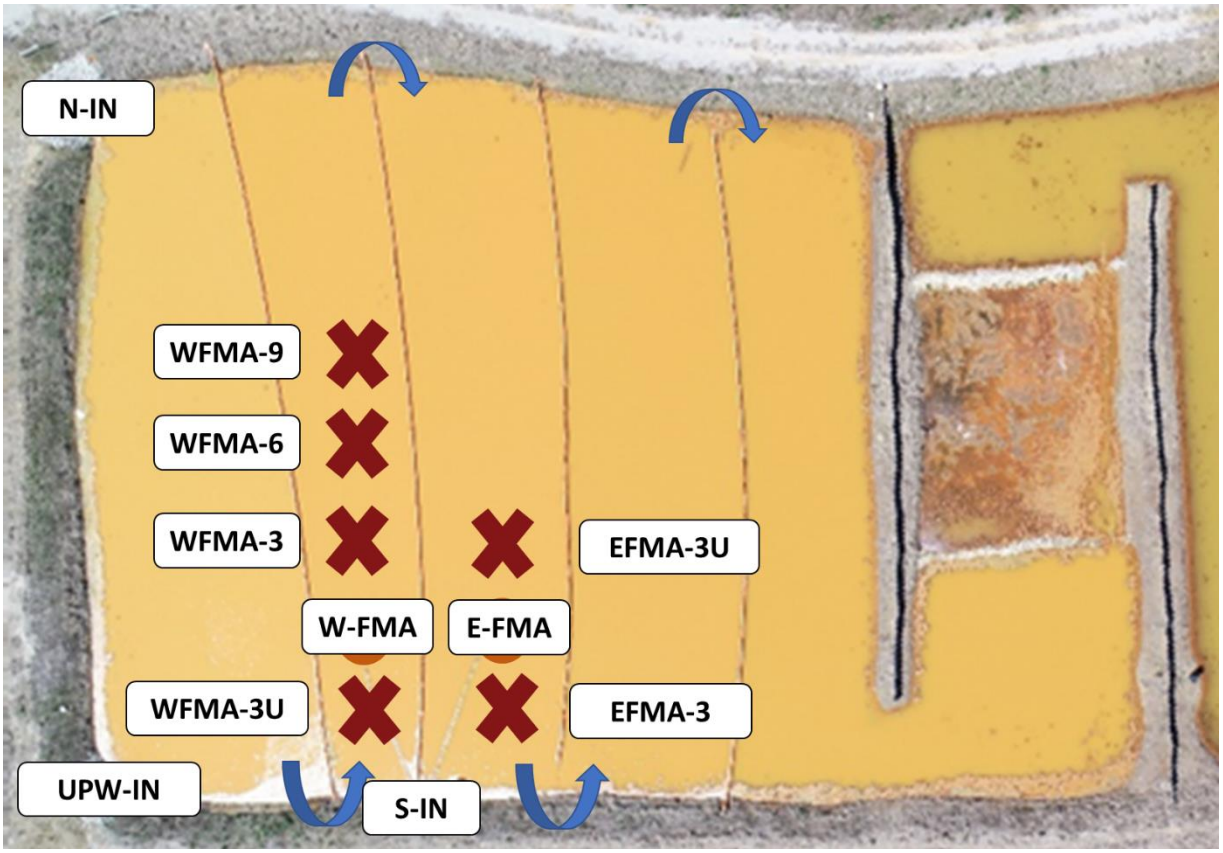

Figure 3.2 Map showing the locations of YSI datasondes deployment and sampling at increasing distance from both the west float-mix aerator (WFMA) and the east float-mix aerator (EFMA) in the Southeast Commerce Passive Treatment System, Oklahoma, USA.

Total suspended solids (TSS), total metals and dissolved metals grab samples were collected at each location from a canoe for the OFF (August 6th, August 12th, and August 20th) and OFF (August 29th, September 17th and September 20th) studies. The samples for dissolved metals were filtered through a 0.45-µm filter for each sample. Turbidity (NTU) was measured on-site using a Hach 2100P portable turbidimeter. Total alkalinity (mg/L $CaCO_3$) was also measured on-site using a Hach digital titrator with 1.6 N H_2SO_4 titrant and bromocresol green-

methyl red indicator (Hach Method 8203). The total and dissolved metals samples were acidified with concentrated trace-metal grade nitric acid and were transported back to the Center for Restoration of Ecosystems and Watersheds (CREW) laboratory for analysis. The metals samples were digested (EPA Method 3015) and then analyzed with a Varian-Vista Pro Inductively Coupled Plasma Optical Emission Spectrometer (ICP-OES) (EPA Method 6010). TSS samples were filtered through a glass fiber filter under vacuum and then dried in a drying oven in accordance with EPA Method 160.2.

3.2.3 pCO_2 Calculation

Temperature, pH and total alkalinity were used to calculate the partial pressure of CO_2 (pCO_2) in the water via the Arrhenius and Henderson-Hasselbalch equations. The Arrhenius equation (Eq. 3.3) is used to correct equilibrium constants for temperature and the series of Henderson-Hasselbalch equations for carbonate species were utilized to calculate pCO_2 (Eq. 3.4). Variables are defined in Chapter 1.

$$K_T = K_{25^\circ} exp\left[\left(\frac{-\Delta H^\circ_{rxn}}{R}\right)\left(\frac{1}{T_{25^\circ}} - \frac{1}{T}\right)\right] \tag{3.3}$$

$$P_{CO_2} = \left[\frac{Alk - [OH^-] + [H^+]}{(\alpha_1 + 2\alpha_2)}\right]\left(\frac{\alpha_0}{K_H}\right) \tag{3.4}$$

For these calculations, DO and pH measurements were represented by continuous data collected every 15 minutes throughout the study. Alkalinity was measured during each

sampling event. Since the alkalinity data set was not continuous, the mean alkalinity between two sampling events was used to calculate pCO_2 values.

3.2.4 Statistical Analyses

Statistical analyses of the datasets were performed using Microsoft Excel and IBM SPSS Statistics Software. The normality of the data was analyzed using the Kolmogorov-Smirnov and Shapiro-Wilk tests. The data were found to be nonparametric and thus the ON and OFF datasets were analyzed using the Mann-Whitney U-test and Mood's Median test. Table 3.2 shows the tests used to perform the statistical analyses and the null hypothesis for each test. A 95% confidence interval was used for all analyses in which a p-value greater than 0.05 means acceptance of the null hypothesis.

Table 3.2 Statistical analyses used to analyze the spatial study datasets and their respective null hypotheses.

Statistical Test	Null Hypothesis
Kolmogorov-Smirnov Test	The samples come from the same distribution
Shapiro-Wilk Test	The population is normally distributed
Mann Whitney U-test	The distributions between variables are identical
Mood's Median Test	The medians of the populations are identical

3.3 Results and Discussion

3.3.1 Dissolved Oxygen and Carbon Dioxide

Since the SECPTS came online in February 2017, water quality samples have been taken at the N-IN, S-IN and UPW-IN inlets and at the outlet of the oxidation pond. These data give insight into how the oxidation pond is performing overall. However, prior to this study, no data had been collected near the FMAs to determine their radius of influence. Data were collected upstream and downstream of the aerators at increasing distances to determine the FMAs' ability to increase DO, degas pCO_2 and raise pH with respect to distance. Box and whisker plots representing DO, pCO_2 and pH data collected from deployed YSIs and sampling events for each FMA are shown in Figures 3.3-3.8. DO saturation values above 100% were recorded, due to non-ideal equilibrium conditions and the contribution of biological productivity to oxygenation. During sampling events, filamentous photosynthetic algae were observed, however algae concentrations and estimates of oxygen produced from the biomass were not quantified. Both the WFMA and EFMA showed greater mean and median DO concentrations with the aerators ON than with the aerators OFF regardless of distance from the aerator. However, only the EFMA showed an increase in pH and a decrease in pCO_2 with aerators ON than with the aerators OFF, both upstream and downstream.

Analysis of the data showed that they were not normally distributed and thus non-parametric statistical analyses were conducted. A Mann-Whitney U-test and Mood's median test were performed at each depth to determine if DO saturation, pH and pCO_2 were significantly different when the aerators were ON compared to when the aerators were OFF.

Comparison of DO, pCO_2 and pH at each location for ON and OFF all resulted in p-values less than 0.001 for the Mann-Whitney U-test and Mood's median test, indicating that the samples from ON and OFF are from different distributions and that their medians are statistically different.

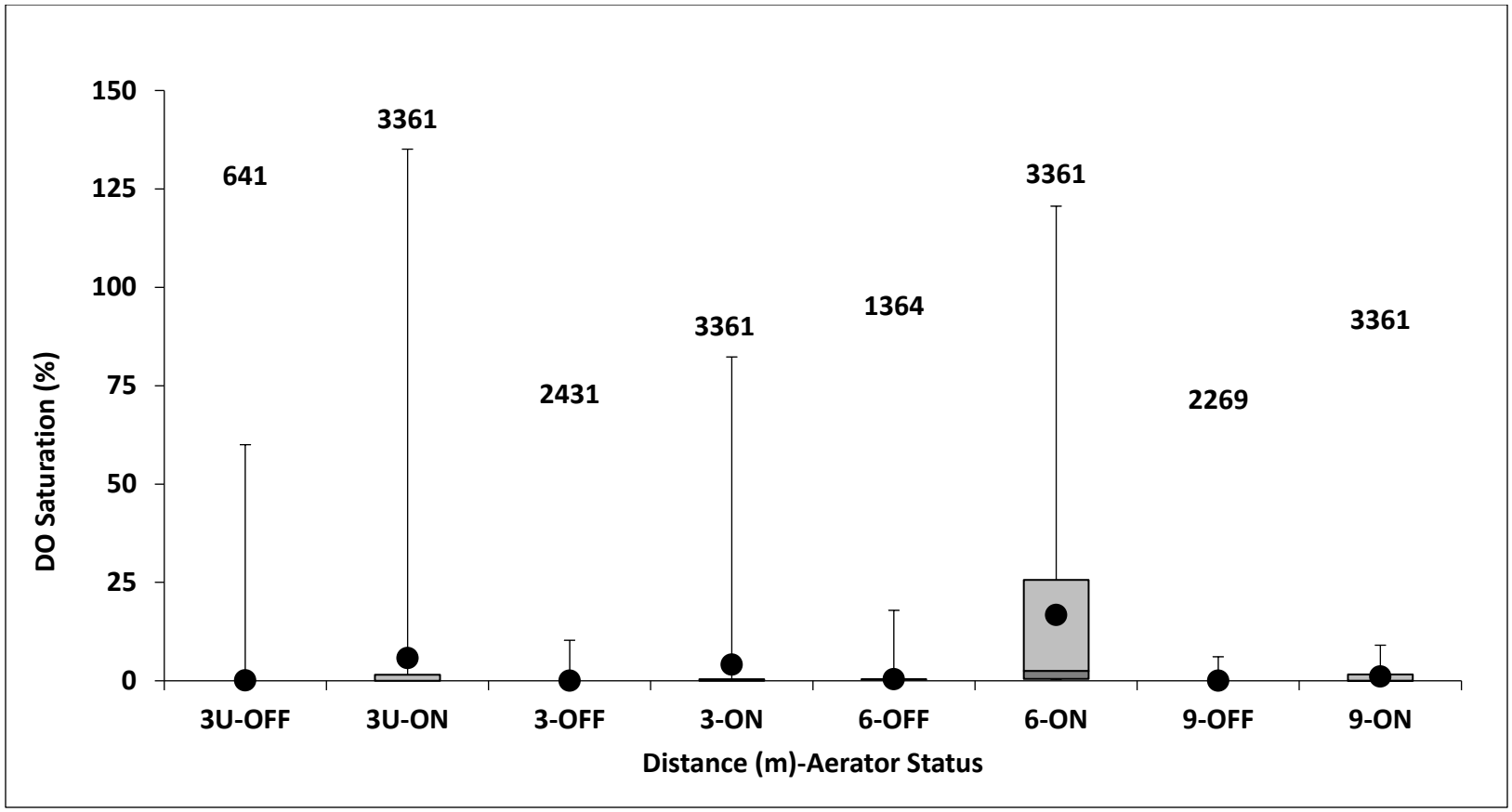

Figure 3.3 Box and whisker plot of dissolved oxygen saturation readings collected at each distance from the west float-mix aerator (WFMA) for the ON and OFF studies. The points represent the mean value for each data set and the numbers above the plot represent n, the sample size for each data set.

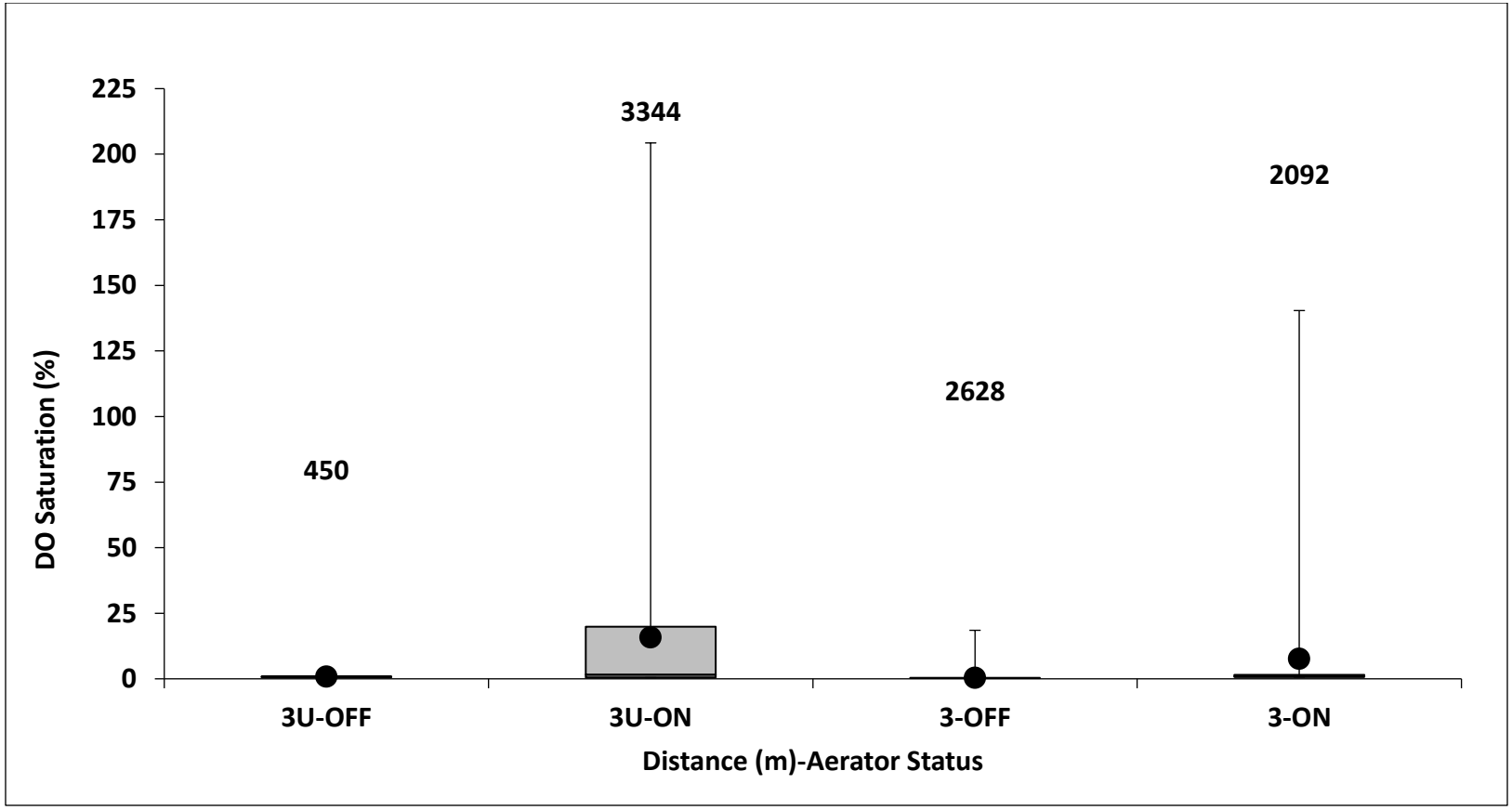

Figure 3.4 Box and whisker plot of dissolved oxygen saturation readings collected at each distance from the east float-mix aerator (EFMA) for the ON and OFF studies. The points represent the mean value for each data set and the numbers above the plot represent n, the sample size for each data set.

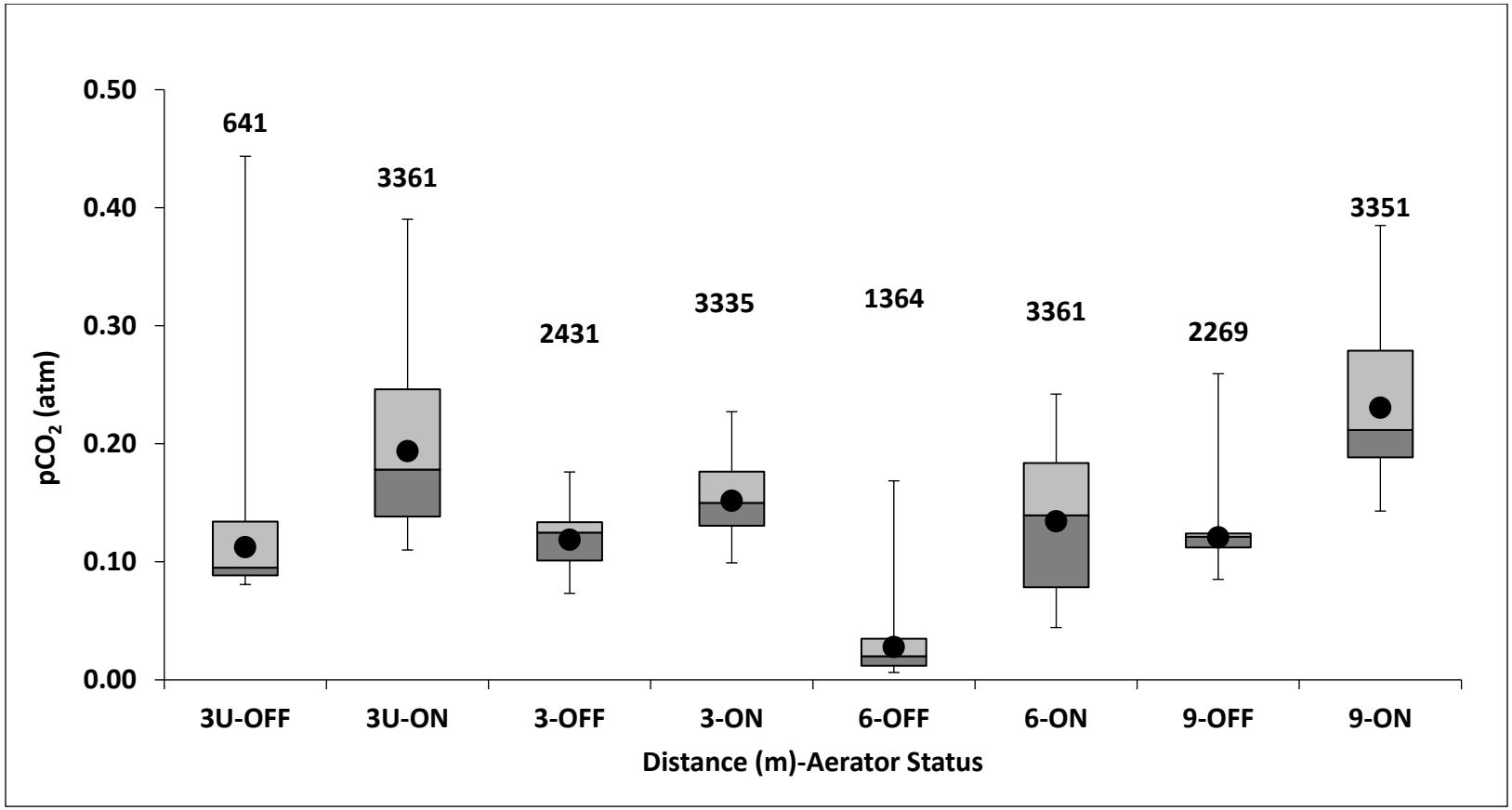

Figure 3.5 Box and whisker plot of dissolved carbon dioxide partial pressures (pCO_2) at each distance from the west float-mix aerator (WFMA) for the ON and OFF studies. The points represent the mean value for each data set and the numbers above the plot represent n, the sample size for each data set.

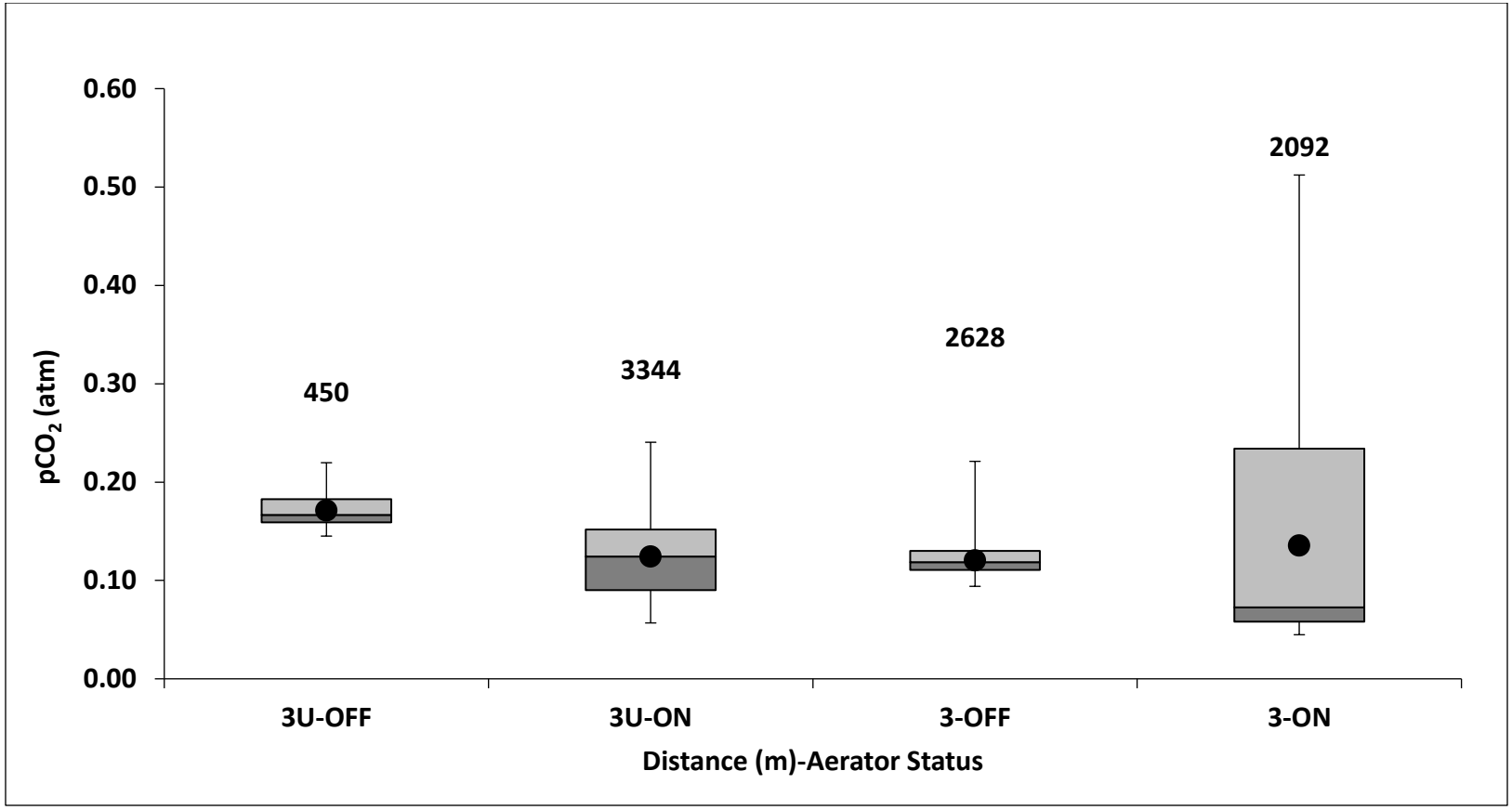

Figure 3.6 Box and whisker plot of dissolved carbon dioxide partial pressures (pCO_2) at each distance from the east float-mix aerator (EFMA) for the ON and OFF studies. The points represent the mean value for each data set and the numbers above the plot represent n, the sample size for each data set.

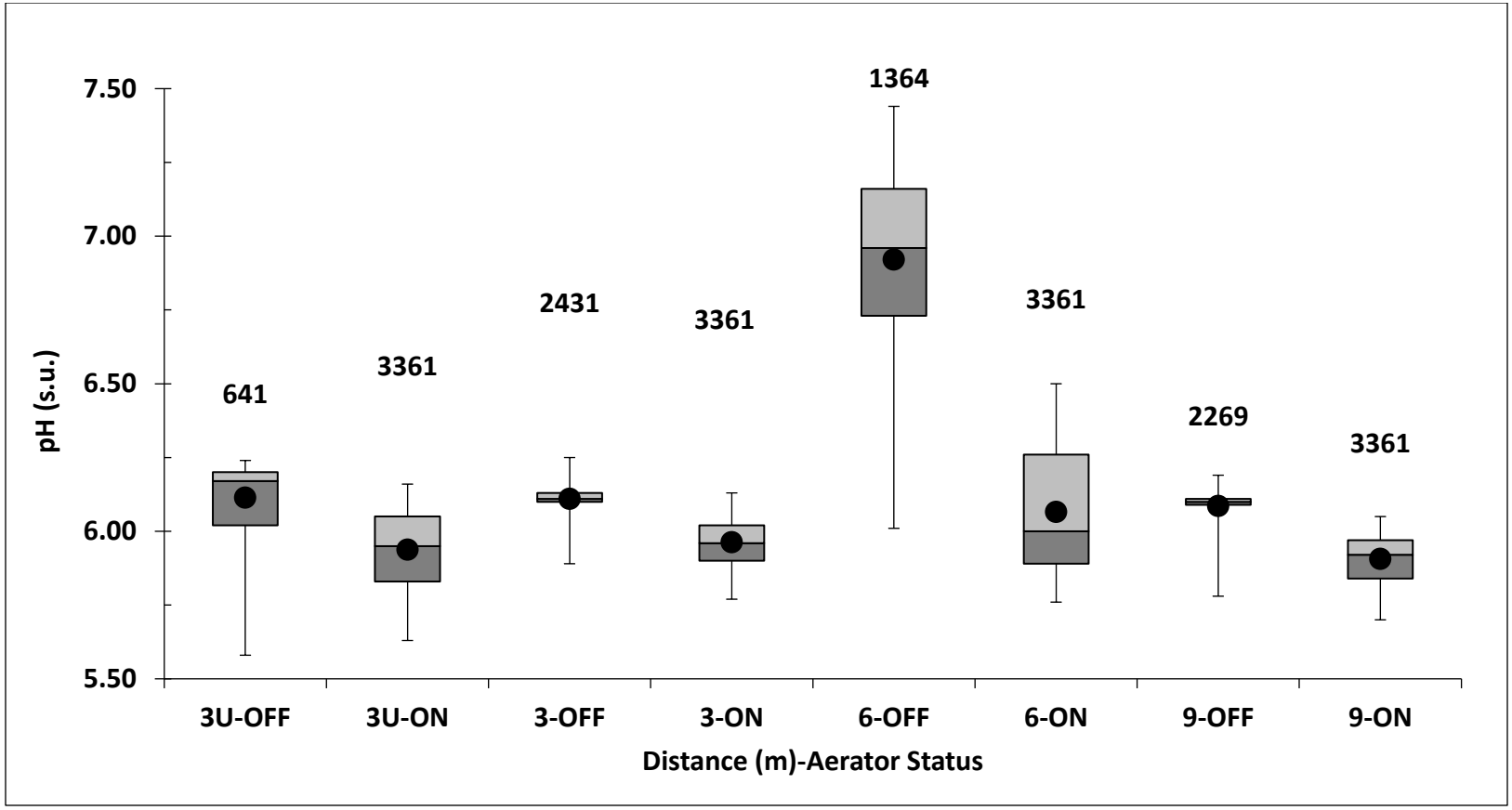

Figure 3.7 Box and whisker plot of pH measurements at each distance from the west float-mix aerator (WFMA) for the ON and OFF studies. The points represent the mean value for each data set and the numbers above the plot represent n, the sample size for each data set.

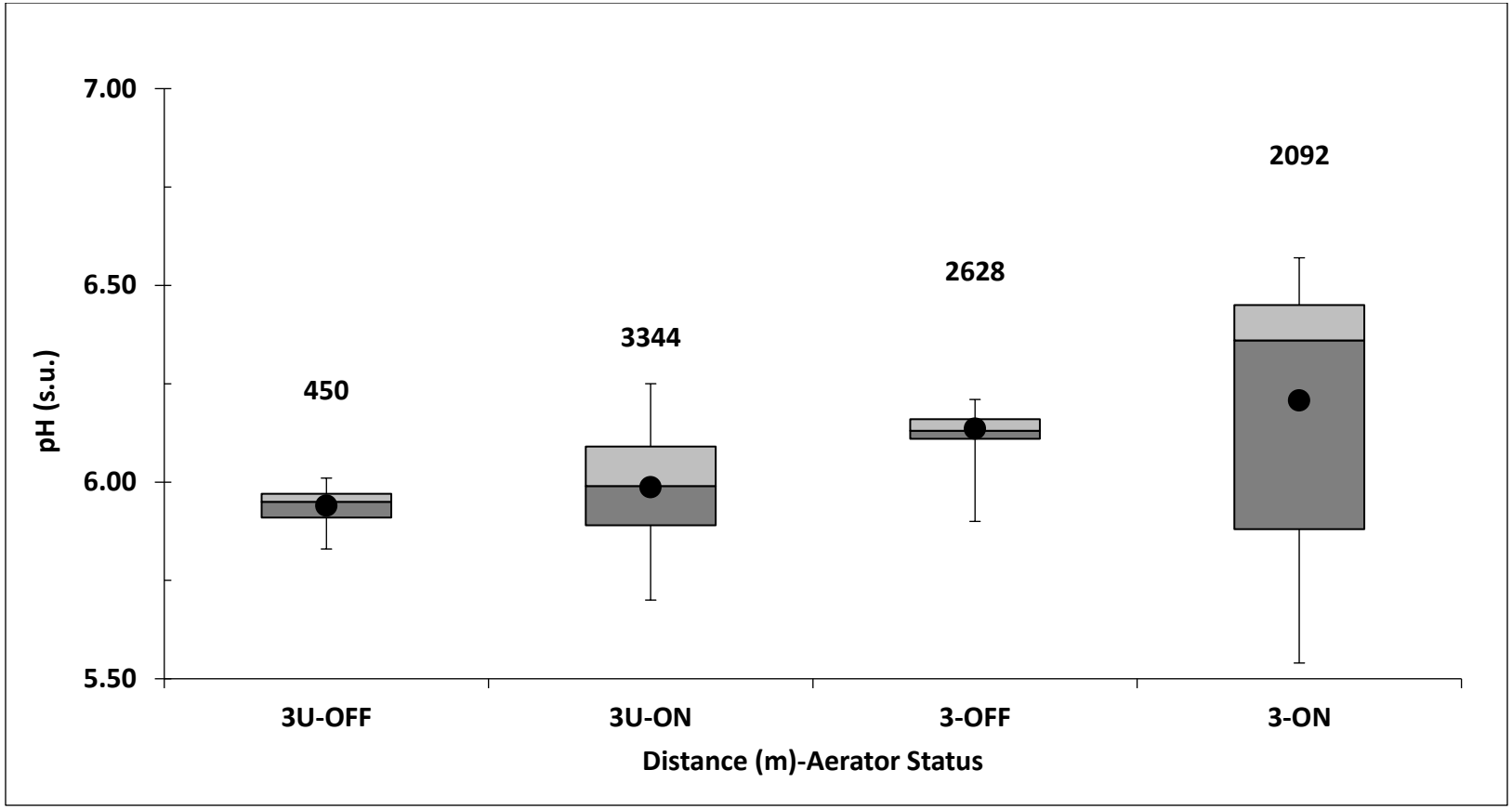

Figure 3.8 Box and whisker plot of pH measurements at each distance from the west float-mix aerator (WFMA) for the ON and OFF studies. The points represent the mean value for each data set and the numbers above the plot represent n, the sample size for each data set.

The pH was lower during the ON study compared to the OFF study for the WFMA; the opposite of what was hypothesized. This result may be due to changes in the water surface elevation of the oxidation pond caused by rainfall and thus the relative depth of the YSI datasondes. Figures 3.9 and 3.10 show the changes in water elevation, the amount of rainfall during the study and the elevation of the YSI datasondes during deployment for each study. The ON study had a water elevation that ranged from 242.04 to 242.27 m above mean sea level with an average water elevation of 242.10 m. The YSI was deployed 0.46 m below the water surface but due to the change in water elevation, the YSI depth ranged from 0.43 to 0.65 m below the water surface. Conversely, during the OFF study, the water surface elevation ranged from 242.05 to 242.34 m above mean sea level with an average elevation of 242.15 m. While the YSI was designed to be deployed approximately 0.46 m below the water surface, its depth ranged from 0.41 to 0.70 m below the water surface due to changes in water surface elevations. Chapter 2 showed that the FMAs have limited effect with increasing depth and thus lower pH values deeper below the surface. Another contributing factor was the WFMA's proximity to the upwelling. Increased rainfall could have caused an increase in discharge from the upwellings with low DO concentrations and elevated dissolved Fe concentrations.

The WFMA data also show higher pCO_2 with the ON compared to the OFF study; opposite of what was hypothesized. A comparison of the alkalinity values collected 0.4 m below the surface for the EFMA and WFMA with the aerators on and off show that the total alkalinity was consistently lower during the ON study compared to the OFF study indicating that CO_2 is being degassed (Figures 3.11 and 3.12). However, since pCO_2 is calculated from alkalinity and pH

values, the factors affecting the pH measurements also affect the calculated pCO_2 values. Therefore, a lower measured pH results in a higher calculated pCO_2.

While the WFMA showed opposite trends for pCO_2 and pH than hypothesized perhaps due to influence from the upwelling, the EFMA showed that increasing the DO concentration degassed more CO_2 and overall raised the pH. Not only was pH higher when the aerators were on, but the pH increased downstream. The EFMA data show that the FMAs have at least a 3 m radius of influence and that aeration can increase pH further downstream as shown in Figure 3.13. Figure 3.14 shows that DO saturation was higher both upstream and downstream of the EFMA when the aerators were on, but the DO saturation did not have an additive effect as the water moved further downstream. This was because DO was consumed in the Fe oxidation process further downstream thus decreasing the DO saturation.

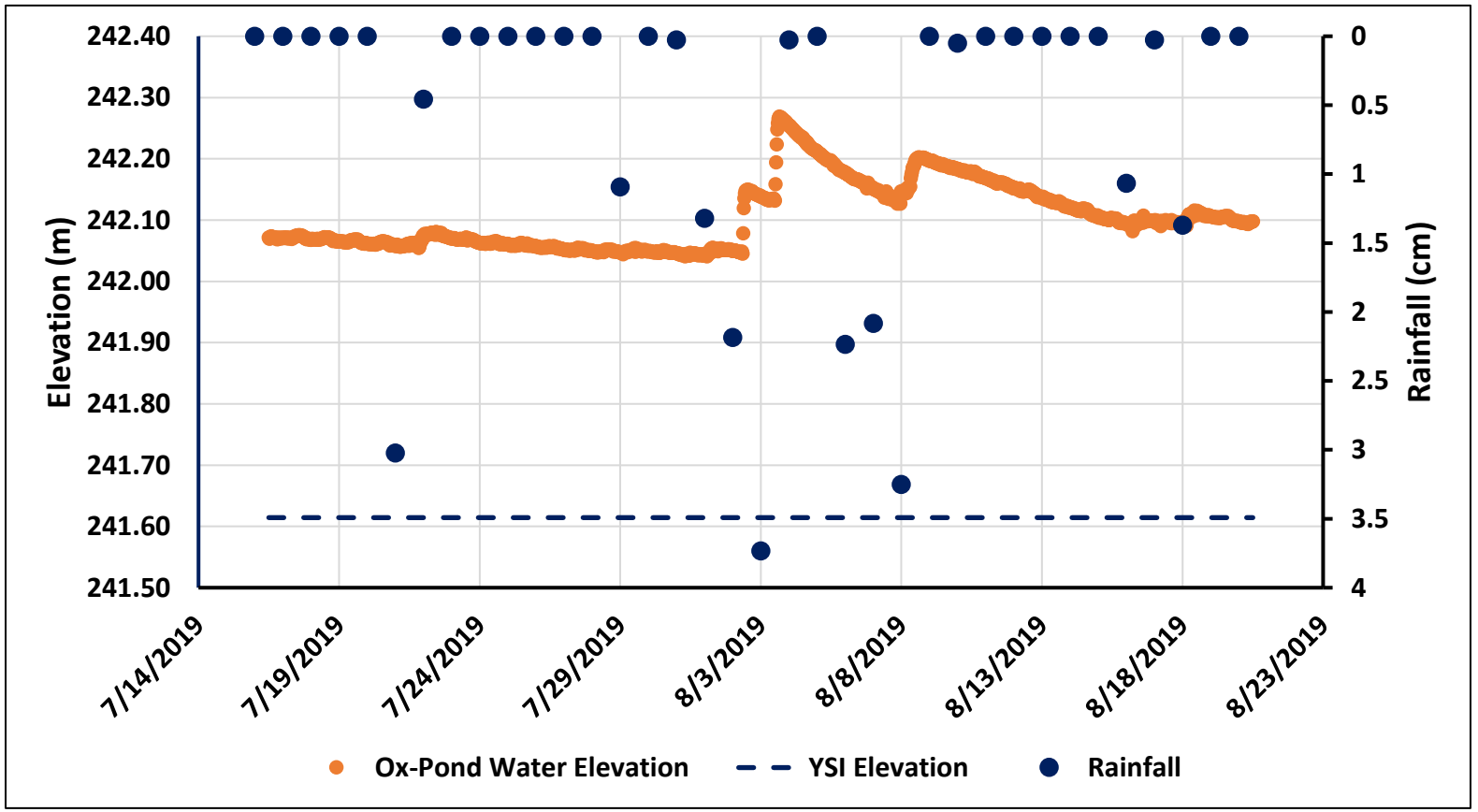

Figure 3.9 Daily rainfall (cm) during the ON study and the oxidation pond water elevation (m) with respect to the deployed YSI elevation.

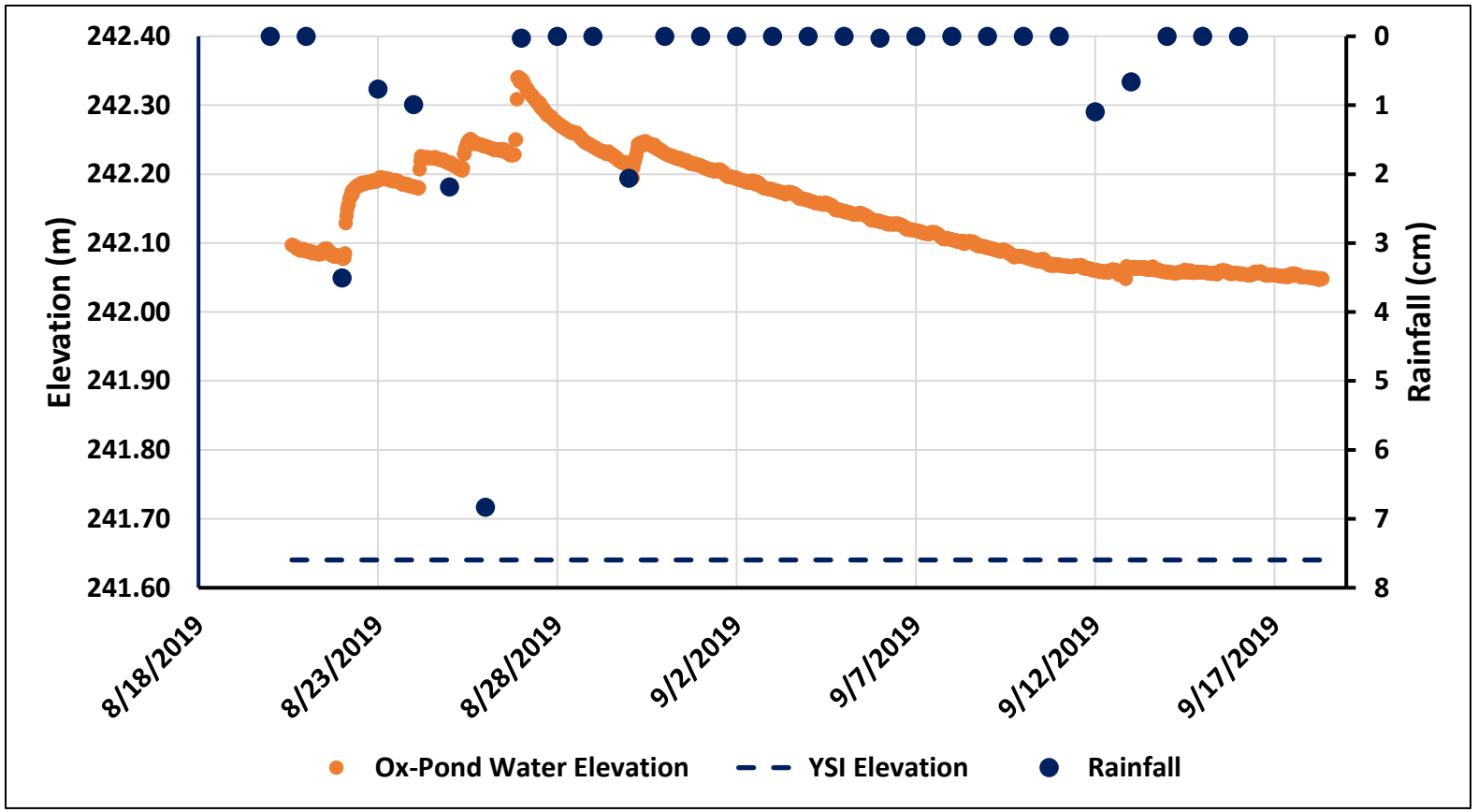

Figure 3.10 Daily rainfall (cm) during the OFF study and the oxidation pond water elevation (m) with respect to the deployed YSI elevation.

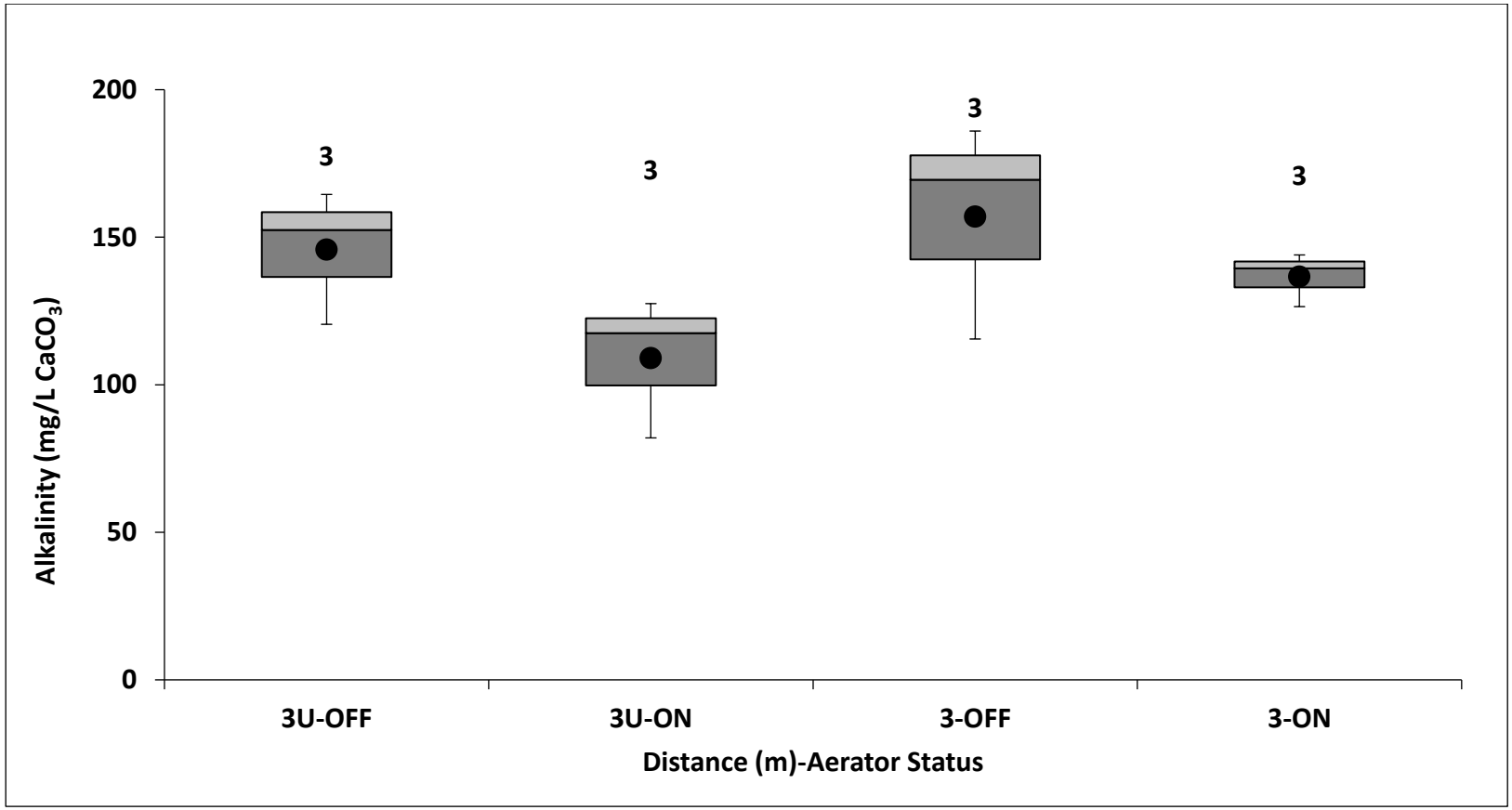

Figure 3.11 Box and whisker plot of alkalinity measurements at each distance from the east float-mix aerator (EFMA) for the ON and OFF studies. The points represent the mean value for each data set and the numbers above the plot represent n, the sample size for each data set.

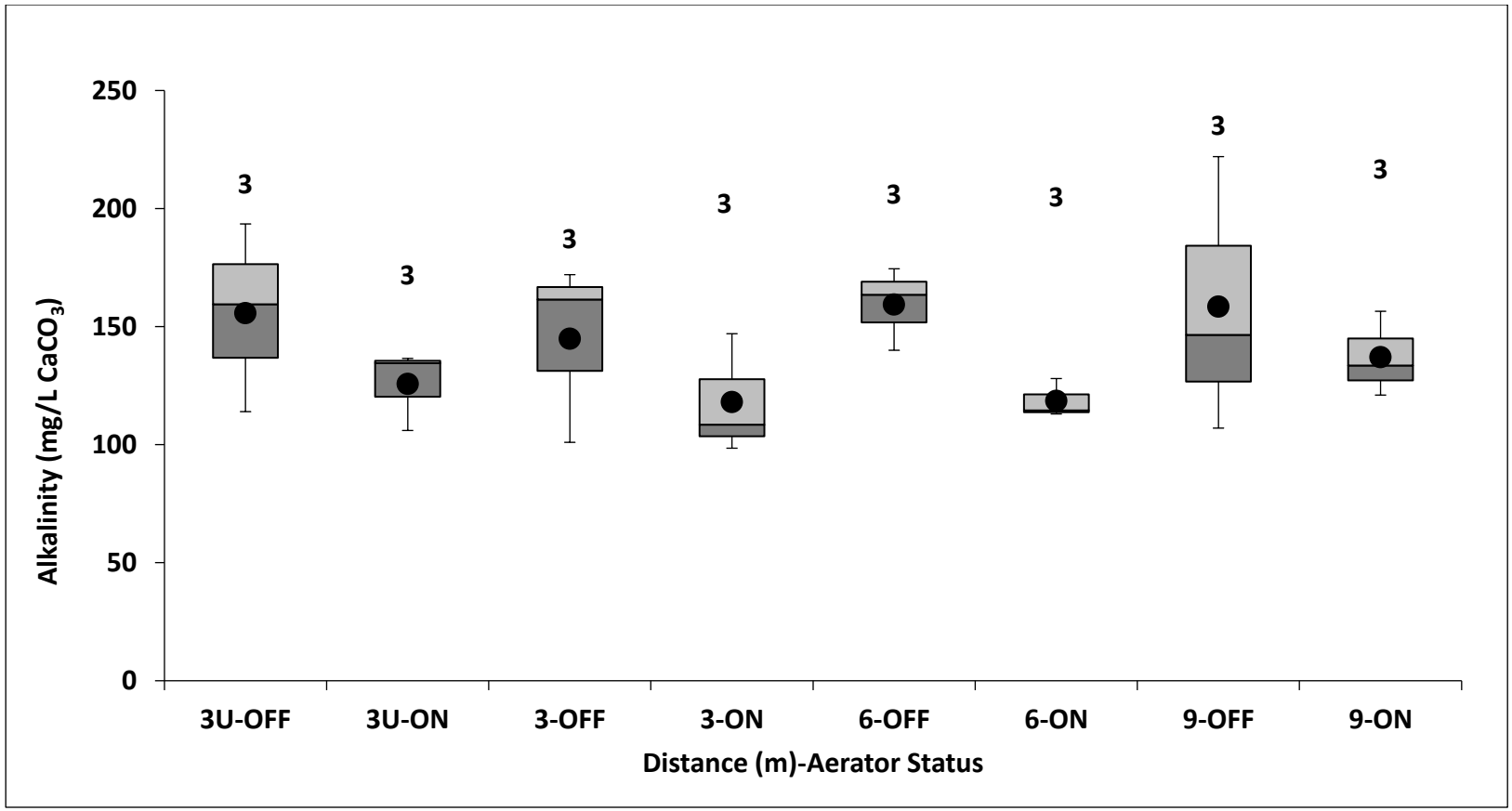

Figure 3.12 Box and whisker plot of total alkalinity measurements at each distance from the west float-mix aerator (WFMA) for the ON and OFF studies. The points represent the mean value for each data set and the numbers above the plot represent n, the sample size for each data set.

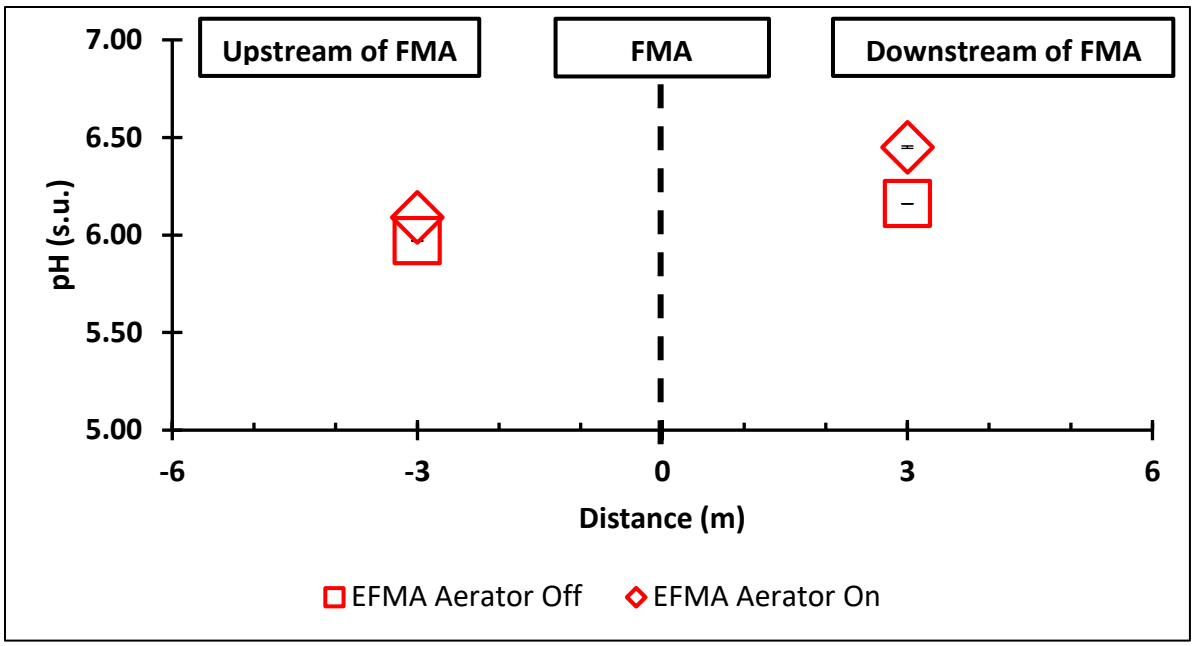

Figure 3.13 Median pH values upstream and downstream 3 m of the EFMA. Standard error bars may be smaller than the data point.

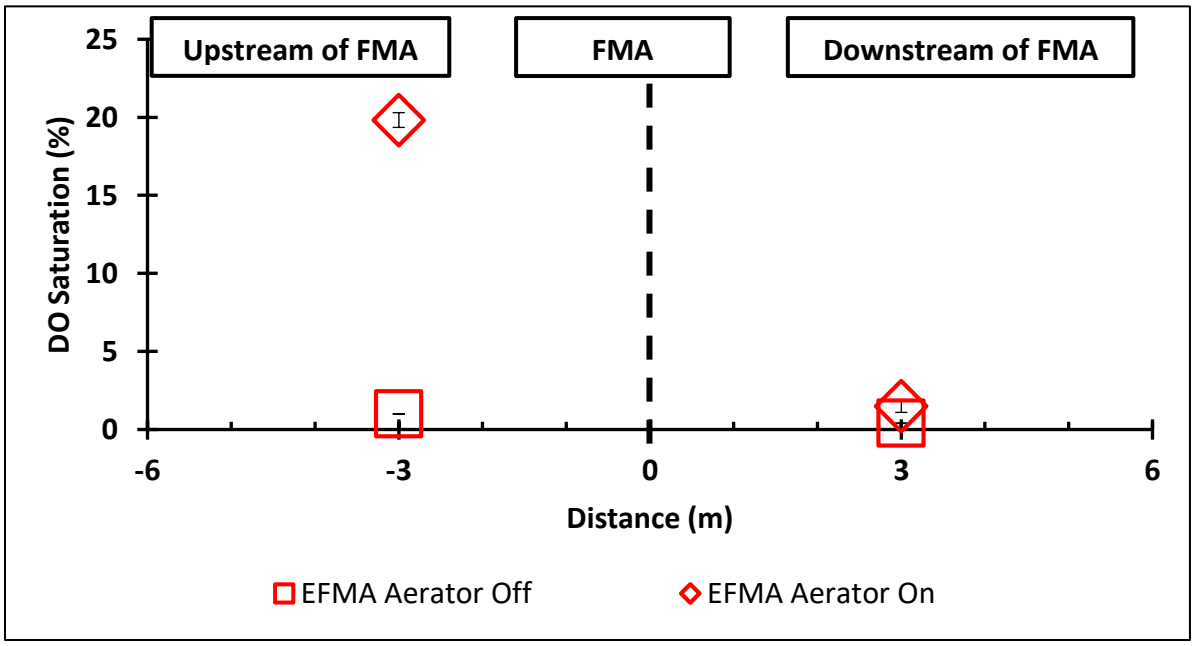

Figure 3.14 Median DO saturation (%) values 3m upstream and downstream of the EFMA. Standard error bars may be smaller than the data point.

3.3.2 Solids and Iron Retention

Total and dissolved Fe concentrations were lower in the pond at increasing distance from the FMAs during the ON study for both the WFMA and EFMA. This indicated that more Fe was being oxidized and precipitated due to the increased DO provided by the FMAs. Figures 3.15 – 3.22 show TSS, total Fe, dissolved Fe and particulate Fe concentration data collected during the sampling events. Particulate Fe concentration was calculated by subtracting the dissolved Fe concentration from the total Fe concentration.

While total and dissolved Fe concentrations decreased, particulate Fe concentrations showed minimal differences between the ON and OFF studies (Figure 3.21 and 3.22). Therefore, the fraction of total Fe present in particulate form was calculated and a Mann Whitney U-test was performed to determine if the mean percent particulate Fe at each location was statistically different between ON and OFF (Table 3.3). The lack of statistical significance may be due to the limited number of sampling events and the large variability in the concentrations.

Table 3.3 Average percentage of total Fe in particulate form at each distance from the west float-mix aerator (WFMA) and east float-mix aerator (EFMA) off and on and p-values calculated using a Mann Whitney U-test comparing the fraction of total Fe in particulate form

Site	OFF	ON	p-value
WFMA-3U	51.3%	59.7%	1.000
WFMA-3	54.2%	66.9%	0.700
WFMA-6	29.2%	85.4%	0.100
WFMA-9	50.7%	89.9%	0.700
EFMA-3U	65.1%	73.4%	1.000
EFMA-3	35.0%	74.6%	0.200

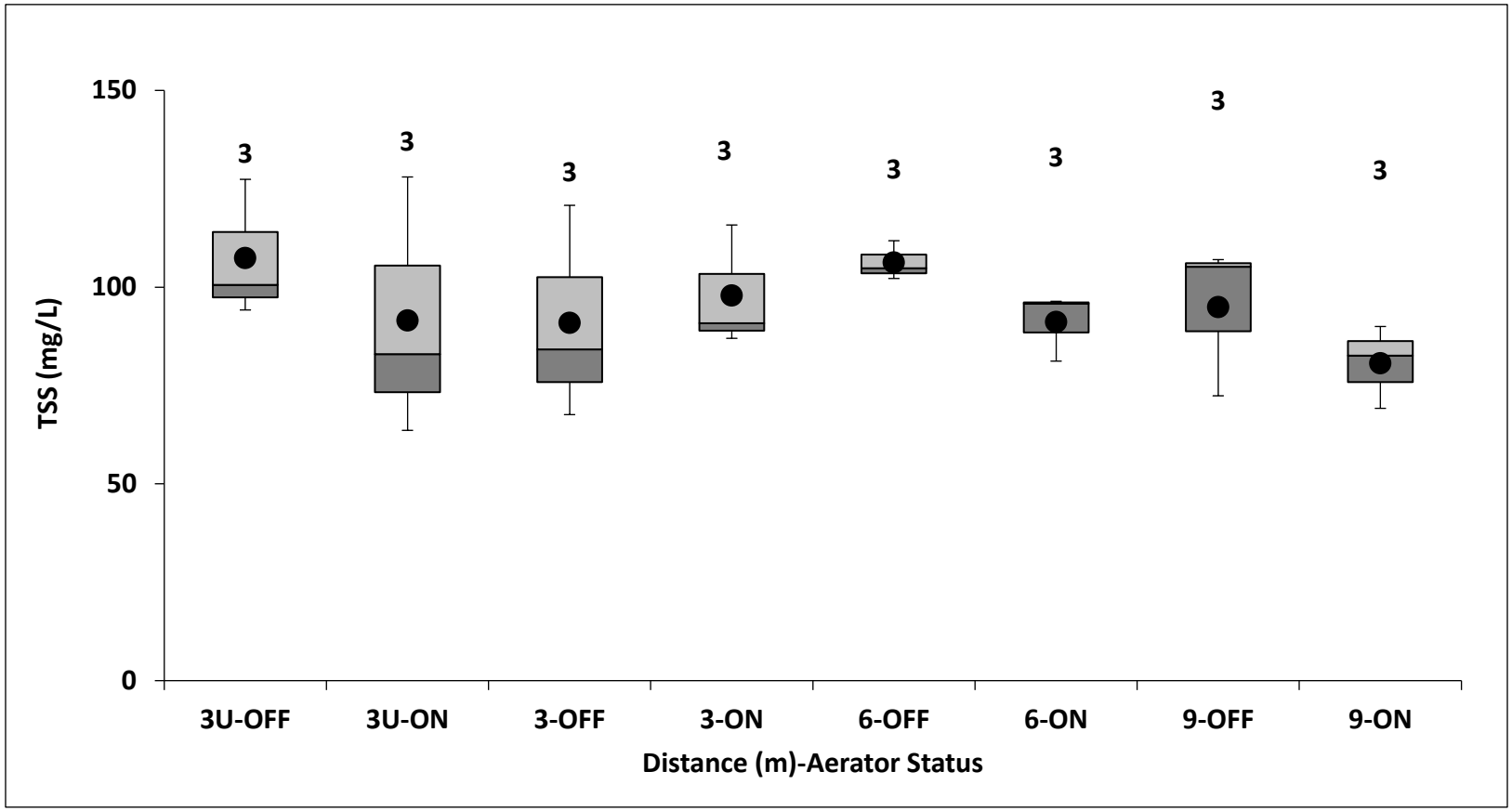

Figure.3.15 Box and whisker plot of TSS concentrations at each distance from the west float-mix aerator (WFMA) for the ON and OFF studies. The points represent the mean value for each data set and the numbers above the plot represent *n*, the sample size for each data set.

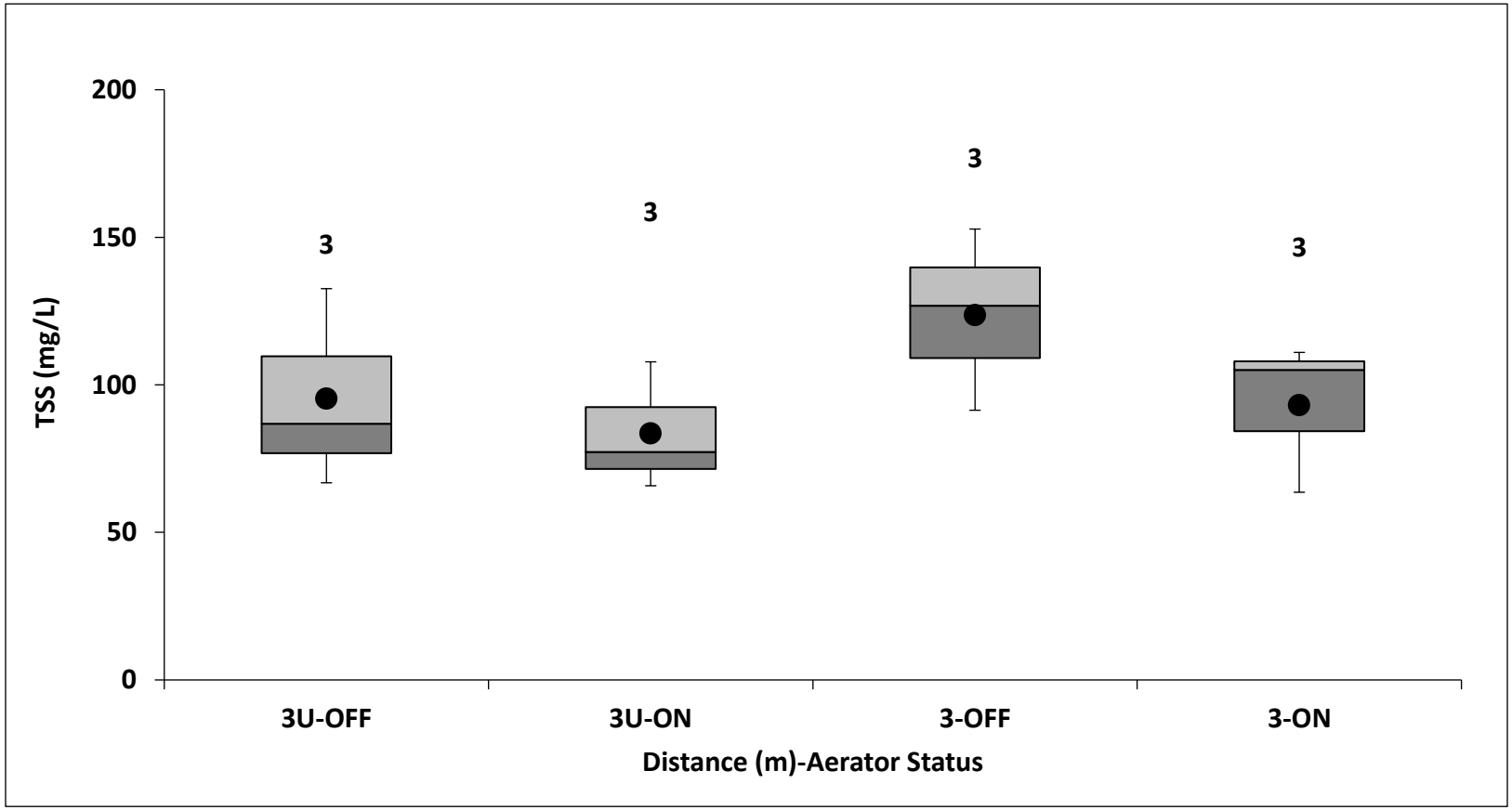

Figure 3.16 Box and whisker plot of TSS concentrations at each distance from the east float-mix aerator (EFMA) for the ON and OFF studies. The points represent the mean value for each data set and the numbers above the plot represent *n*, the sample size for each data set.

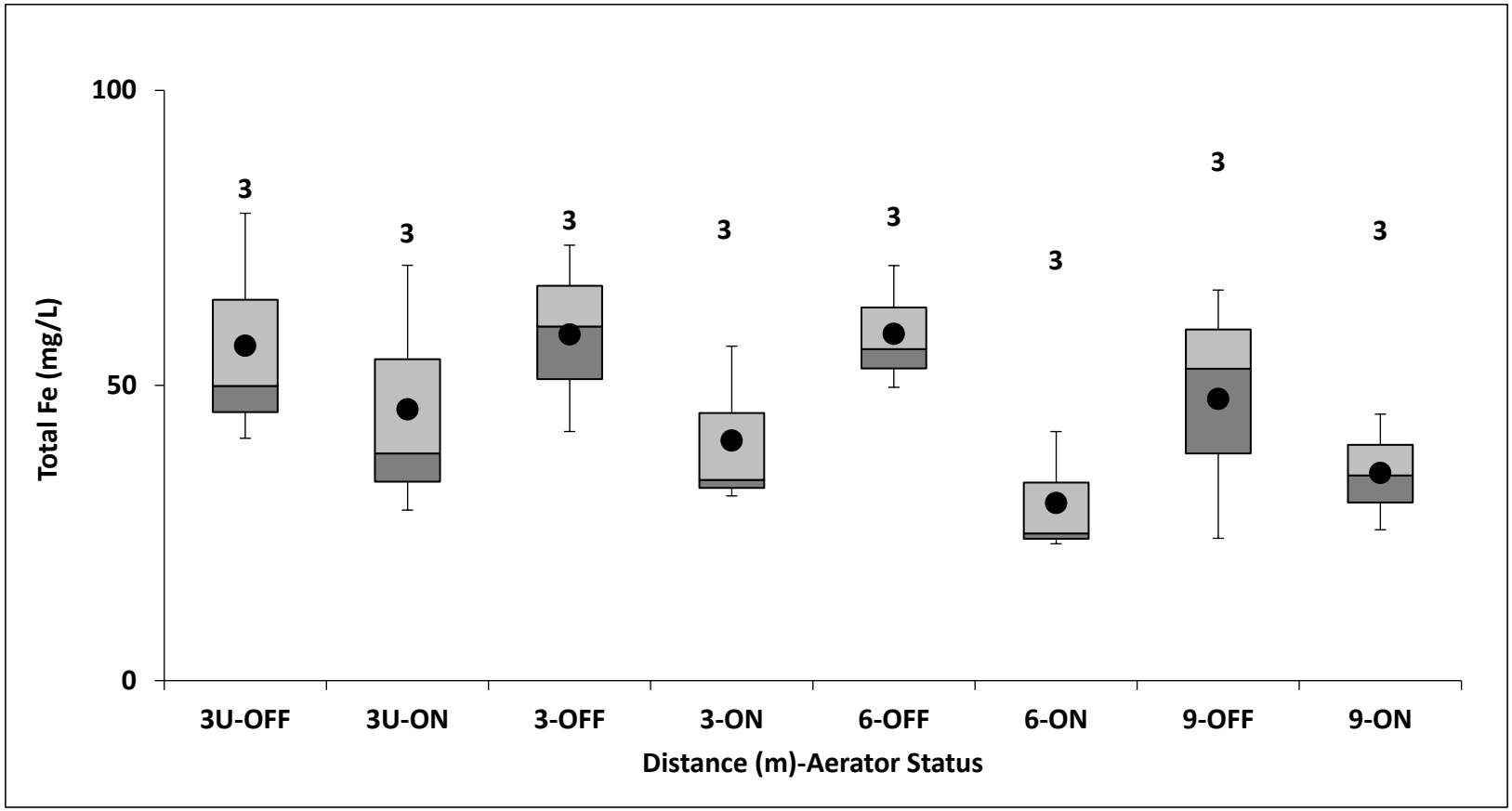

Figure 3.17 Box and whisker plot of total Fe concentrations at each distance from the west float-mix aerator (WFMA) for the ON and OFF studies. The points represent the mean value for each data set and the numbers above the plot represent *n*, the sample size for each data set.

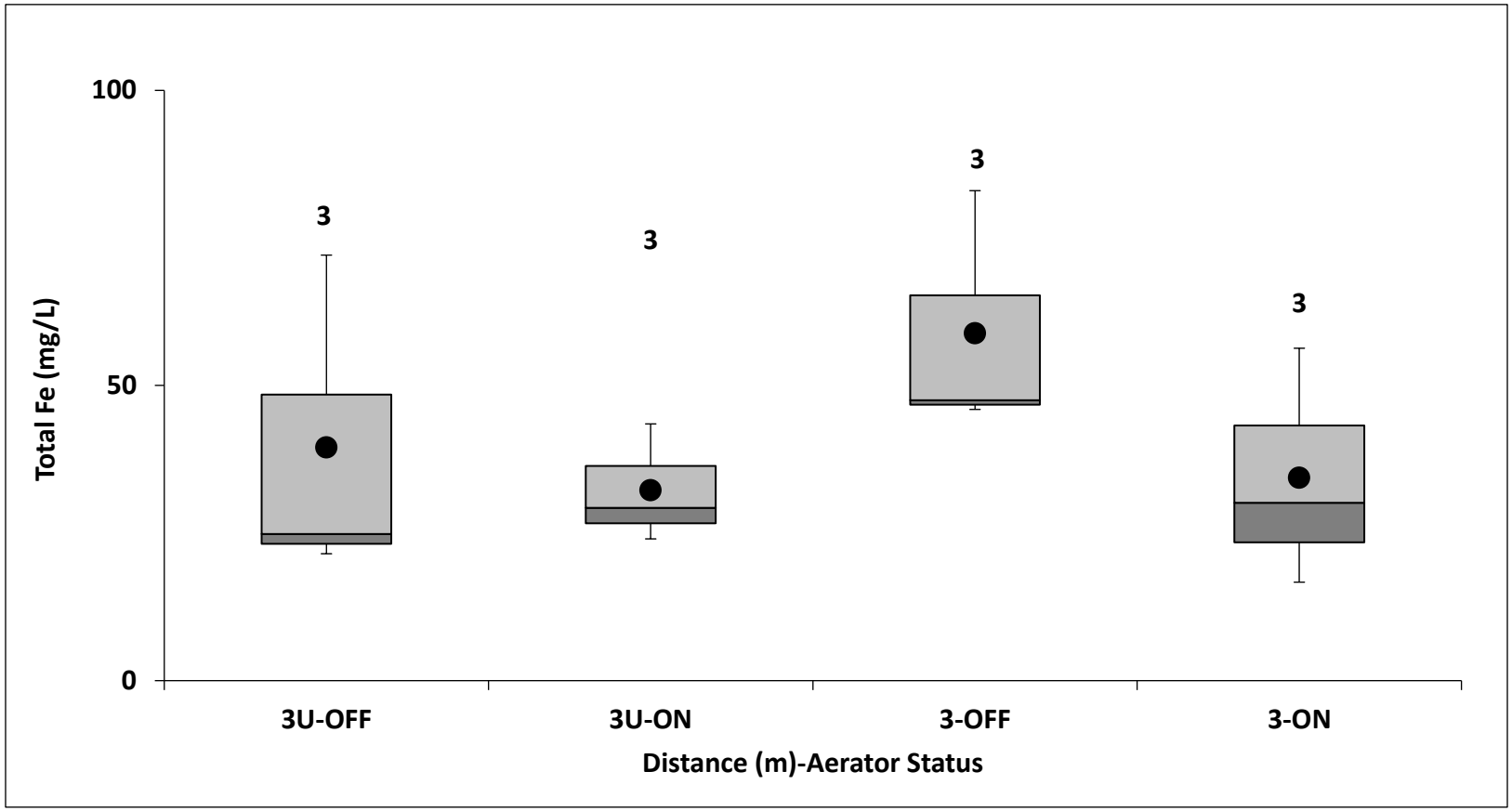

Figure 3.18 Box and whisker plot of total Fe concentrations at each distance from the east float-mix aerator (EFMA) for the ON and OFF studies. The points represent the mean value for each data set and the numbers above the plot represent *n*, the sample size for each data set.

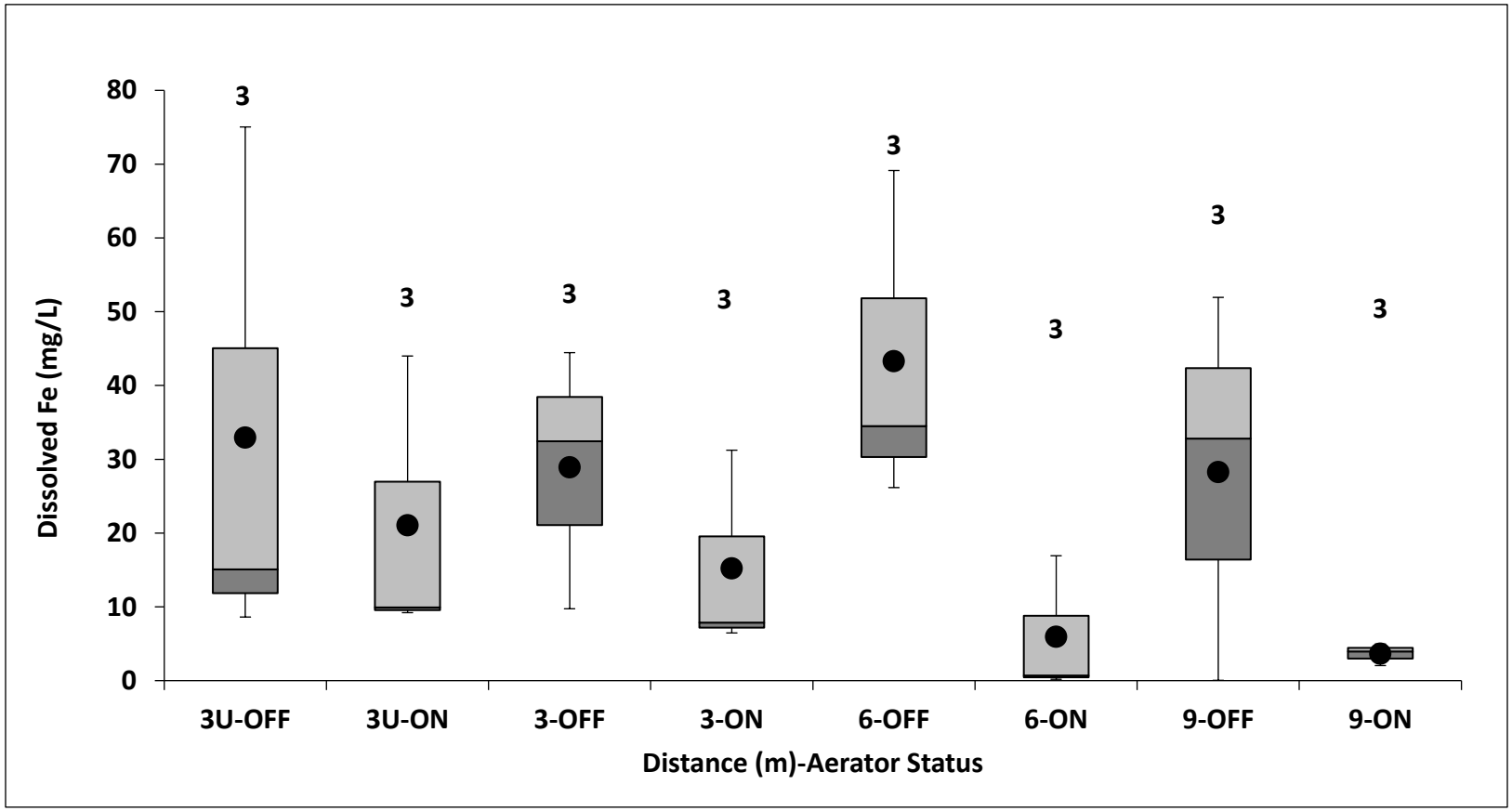

Figure 3.19 Box and whisker plot of dissolved Fe concentrations at each distance from the west float-mix aerator (WFMA) for the ON and OFF studies. The points represent the mean value for each data set and the numbers above the plot represent *n*, the sample size for each data set.

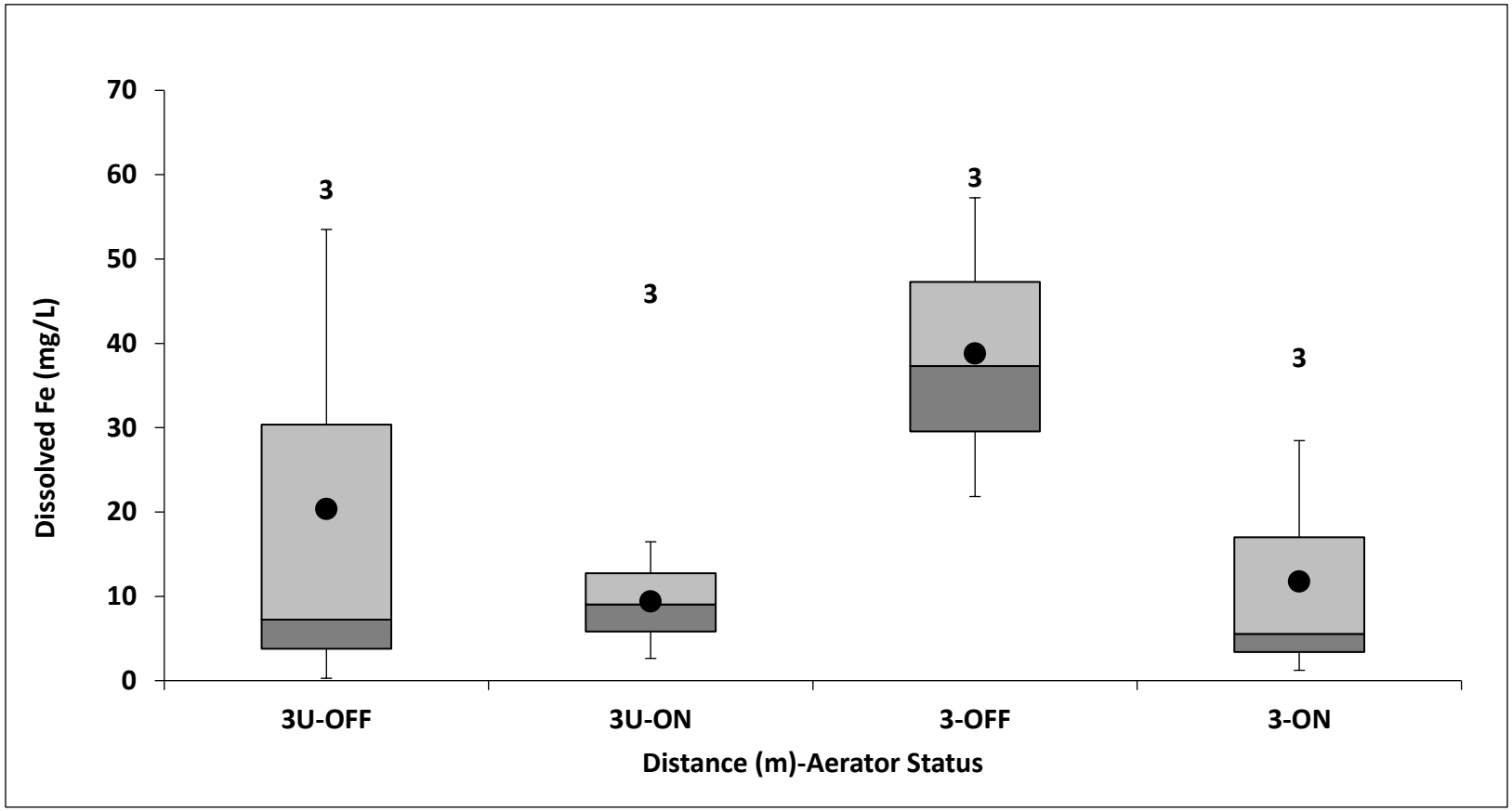

Figure 3.20 Box and whisker plot of dissolved Fe concentrations at each distance from the east float-mix aerator (EFMA) for the ON and OFF studies. The points represent the mean value for each data set and the numbers above the plot represent *n*, the sample size for each data set.

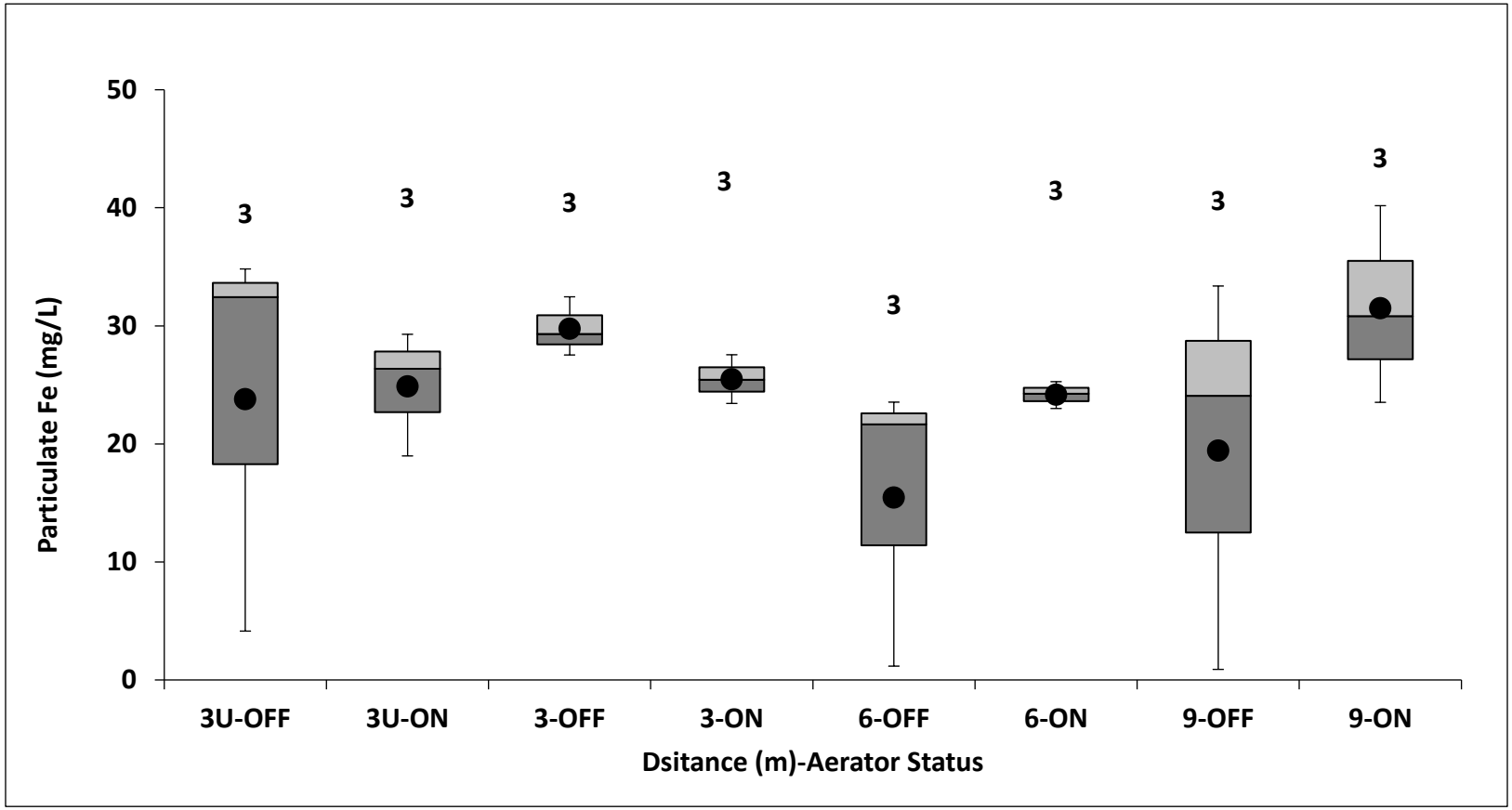

Figure 3.21 Box and whisker plot of particulate Fe concentrations at each distance from the west float-mix aerator (WFMA) for the ON and OFF studies. The points represent the mean value for each data set and the numbers above the plot represent *n*, the sample size for each data set.

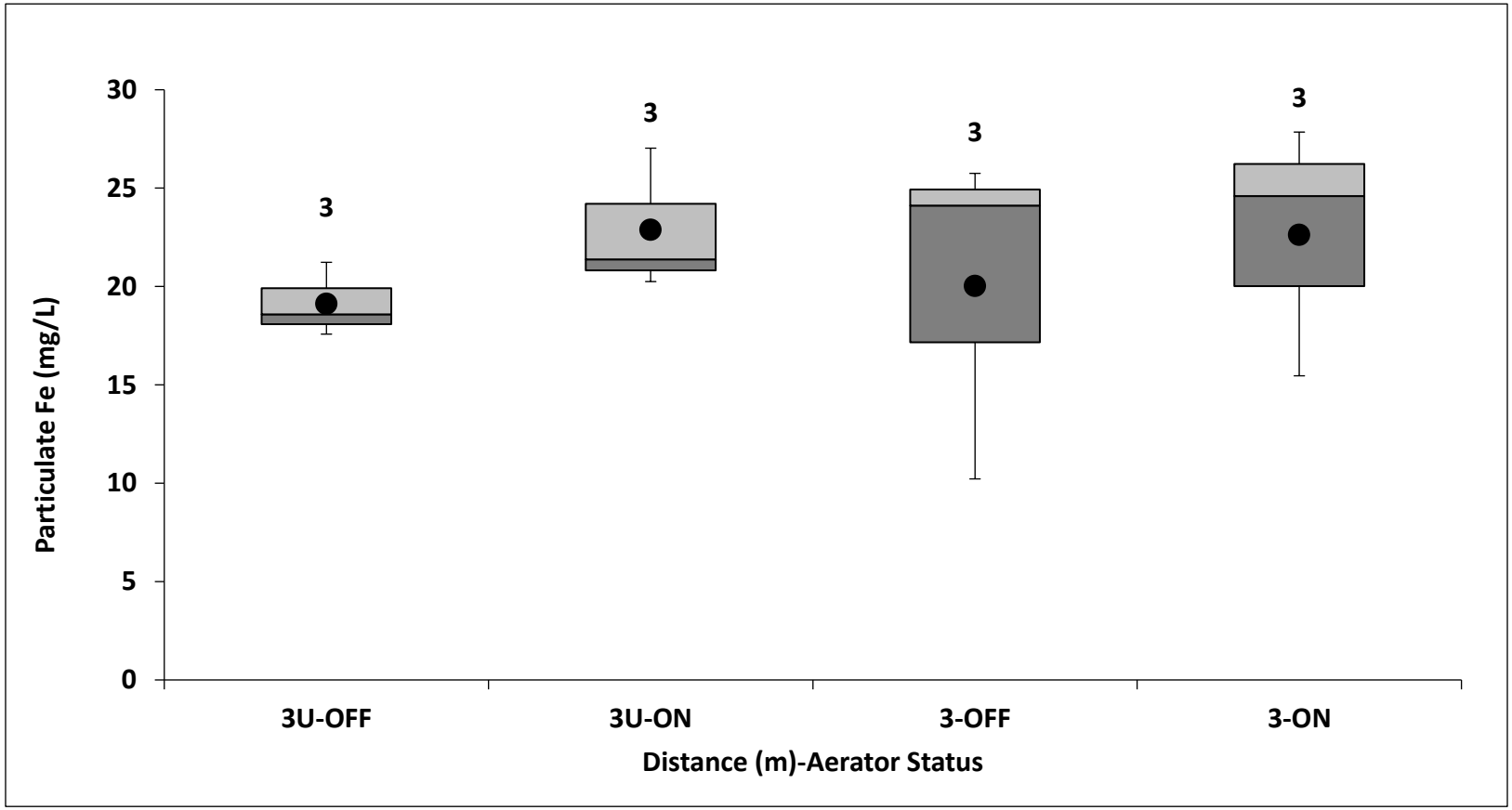

Figure 3.22 Box and whisker plot of particulate Fe concentrations at each distance from the east float-mix aerator (EFMA) for the ON and OFF studies. The points represent the mean value for each data set and the numbers above the plot represent *n*, the sample size for each data set.

It was hypothesized that the aerators ON would increase the amount of Fe precipitated and that the aerators would have a diminished effect with increasing distance from the aerator. The WFMA and EFMA both did not have a statistical difference in particulate Fe between the ON and OFF studies and the WFMA seemed to have a greater effect at 6 m and greater. The greater difference in percent particulate Fe at 6 and 9 m from the WFMA may be due to less interference from the upwellings which discharges raw mine drainage with low DO content and elevated dissolved Fe (II) concentrations.

The lack of statistical difference may also be due rainfall effects on Fe transport. Oxenford (2016) found that there is a positive linear relationship between the amount of Fe transported out of a passive treatment system and the average frequency of storms, because rainfall events disrupt the settling of precipitated flocs within the water column. Table 3.4 shows that the ON study had a higher frequency of rainfall events than the OFF study which means that Fe flocs were less likely to aggregate and settle, thus causing a lower particulate Fe concentration than anticipated.

Table 3.4 Summary of rainfall data collected at the Miami Mesonet station approximately 5 km southeast of the SECPTS

	OFF	**ON**
Maximum Daily Rainfall (cm)	6.83	3.73
Maximum 5-Minute Rainfall Intensity (cm/hr)	13.1	10.7
Total Rainfall During Study Period (cm)	18.1	21.9
Number of Days in Study with Rainfall	10	15
% Days of Study with Rainfall	36%	42%

Another contributing factor from rainfall is a dilution effect on the Fe concentrations. On August 3, 2019 approximately 3.73 cm of rainfall occurred which caused the oxidation pond volume to increase about 5% due to direct precipitation and runoff. This change in volume did not include the three days of rainfall that occurred before that event in which approximately 3.5 cm of rainfall fell. A sampling event was performed on August 6th, 2019. Table 3.5 shows the comparison of percent particulate Fe measured on August 6th compared to the average percent particulate Fe calculated during the other two events. This shows that rainfall dilution and settling disruption caused by rainfall had a substantial effect on particulate Fe concentrations.

Table 3.5 Comparison of percentage of total Fe in particulate form at each distance from the west float-mix aerator (WFMA) and east float-mix aerator (EFMA) for the August 6th, 2019 event to the average between the August 12th and August 20th, 2019 sampling events.

Site	8/6/2019	Average of 8/12/2019 and 8/20/2019 events
WFMA-3U	37.5%	70.9%
WFMA-3	44.9%	77.9%
WFMA-6	59.9%	98.2%
WFMA-9	89.0%	90.3%
EFMA-3U	62.1%	79.1%
EFMA-3	49.5%	87.1%

Although rainfall interference made it difficult to determine if there was statistically greater particulate Fe with the aerators ON compared to when the aerators were OFF, overall,

there was a higher percentage of particulate iron at each sampling location with the aerators ON.

3.4 Conclusions

Aeration technologies that do not require a hydraulic head difference to aerate the water are needed for PTS located in relatively flat landscapes. FMAs are a potential technology that can fill this need. This chapter looked at the FMAs effectiveness with increasing distance from the FMA to determine their radius of influence. It was hypothesized that aeration provided by the FMAs would increase DO and decrease CO_2 concentrations closer to the aerators resulting in more Fe retention nearer to the aerators. This hypothesis was partially accepted because the DO saturation was higher at each location when the FMAs were on compared to when they were off, and this did allow for more Fe to be oxidized thus decreasing the total Fe concentrations and increasing the percent particulate Fe when the aerators were on.

However, pCO_2 concentrations were not always lower when the aerators were on compared to when the aerators were off. This may be attributed to grab alkalinity values not representing the continuous change in pCO_2 and pH. The EFMA showed an increase in pH with the aerators on compared to the aerators off and the pH increased downstream. The WFMA, however, consistently had lower pH when the aerators were on compared to when the aerators were off. This may be due to increased discharge of lower pH mine drainage from the upwelling due to high rainfall events or due to the extreme rise in oxidation pond water elevation that caused the YSI datasonde to be deployed deeper than designed.

Overall, the FMAs improved the water quality of the oxidation pond by increasing DO and facilitating Fe oxidation. The FMAs have a limited influence on pCO_2 and pH at distances greater than 3 m which can limit Fe oxidation rates further downstream.

Chapter 4: Analysis of the Effectiveness of Float-Mix Aerators to Promote Iron Retention Within an Oxidation Pond

4.1 Introduction

Passive treatment systems (PTS) are generally economically favorable technologies for treating mine drainage (Hedin et al. 1994; Hedin 2008; Johnson and Hallberg 2005; Nairn et al. 2009; Skousen et al. 2017; Watzlaf et al. 2004; Younger et al. 2002). PTS are ecologically engineered systems that utilize a combination of geochemical, biological, and physical processes and renewable energy sources to treat mine drainage with little to no chemical or energy inputs (Johnson and Hallberg 2005; Nairn et al. 2009; Skousen et al. 2017; Watzlaf et al. 2004; Younger et al. 2002). Passive treatment is particularly reliable for net-alkaline mine drainage where iron (Fe) can be precipitated as an iron hydroxide or oxyhydroxide and natural alkalinity can buffer increases in proton acidity and maintain a circumneutral pH (Hedin et al. 1994; Hedin 2008; Nairn et al. 2009).

Due to the natural buffering capacity provided by bicarbonate, oxidation ponds are a common initial process unit used to treat net alkaline mine drainage (Hedin et al. 1994; Johnson and Hallberg 2005). Oxidation ponds promote either passive or active aeration which increases dissolved oxygen (DO) concentrations. In net-alkaline waters, a concentration gradient for carbon dioxide (CO_2) exists which causes CO_2 to readily degas into the atmosphere, effectively raising the pH by reducing the amount of carbonic acid in the water. An increase in DO and rise in pH facilitates faster Fe oxidation rates. Under circumneutral pH conditions, dissolved Fe (III)

iron quickly hydrolyzes with water and precipitates to form various Fe oxide and hydroxide species (Younger et al. 2002). Oxidation ponds are recommended to be the first unit in a PTS for mine drainage with an Fe concentration greater than 50 mg/L so that Fe can settle in the oxidation pond before entering wetland or vertical flow bioreactor systems that are more difficult to maintain (Hedin et al. 1994; Younger et al. 2002). For net-alkaline mine water, oxidation ponds are designed using an Fe removal rate of 10 to 20 g Fe m^{-2} day^{-1}, with a retention time based on the initial Fe concentration and acid load (Nairn et al. 2009; Nairn et al. 2018; Skousen et al. 2017; Watzlaf et al. 2004; Younger et al. 2002).

Although oxygen is readily available in the atmosphere and passive diffusion contributes to water quality changes, greater Fe oxidation rates can be achieved by actively introducing oxygen into the water column (Geroni et al. 2012; Hedin 2008; Kirby et al 2007; Leavitt 2011; Nairn et al. 2009; Nairn et al. 2018; Oh et al. 2015; Schmidt 2004). A variety of aeration techniques exist, including cascade aeration and mechanical technologies that actively add air into the system such as air sparging, fine bubble diffusers and floating surface aerators (Geroni et al. 2012; Hedin 2008; Kirby et al 2007; Leavitt 2011; Nairn et al. 2009; Nairn et al. 2018; Oh et al. 2015; Parker and Suttle 1987; Schmidt 2004; Shammas 2007; Zhang et al. 2000). Although cascade aeration effectively aerates the water and is commonly used in PTS, its use is limited to sites that have adequate hydraulic head differences (Geroni et al. 2012). Therefore, a need exists for novel aeration techniques that do not rely on hydraulic head for PTS located in relatively flat landscapes.

Airlift aerators are an aeration technology that can potentially fulfill this need for aeration devices applicable for PTS located in flat landscapes. A literature gap exists regarding the effectiveness of airlift aerators, or float-mix aerators (FMAs), to oxygenate the water, degas CO_2 and promote Fe retention in initial oxidative units of PTS. Chapter 2 study showed that the FMAs increased DO concentrations and decreased dissolved CO_2 partial pressures at depths of 0.4 m and shallower. Chapter 3 showed that FMAs have a limited influence at horizontal distances greater than 3 m. However, no research has been performed analyzing how FMAs affect the overall performance of oxidative units. This chapter investigated the role the FMAs play in improving the performance of the oxidation pond at the Southeast Commerce Passive Treatment System (SECPTS) in Oklahoma, USA. It was hypothesized that the FMAs would increase DO concentrations, decrease dissolved pCO_2 concentrations, increase pH and promote a higher Fe retention rates when compared to the oxidation pond without active aeration.

4.2 Methods

4.2.1 Site Background and Description

The Tar Creek Superfund Site is an approximately 100 km^2 site in northeastern Oklahoma, located within the Tri-State Mining District which is a 3,077 km^2 area including parts of Jasper and Newton Counties in southwestern Missouri, Cherokee County in southeastern Kansas and Ottawa County in northeastern Oklahoma. Underground mining operations were active in the region from the 1800s to the 1970s in which Pb and Zn sulfide ores were extracted. The mines were abandoned, and the dewatering pumps used by the mines were deactivated in

the 1960s allowing the aquifer to recharge and fill the mines. This resulted in artesian flowing mine discharges and the Tar Creek Superfund Site to become listed on the Comprehensive Environmental Response, Compensation, and Liability Act (CERCLA) National Priorities List (NPL) in 1983.

The SECPTS is one of two PTS constructed to address artesian flowing ferruginous net-alkaline mine drainage discharges in the Tar Creek Superfund Site. The SECPTS has been in operation since February 2017 and treats approximately 500 L/min of mine drainage with elevated metals concentrations (Table 4.1). The SECPTS consists of an initial oxidation pond designed for Fe retention and trace metal sorption, a surface flow wetland that provides additional Fe and trace metal retention, a vertical flow bioreactor that utilizes sulfate-reducing bacteria to promote the formation and retention of metal sulfides, and a final polishing unit consisting of two open-water pools with a wetland shelf in between that removes any remaining sulfide and oxygen demand and reaerates the water before it is discharged into an unnamed tributary of Tar Creek.

Table 4.1 Influent and effluent water quality for the Southeast Commerce passive treatment system in the Tri-State Lead-Zinc Mining District, Oklahoma, USA. Values less than the practical quantitation limit (PQL) are reported as <PQL. The number of sampling events is reported as n.

Sampling location	pH	DO Saturation (%)	Total Alkalinity (mg/L $CaCO_3$)	Cd (µg/L)	Fe (mg/L)	Pb (mg/L)	Zn (mg/L)
S-IN (n=32)	6.06	39.8	387	15	153	0.15	6.89
N-IN (n=29)	6.16	40.6	344	14	133	0.14	6.72
UPW-IN (n=9)	5.88	41.6	305	21	143	0.28	7.062
Effluent (n=34)	6.79	69.4	139	<PQL*	1.31	0.024	0.81

The oxidation pond and final polishing unit each have a set of two FMAs. Each set delivers approximately 50 m^3/min of air via a blower. Figure 4.1 shows a schematic of an FMA used in the oxidation pond and FPU. Air is delivered via an airline and enters the airlift pipe approximately 0.4 m below the water surface. The air-water mixture becomes more buoyant and travels up the airlift pipe and spills across the 1.2 m diameter aluminum plate allowing additional passive diffusion of oxygen to occur.

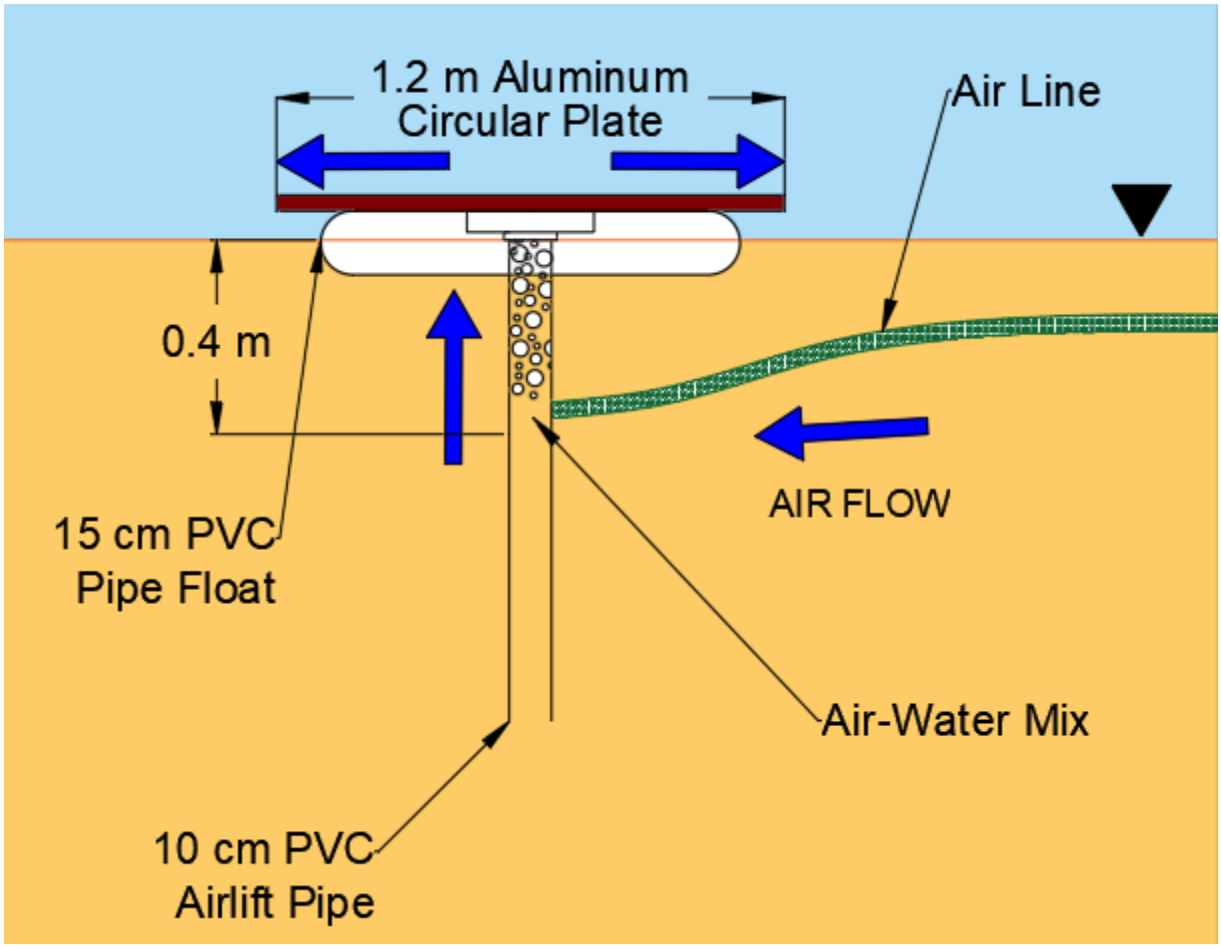

Figure 4.1 Schematic of the float-mix aerator, also known as an airlift aerator, used in the SECPTS.

4.2.2 Water Sample Collection and Analysis

In-situ physical water quality parameters including temperature, specific conductance, ORP, pH and DO were collected every 15 minutes from deployed YSI multiparameter datasondes deployed at the locations shown in Figure 4.2 when the FMAs were off (OFF) and again when they were on (ON). The YSI datasondes were attached to a flotation device so that they could rise and fall with the water elevation and maintain a depth of 0.4 m below the water surface. The YSI datasondes were deployed 0.4 m below the water surface to reduce possible interference of wind and rain on the water quality yet still be shallow enough to record possible changes caused by active aeration. Continuous YSI data for the pond study were collected for the OFF study starting September 21st, 2019 until October 5th, 2019 and for the ON study from October 6th, 2019 to October 31st, 2019 at the locations shown in Figure 4.2. Water quality samples for analysis of alkalinity, turbidity, total and dissolved metals and total suspended solids (TSS) were collected at each location. Water quality samples and physical parameters were collected and measured at each sampling location during the depth and spatial studies as well as during the pond study. Table 4.2 shows the sampling event dates for the ON and OFF studies for each location. A review of historical monthly water quality and quantity data collected for the SECPTS by CREW (2017-2019) was performed to supplement the analysis of the FMAs influence on the oxidation pond. Analyses of water quality samples followed US Environmental Protection Agency (USEPA) methods.

Table 4.2 Dates grab samples were collected for both the ON and OFF studies. Some of these samples were collected during the depth and spatial studies.

	ON	OFF
Grab Samples	April 12th, 2019 June 18th, 2019 June 26th, 2019 July 15th, 2019 August 6th, 2019 August 20th, 2019 October 18th, 2019	August 29th, 2019 September 18th, 2019 September 20th, 2019 September 26th, 2019 October 5th, 2019

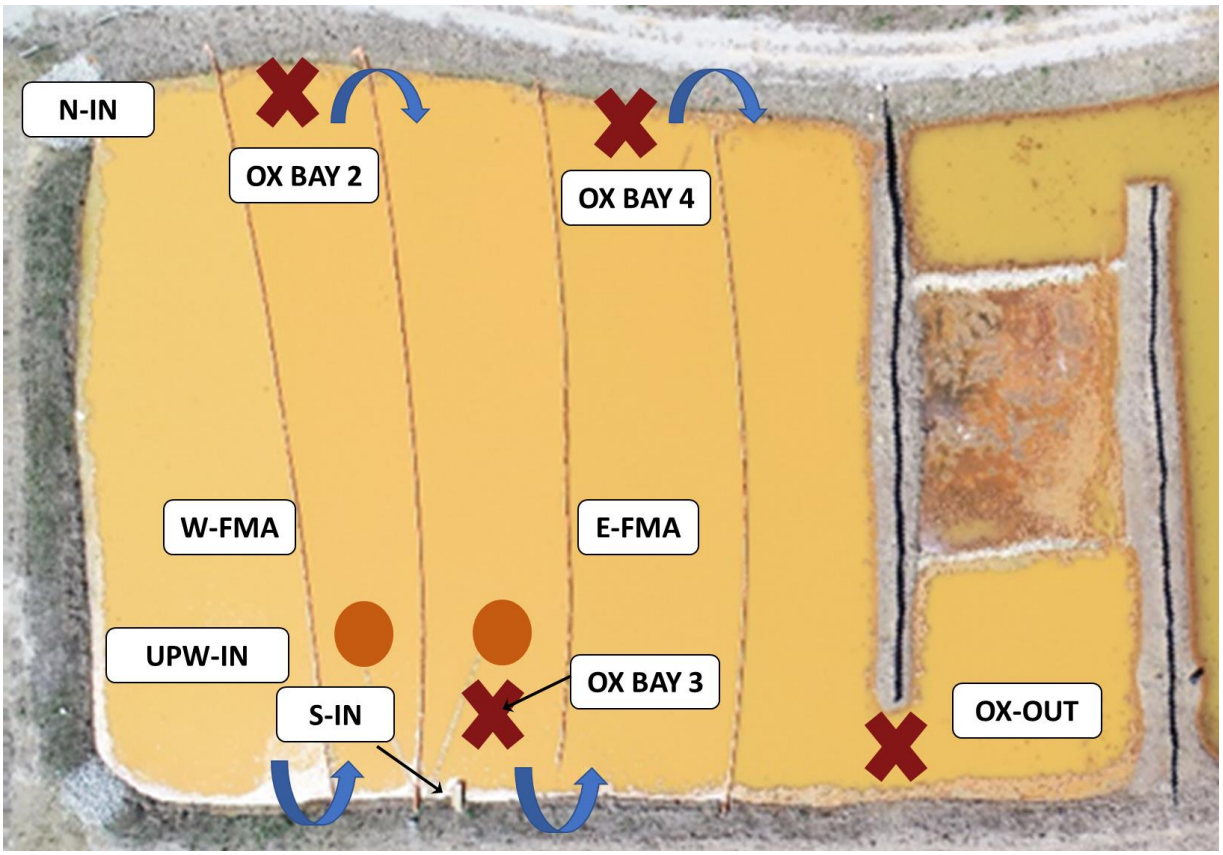

Figure 4.2 Map showing the locations of YSI datasondes deployment and sampling in the Southeast Commerce Passive Treatment System, Oklahoma, USA

4.2.3 pCO_2 Calculation

Temperature, pH and total alkalinity were used to calculate the partial pressure of CO_2 (pCO_2) in the water via the Arrhenius and Henderson-Hasselbalch equations. The Arrhenius equation (Eq. 4.1) is used to correct equilibrium constants for temperature using the enthalpy of the reaction at standard conditions ($\Delta H°_{rxn}$) and the universal gas constant (R) equal to 8.314 J $mole^{-1}$ K^{-1}. The temperature adjusted equilibrium constants, pH and alkalinity were used in the series of Henderson-Hasselbalch equations for carbonate species to calculate pCO_2 as represented by the ionization fraction of CO_2* (α_0), ionization fraction of HCO_3^- (α_1) and the ionization fraction of CO_3^{2-} (α_2), as shown in Equation 4.2 (Jensen 2003; Moran 2010a). The variables are further defined in Chapter 1.

$$K_T = K_{25°}\, exp\left[\left(\frac{-\Delta H°_{rxn}}{R}\right)\left(\frac{1}{T_{25°}} - \frac{1}{T}\right)\right] \tag{4.1}$$

$$P_{CO_2} = \left[\frac{Alk - [OH^-] + [H^+]}{(\alpha_1 + 2\alpha_2)}\right]\left(\frac{\alpha_0}{K_H}\right) \tag{4.2}$$

For these calculations, temperature and pH measurements were represented by continuous data collected every 15 minutes throughout the study. Alkalinity was measured during each sampling event. When the alkalinity measurement did not temporally match the temperature and pH measurements, the mean alkalinity between two sampling events was used to calculate pCO_2 values.

4.2.4 Statistical Analyses

Statistical analyses were performed on each of the datasets generated using Microsoft Excel and IBM SPSS Statistics software. The Kolmogorov-Smirnov and Shapiro-Wilk test were used to determine the normality of the dataset. All datasets were found to be non-parametric and thus the Mann-Whitney U-test and Mood's Median test were used to compare the independent ON and OFF datasets. The null hypothesis for the Mann-Whitney U-test is that the distributions between variables were identical. The null hypothesis for the Mood's Median test was that the medians of the populations are identical. A 95% confidence interval was used for all analyses in which a p-value greater than 0.05 means acceptance of the null hypothesis.

4.3 Results and Discussion

4.3.1 Dissolved Oxygen and Carbon Dioxide

Since SECPTS came online in February 2017, monthly water quality and quantity data have been collected at the inlets of the system and the outlet of each unit in order to assess the performance of each unit in the system. The data in Table 4.3 represent the performance of the oxidation pond when the aerators are on as designed. This historical data shows that the oxidation pond increases DO by over 100%, degasses approximately half of the CO_2 that comes into the pond, raises pH and removes approximately 93% of the Fe loading before the water enters the wetland unit.

Table 4.3 Comparison of DO saturation (%), pCO_2 (atm), pH, total Fe concentration and Fe loadings for in the influents and effluent of the oxidation pond in the Southeast Commerce Passive Treatment System in Oklahoma, USA based on monthly sampling.

	Site	DO Sat. (%)	pCO_2 (atm)	pH	Total Fe (mg/L)	Fe Loading (kg/d)
	N-IN	40.6 ± 19.5	0.299 ± 0.071	6.16 ± 0.12	133 ± 13	12.4 ± 6.40
Influent	**UPW-IN**	41.6 ± 12.8	0.532 ± 0.095	5.87 ± 0.08	151 ± 11	84 ± 33
	S-IN	39.8 ± 25.0	0.430 ± 0.112	6.06 ± 0.11	153 ± 12	3.09 ± 1.23
Effluent	**OX-OUT**	88.2 ± 37.4	0.160 ± 0.073	5.95 ± 0.18	12.8 ± 8.9	7.83 ± 4.34

In order to determine if the FMAs had an impact on the effectiveness of the oxidation pond, water quality data for locations throughout the oxidation pond were collected and compared when the aerators were off and on. Figures 4.3-4.5 display the descriptive statistics for DO, pCO_2 and pH data collected from deployed YSIs and sampling events at each location (OX BAY 2, OX BAY 3, OX BAY 4 and OX-OUT) for the ON and OFF study. Continuous YSI data generated for OX BAY 2 from September 21st 0:00 to 21:45 were removed due to temporary fouling of the sensors. Similarly, alkalinity values collected on September 26, 2019 were removed due to dilution by excessive rainfall. Approximately 5.48 cm of rainfall fell between September 21st and September 26th causing the water surface elevation of the oxidation pond to rise 0.32 m and the volume to increase by approximately 1,300 m^3. Figures 4.6 and 4.7 show the rainfall amounts and corresponding oxidation pond water surface elevations during the OFF and ON studies, respectively. This increase of water surface elevation and additional volume from rainfall affected water quality. Total alkalinity values in the pond typically range from 100-150 mg/L $CaCO_3$, but on September 26th values around 60 mg/L $CaCO_3$ were measured.

The aerators increased the DO saturation (%) at each location and progressively increased the DO saturation as the water moved from the inlets to the outlet of the oxidation pond (Figures 4.3 and 4.8). This was not the trend observed during the spatial study as discussed in Chapter 3. This is likely because the spatial study looked at changes in DO at a much smaller scale. Therefore, oxygen consumed during the oxidation of Fe was observed in the smaller scale spatial study but was less evident in the pond study. Similarly, elevated DO saturation was observed at all sampling location within the oxidation pond. This may be because biological productivity can contribute to oxygenation. Biomass was observed during sampling events but was not quantified.

It was hypothesized that the increase in DO would decrease pCO_2 and increase pH. However, minimal change was observed in pCO_2 and pH between the ON and OFF studies at each location (Figure 4.9 and Figures 4.10). Table 4.4 shows p-values from a Mann-Whitney U-test which shows that the data from each location besides OX BAY 3 had different distributions. The Mood's median test (Table 4.5) shows that the median pCO_2 were statistically different for every location except for OX-OUT and that pH values were not statistically different between the ON and OFF datasets for each location outside of OX BAY 2, which is supported by Figures 4.9 and 4.10. By the time the water reaches OX-OUT, CO_2 had readily degassed regardless of active aeration resulting in similar median values between the ON and OFF studies.

Table 4.4 Resulting p-values from a Mann-Whitney U-test comparing dissolved oxygen saturation (DO %Sat), carbon dioxide partial pressure (pCO_2) and pH at each location when aerators were on and then off.

Site	DO Saturation	pCO_2	pH
OX BAY 2	<0.001	<0.001	<0.001
OX BAY 3	<0.001	0.297	0.429
OX BAY 4	<0.001	<0.001	<0.001
OX -OUT	<0.001	<0.001	<0.001

Table 4.5 Median values and resulting p-values from a Mood's median test comparing dissolved oxygen saturation (DO %Sat), carbon dioxide partial pressure (pCO_2) and pH at each location when aerators were on and then off.

Site		DO Saturation (%)	pCO_2 (atm)	pH (s.u.)
OX BAY 2	**Off**	0.6	0.036	6.54
	On	39.6	0.135	6.04
	p-value	<0.001	<0.001	<0.001
OX BAY 3	**Off**	0.6	0.117	6.08
	On	46.7	0.118	6.08
	p-value	<0.001	0.014	0.461
OX BAY 4	**Off**	1.0	0.149	5.95
	On	65.7	0.166	5.96
	p-value	<0.001	<0.001	0.122
OX OUT	**Off**	0	0.097	6.16
	On	72.0	0.096	6.15
	p-value	<0.001	0.420	0.870

The OX BAY 3 ON and OFF data were assumed to have similar distributions due to the sampling and deployment location's proximity to S-IN. Water quality from S-IN was consistently highly alkaline with a low DO concentration and circumneutral pH. Although the EFMA was able to aerate the water and increase DO, the constant discharge of mine drainage near the OX BAY 3 location did not allow for much change in the pH and pCO_2 values between the ON and OFF

studies. The lack of statistically significant difference between the median pH and pCO_2 values between the ON and OFF datasets was also likely influenced by the rainfall and change in water elevation and volume. The aerators were able to add oxygen to the water, but the increased volume of water and changes to chemistry of the water due to excessive rain, changes in pCO_2 and pH were more difficult to delineate between the ON and OFF studies.

Chapter 3 showed that the FMAs have limited influence at distances greater than 3 m. The only sampling location near an FMA in this study was OX BAY 3 which was also located near S-IN as previously discussed. OX BAY 2 is located approximately 40 m downstream of the WFMA, while OX BAY 3, OX BAY 4 and OX-OUT are located approximately 10 m, 50 m and 100 m downstream of the EFMA, respectively. Therefore, due to their distance from the FMAs, data from the sampling locations show minimal change in pH and pCO_2. Although steady-state DO concentrations are strictly a function of total air injection rate, steady-state CO_2 concentrations vary with the total air injection rate and the total number of airlift aerators used (Loyless and Malone 1998). Therefore, more significant changes in pCO_2 and pH might be seen if there were more FMAs located throughout the pond delivering the same total air rate.

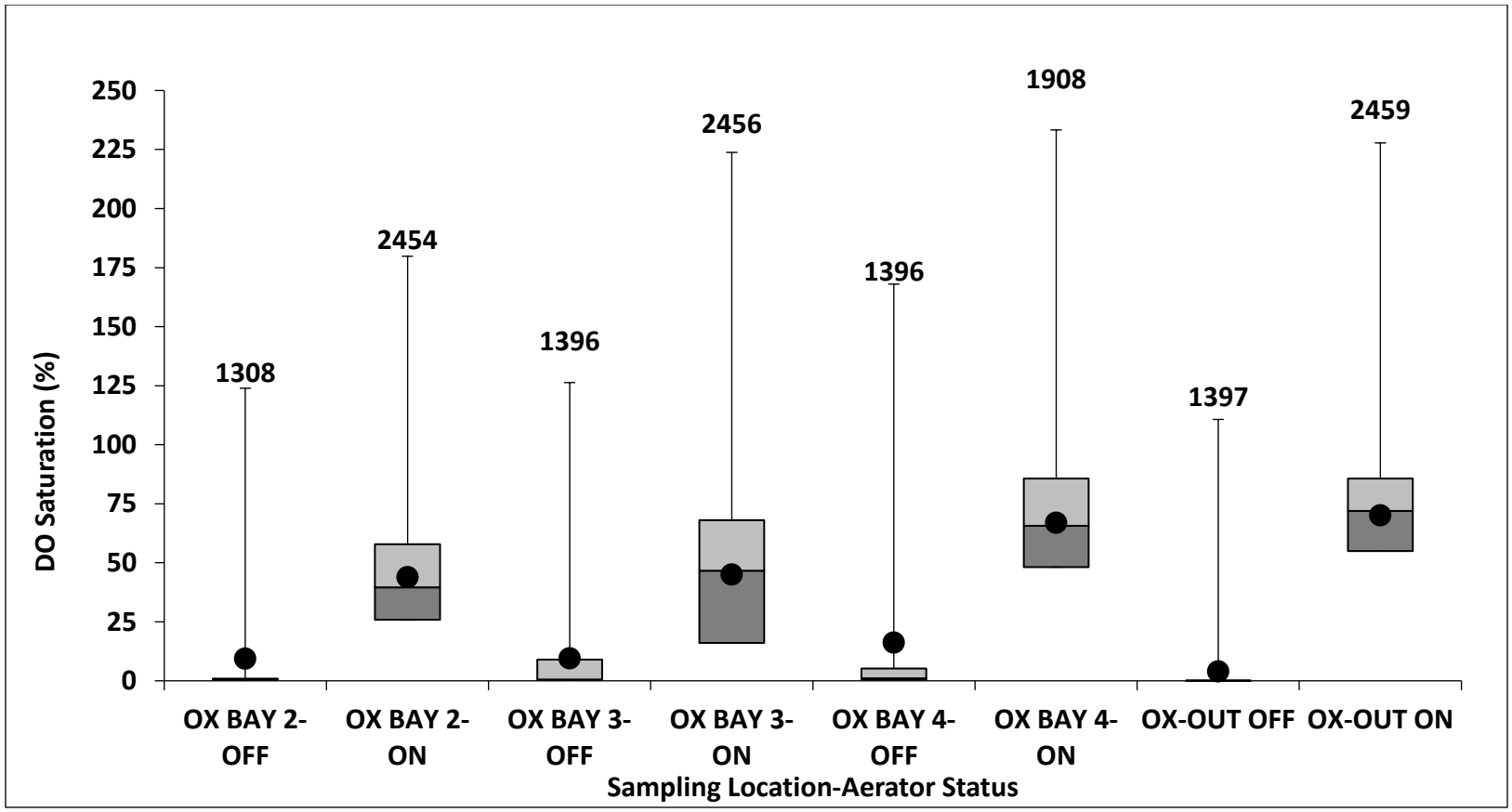

Figure 4.3 Box and whisker plot of dissolved oxygen saturation readings collected at each location within the oxidation pond for the ON and OFF studies. The points represent the mean value for each data set and the numbers above the plot represent n, the sample size for each data set.

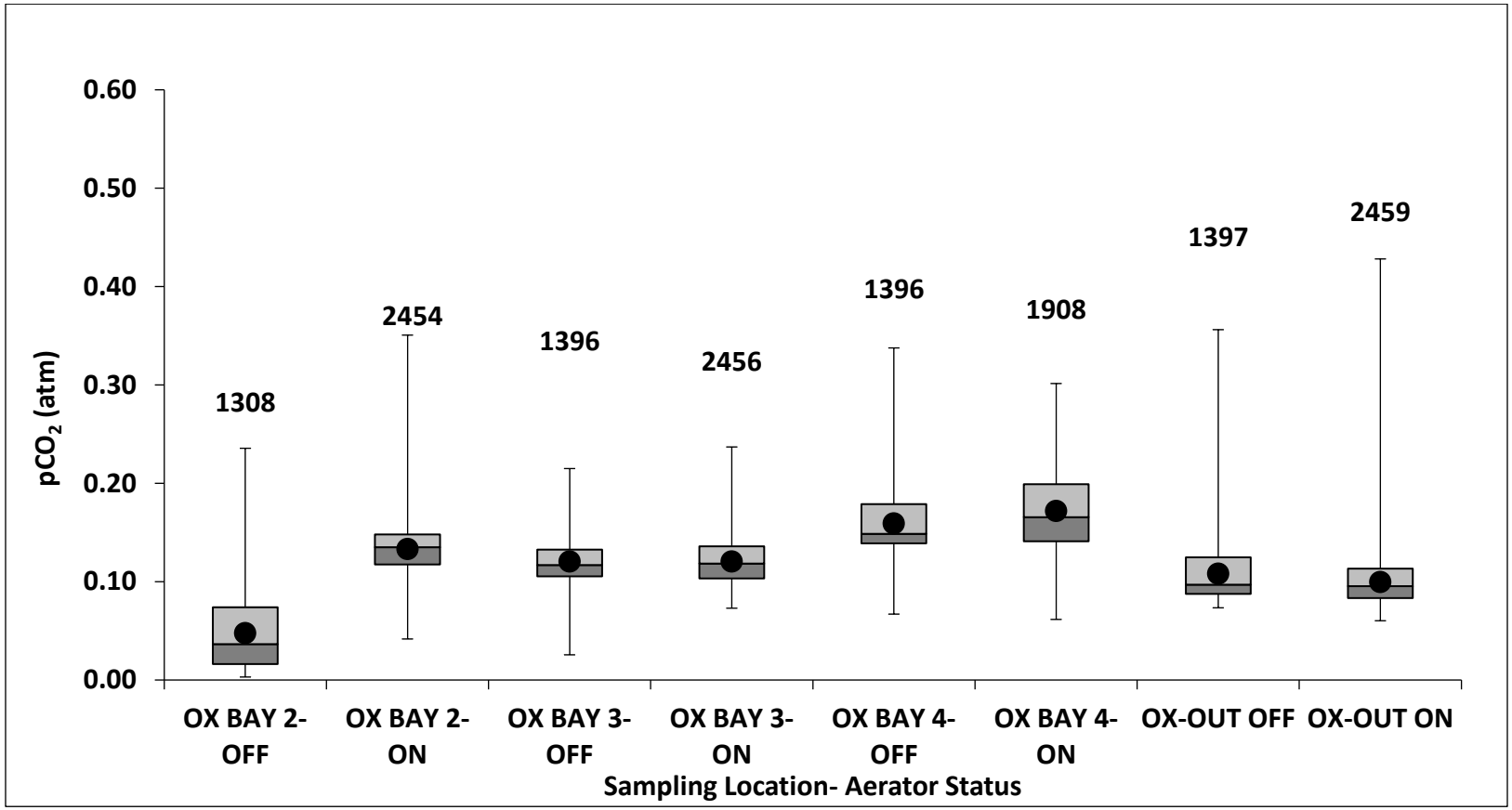

Figure 4.4 Box and whisker plot of dissolved carbon dioxide partial pressures (pCO_2) at each location within the oxidation pond for the ON and OFF studies. The points represent the mean value for each data set and the numbers above the plot represent n, the sample size for each data set.

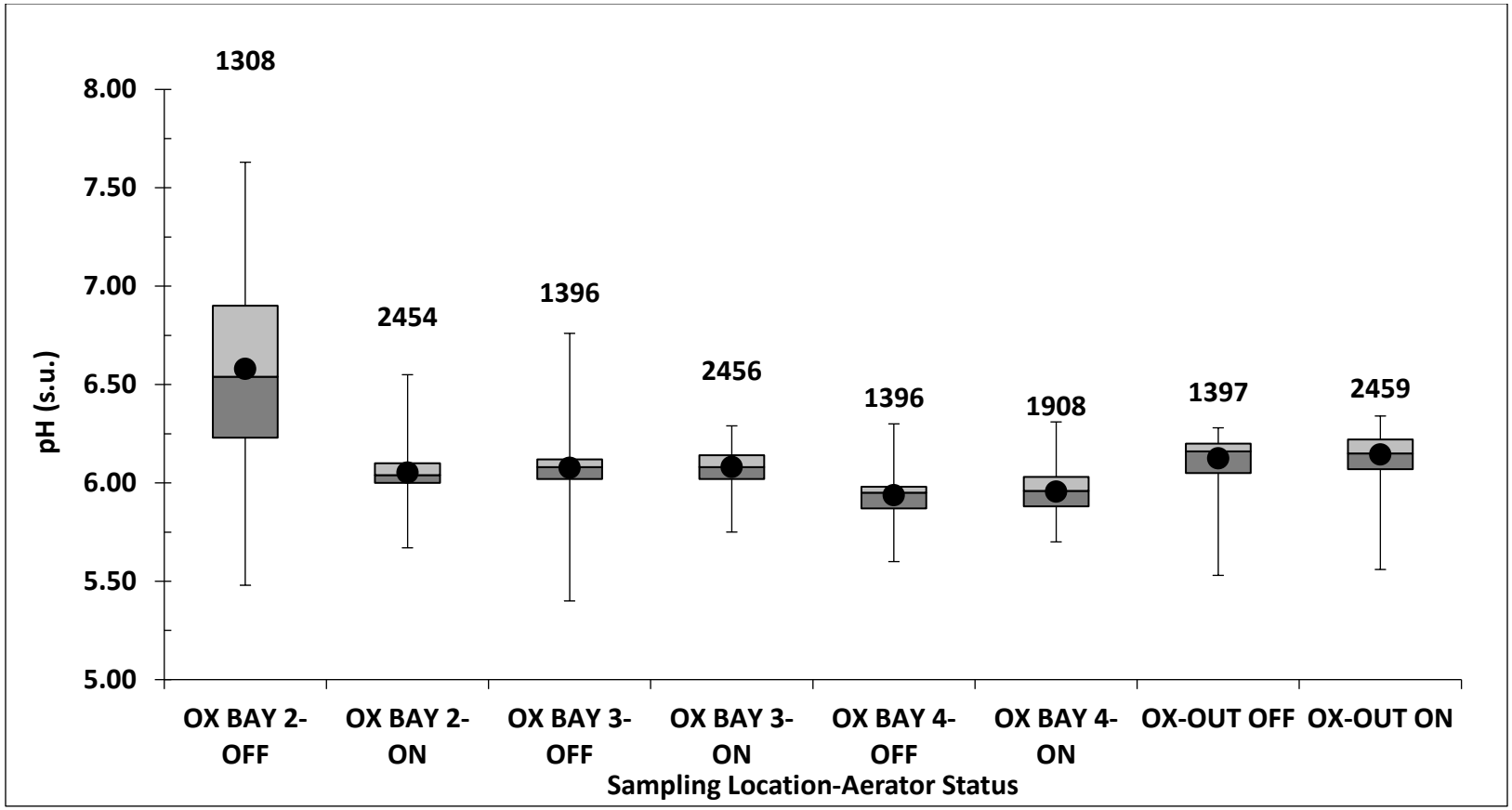

Figure 4.5 Box and whisker plot of pH measurements at each location within the oxidation pond for the ON and OFF studies. The points represent the mean value for each data set and the numbers above the plot represent n, the sample size for each data set.

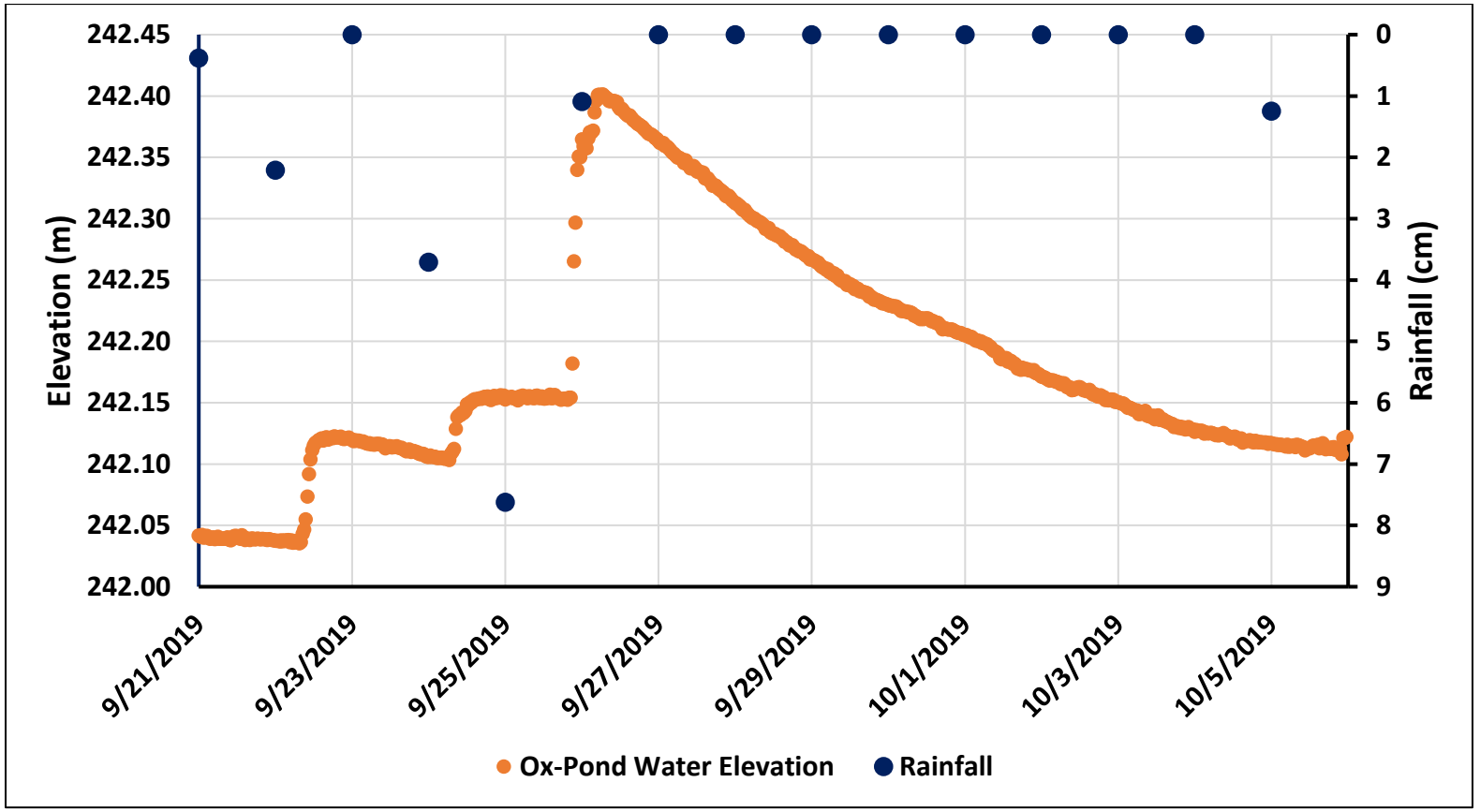

Figure 4.6 Daily rainfall (cm) during the OFF study and the corresponding oxidation pond water elevation (m).

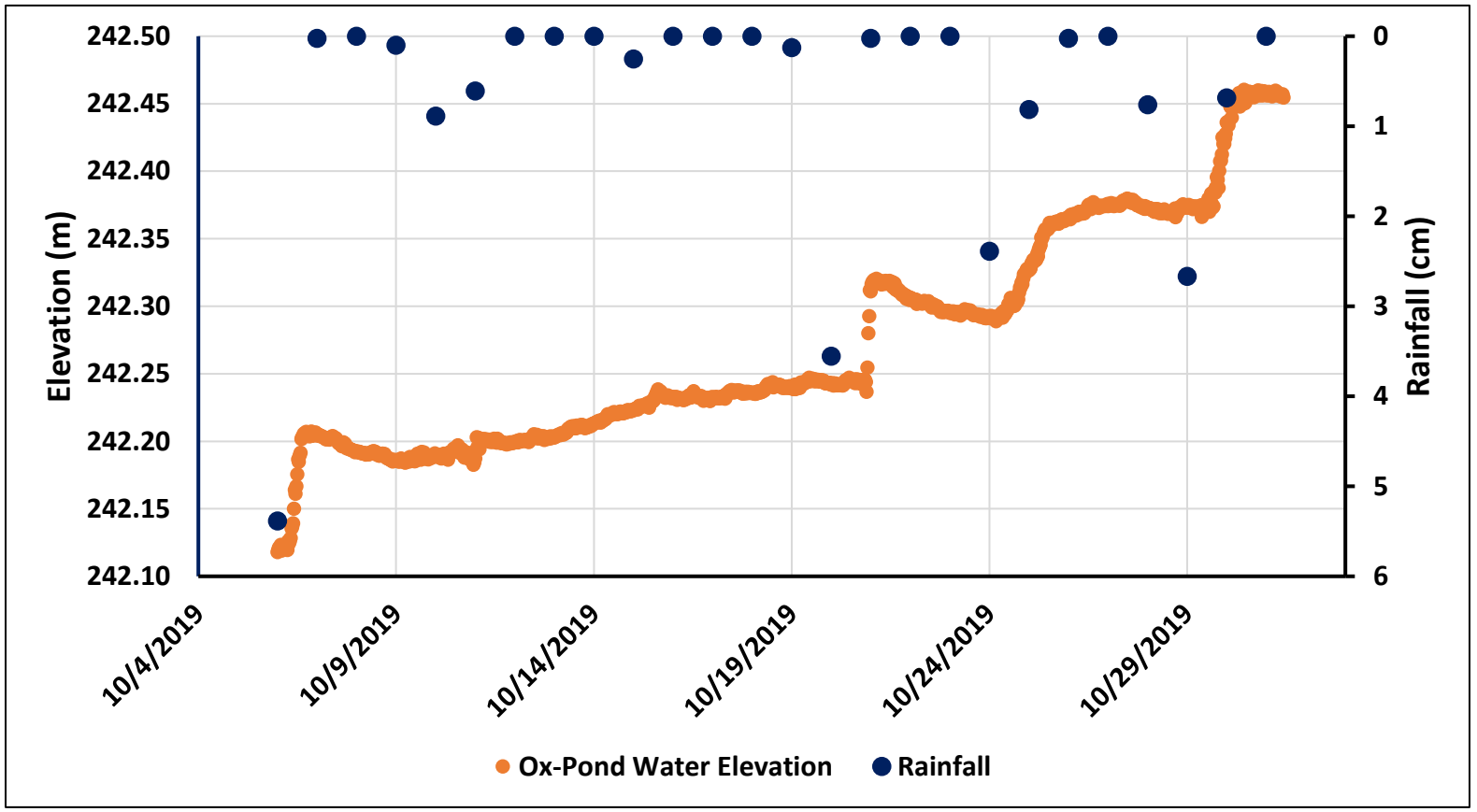

Figure 4.7 Daily rainfall (cm) during the ON study and the corresponding oxidation pond water elevation (m).

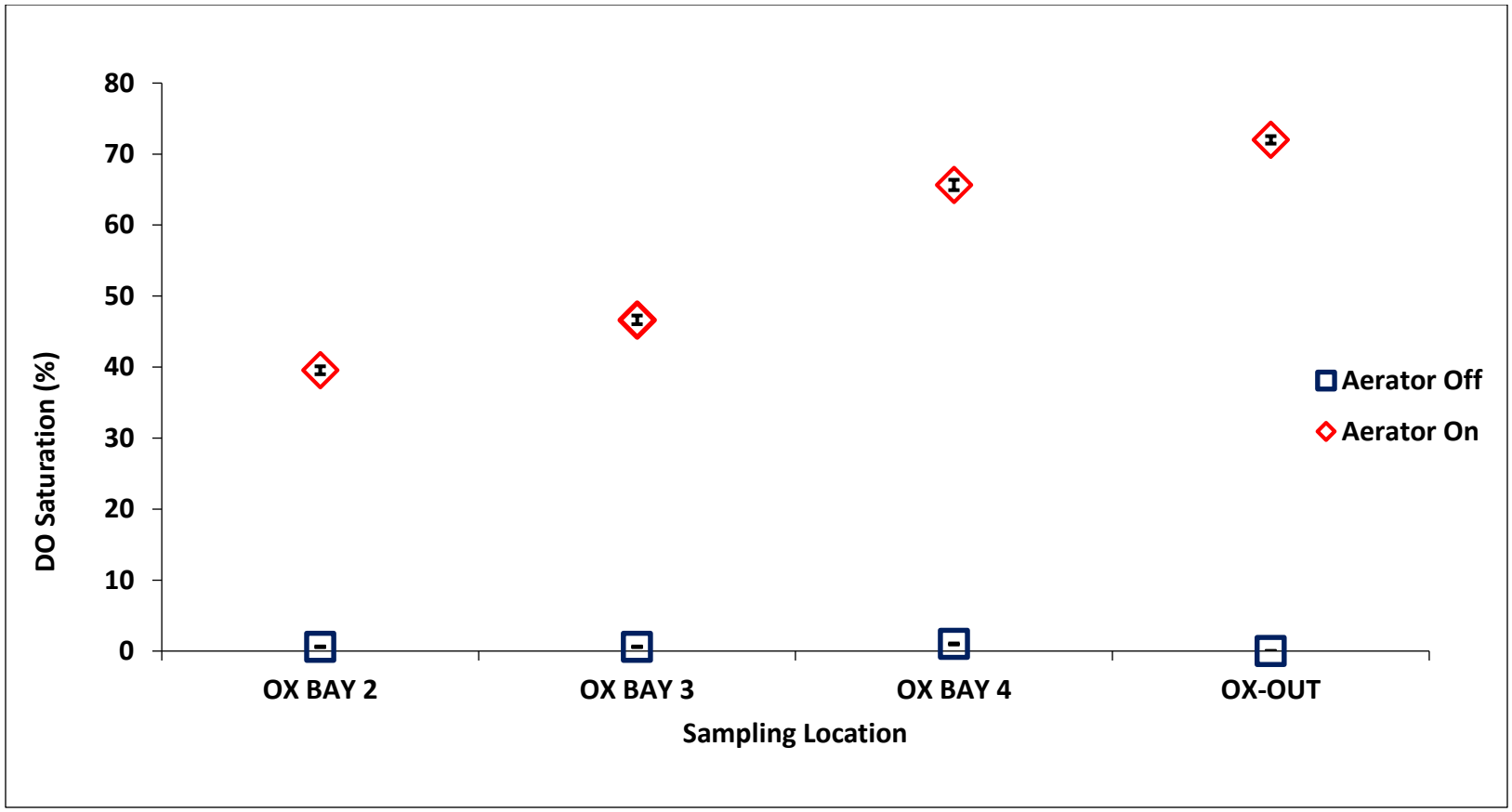

Figure 4.8 Median dissolved oxygen saturation (%) data with standard error bars for each sampling location within the oxidation pond for the ON and OFF studies. Standard error bars may be smaller than the data point.

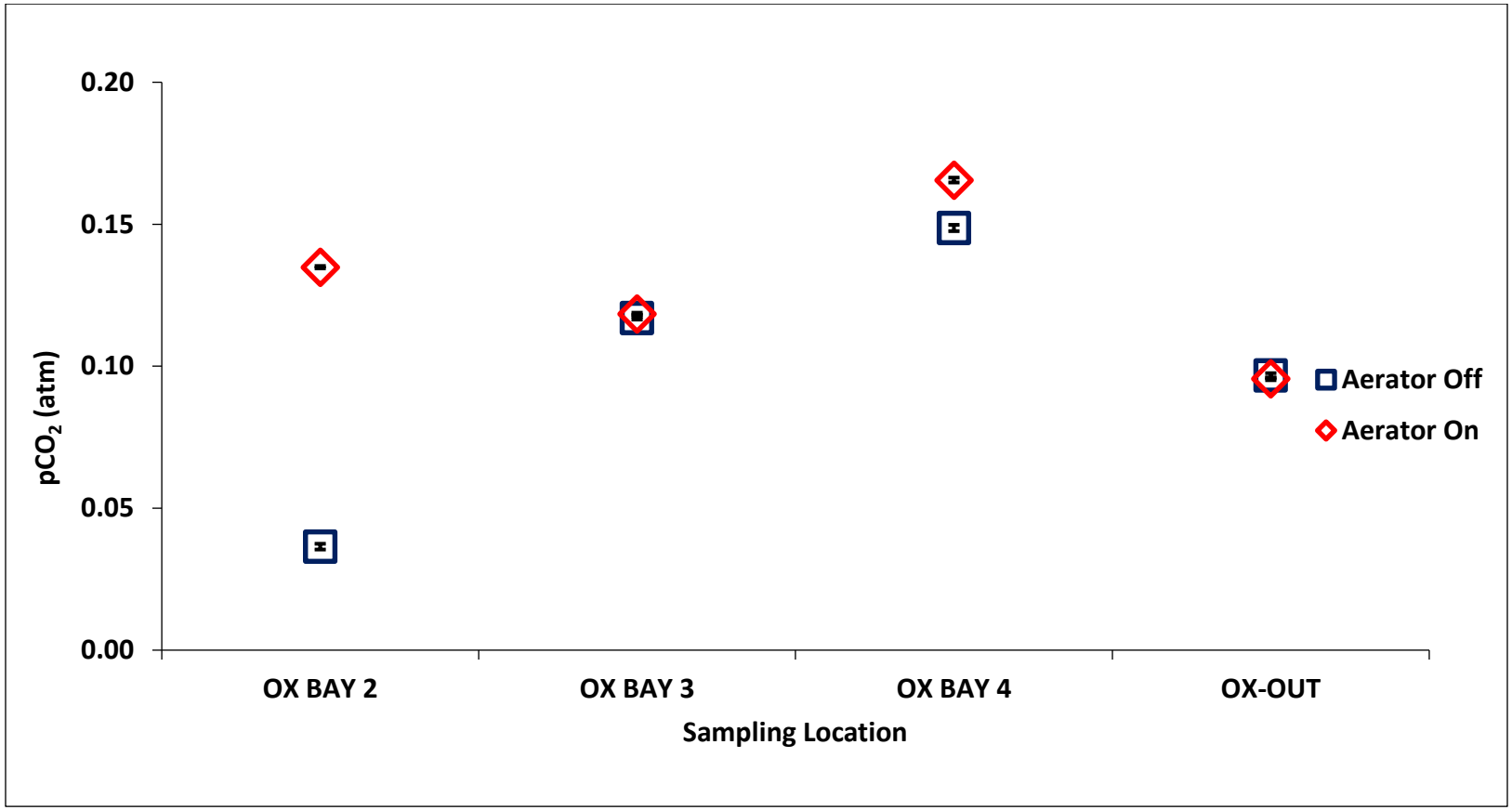

Figure 4.9 Median carbon dioxide partial pressures (pCO_2) data with standard error bars for each sampling location within the oxidation pond for the ON and OFF studies. Standard error bars may be smaller than the data point.

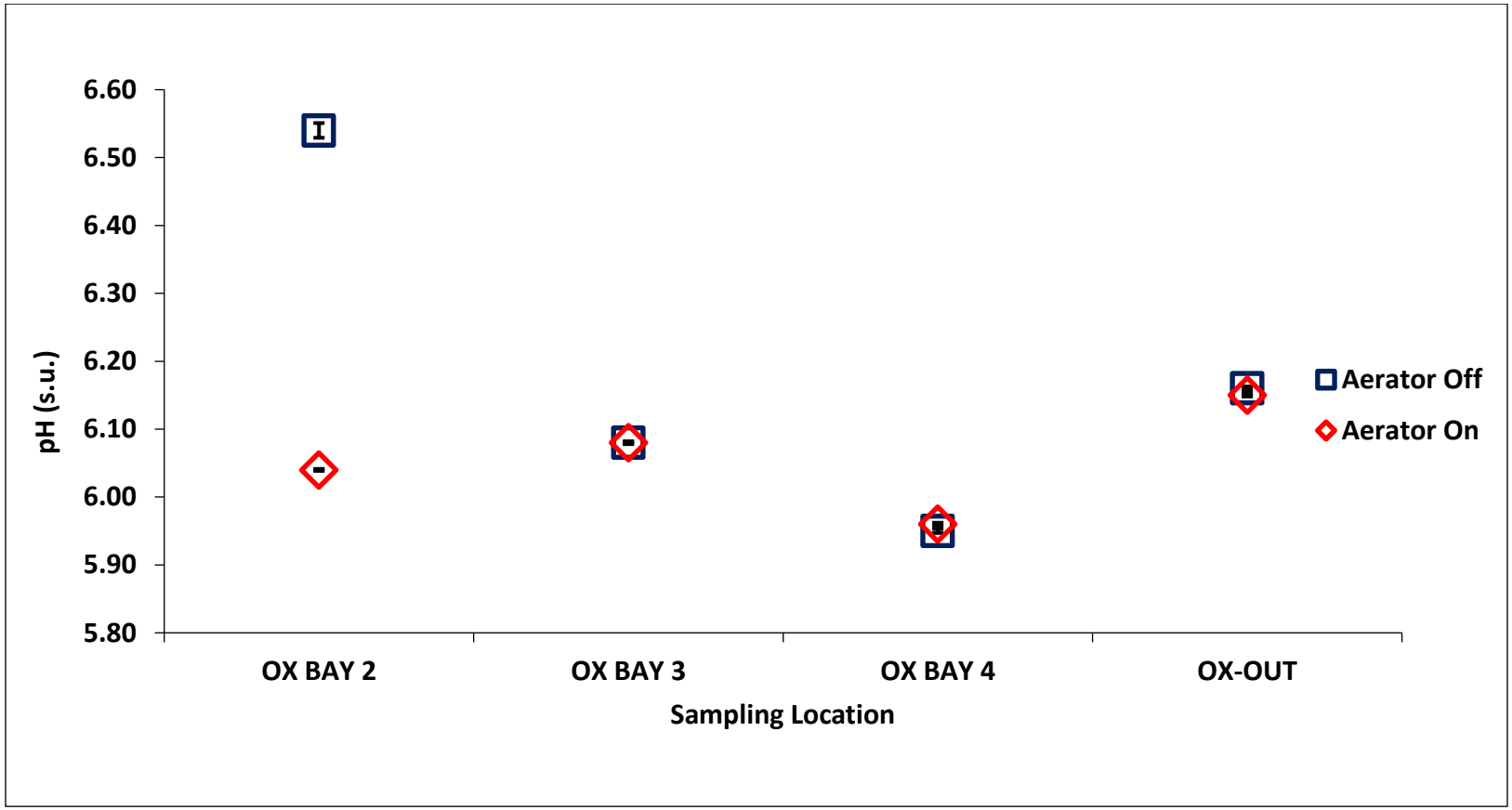

Figure 4.10 Median pH data with standard error bars for each sampling location within the oxidation pond for the ON and OFF studies. Standard error bars may be smaller than the data point.

4.3.2 Solids and Iron Retention

Figures 4.11- 4.14 show box and whisker plots representing TSS, total Fe, dissolved Fe and particulate Fe concentration data collected during the sampling events. Particulate Fe concentration was calculated by subtracting the dissolved Fe concentration from the total Fe concentration. Total Fe, particulate Fe and TSS concentrations were lower during the ON study for every sampling location and decreased from the inlets and outlet of the oxidation pond (Figures 4.15 -4.17). This suggests that aeration promotes faster Fe oxidation which allows for more Fe to be precipitated earlier in the oxidation pond. While the Mood's median test showed there was no statistical difference between the median values, the Mann Whitney U-test showed particulate Fe samples for OX BAY 3 and OX BAY 4 have different distributions (Table 4.6).

Table 4.6 Resulting p-values from a Mann-Whitney U-test comparing total suspended solids (TSS), total, dissolved and particulate Fe concentrations at each location within the oxidation pond when aerators were off and then on.

Site	TSS	Total Fe	Dissolved Fe	Particulate Fe
OX BAY 2	1.00	0.931	1.000	0.931
OX BAY 3	0.073	0.177	0.329	**0.030**
OX BAY 4	0.082	**0.017**	0.792	**0.017**
OX -OUT	0.177	0.181	0.088	0.368

The fraction of total Fe in particulate form was calculated to confirm that the aerators were promoting more Fe oxidation and retention. While the FMAs increased the amount of Fe present in the particulate form, there were no statistical differences in percentage of particulate Fe between the ON and OFF studies. Data from OX BAY 2 showed no difference in

percent particulate Fe between ON and OFF, perhaps due to the distance from the WFMA and from the N-IN and upwelling discharges. By the time the mine drainage from N-IN and the upwellings reached the OX BAY 2 location, enough retention time had passed for passive diffusion of oxygen and thus oxidation of Fe to occur. Water samples collected during this study showed that over 80% of the Fe coming into the system was removed by the time it reached the first sampling location, OX BAY 2. Total Fe concentrations decreased from approximately 140 mg/L in the inlets to about 16 mg/L by the time the water reached the OX BAY 2 location.

However, aeration showed greater effects on increasing percent particulate Fe at the OX BAY 3, which is located near the S-IN inlet. Without active aeration from the FMAs, the dissolved Fe from the S-IN inlet takes longer to oxidize and precipitate as showcased by the lower percentage of particulate Fe when the FMAs were off compared to when they were on. By the time the water reaches the OX BAY 4 location, enough passive diffusion had occurred and retention time had elapsed, for about the same percentage of dissolved Fe to oxidize as when actively aerated by the FMAs. However, active aeration allows for more dissolved Fe to oxidize and precipitate earlier in the oxidation pond allowing more time for the Fe flocs to settle by the time the water exits the oxidation pond. This was evidenced by lower total and particulate Fe concentrations and the increase in percent particulate Fe at the OX-OUT location.

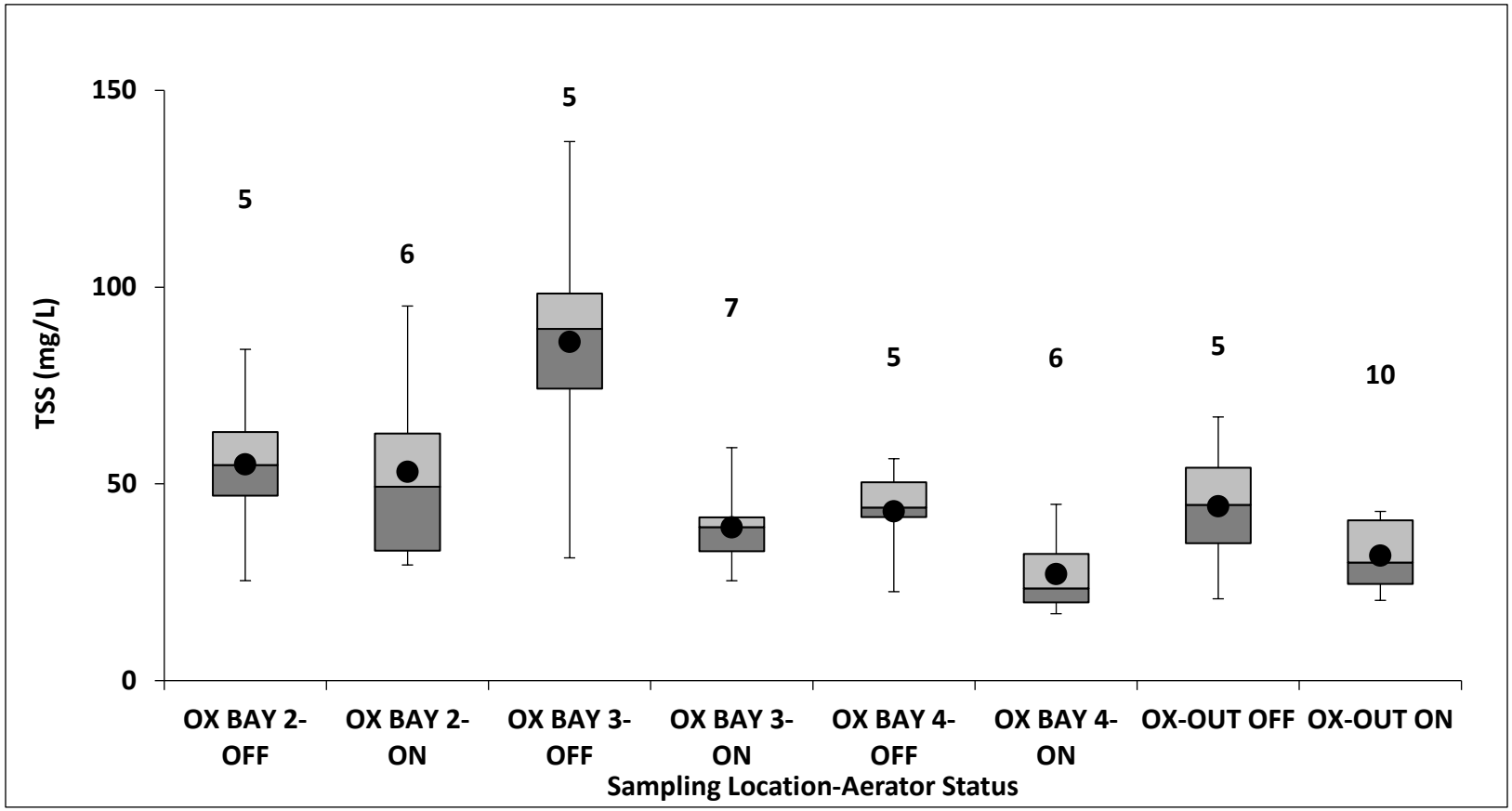

Figure 4.11 Box and whisker plot of TSS concentrations at each location within the oxidation pond for the ON and OFF studies. The points represent the mean value for each data set and the numbers above the plot represent *n*, the sample size for each data set.

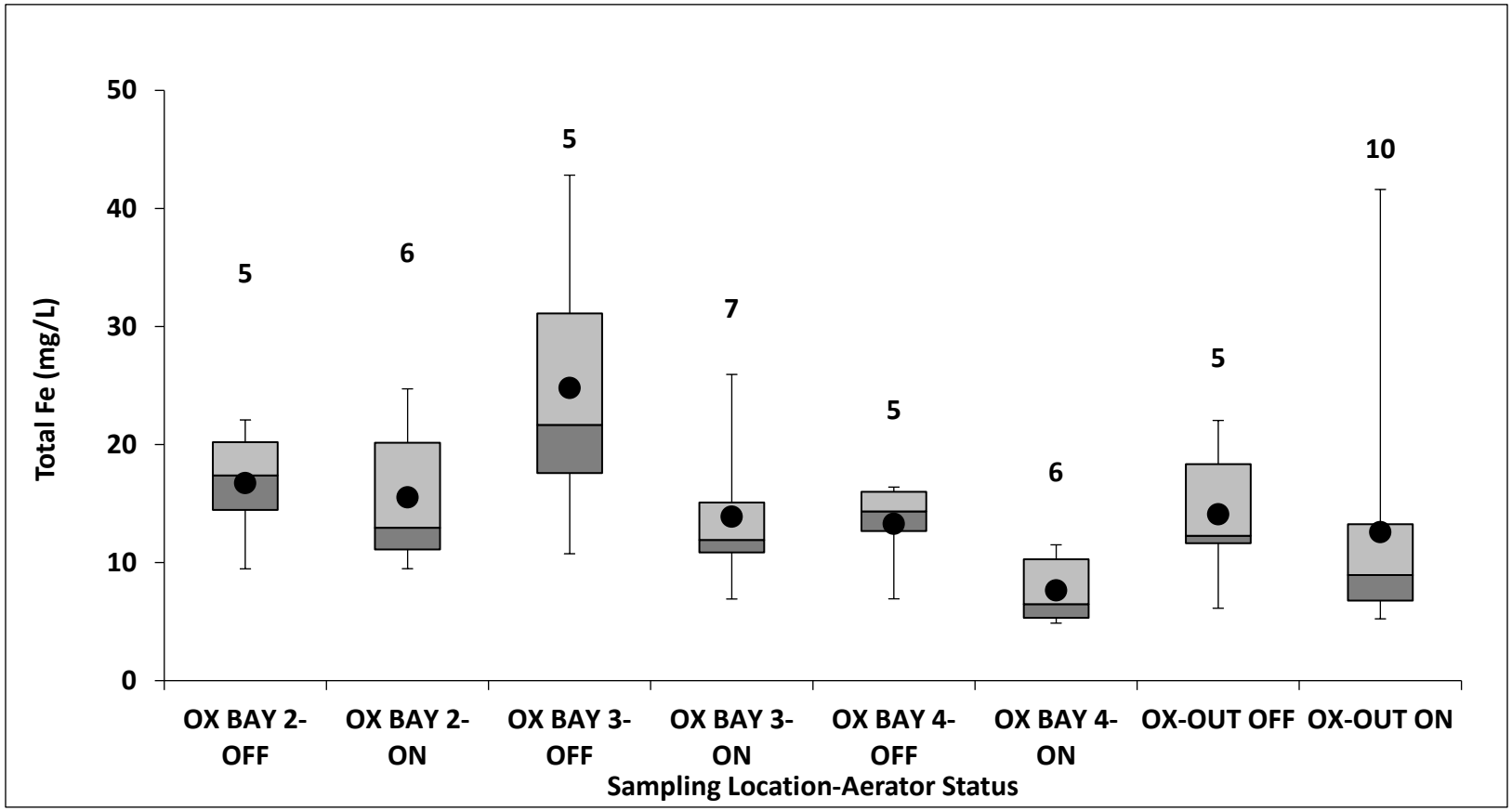

Figure 4.12 Box and whisker plot of total Fe concentrations at each location within the oxidation pond for the ON and OFF studies. The points represent the mean value for each data set and the numbers above the plot represent *n*, the sample size for each data set.

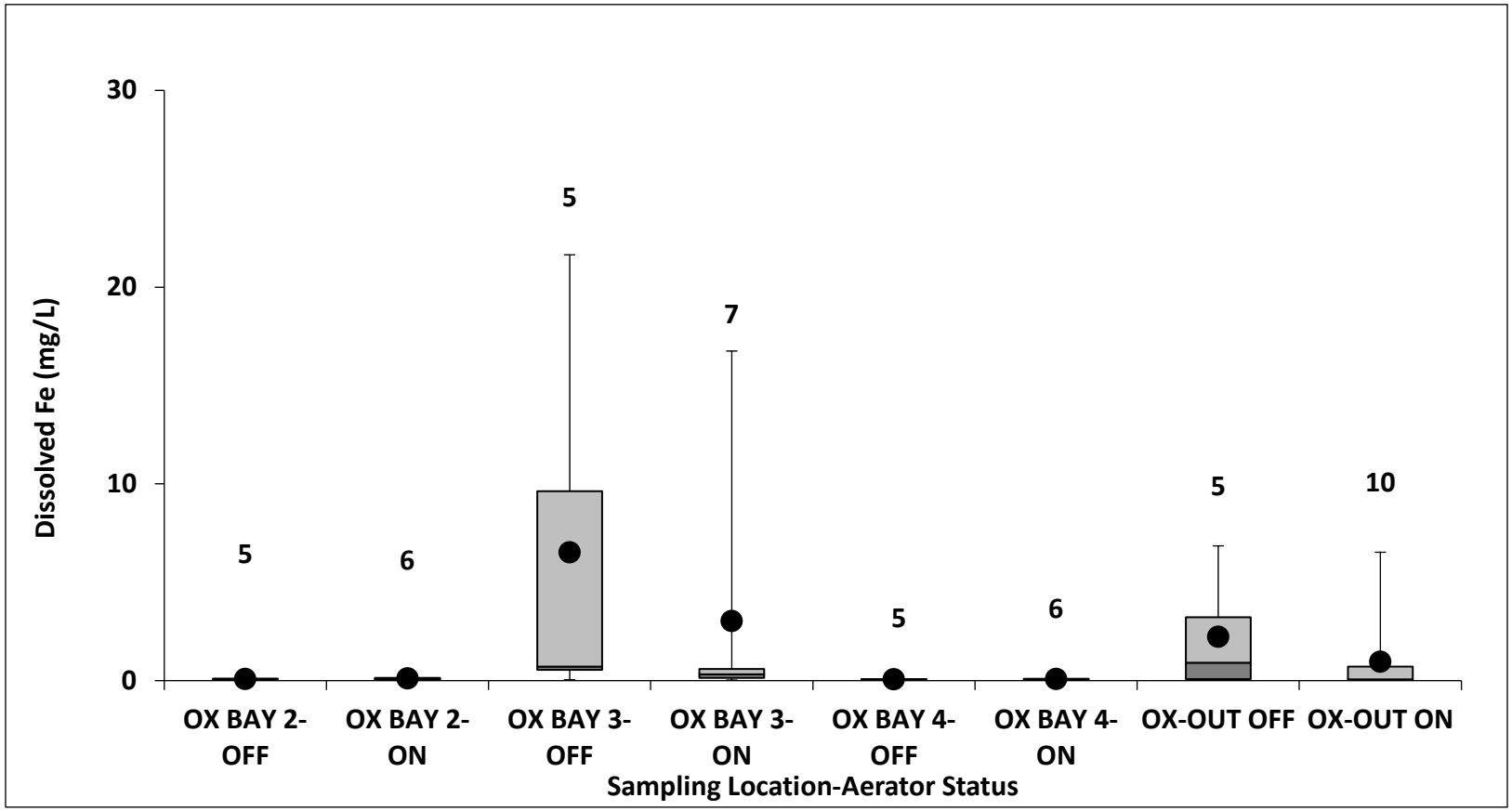

Figure 4.13 Box and whisker plot of dissolved Fe concentrations at each location within the oxidation pond for the ON and OFF studies. The points represent the mean value for each data set and the numbers above the plot represent *n*, the sample size for each data set.

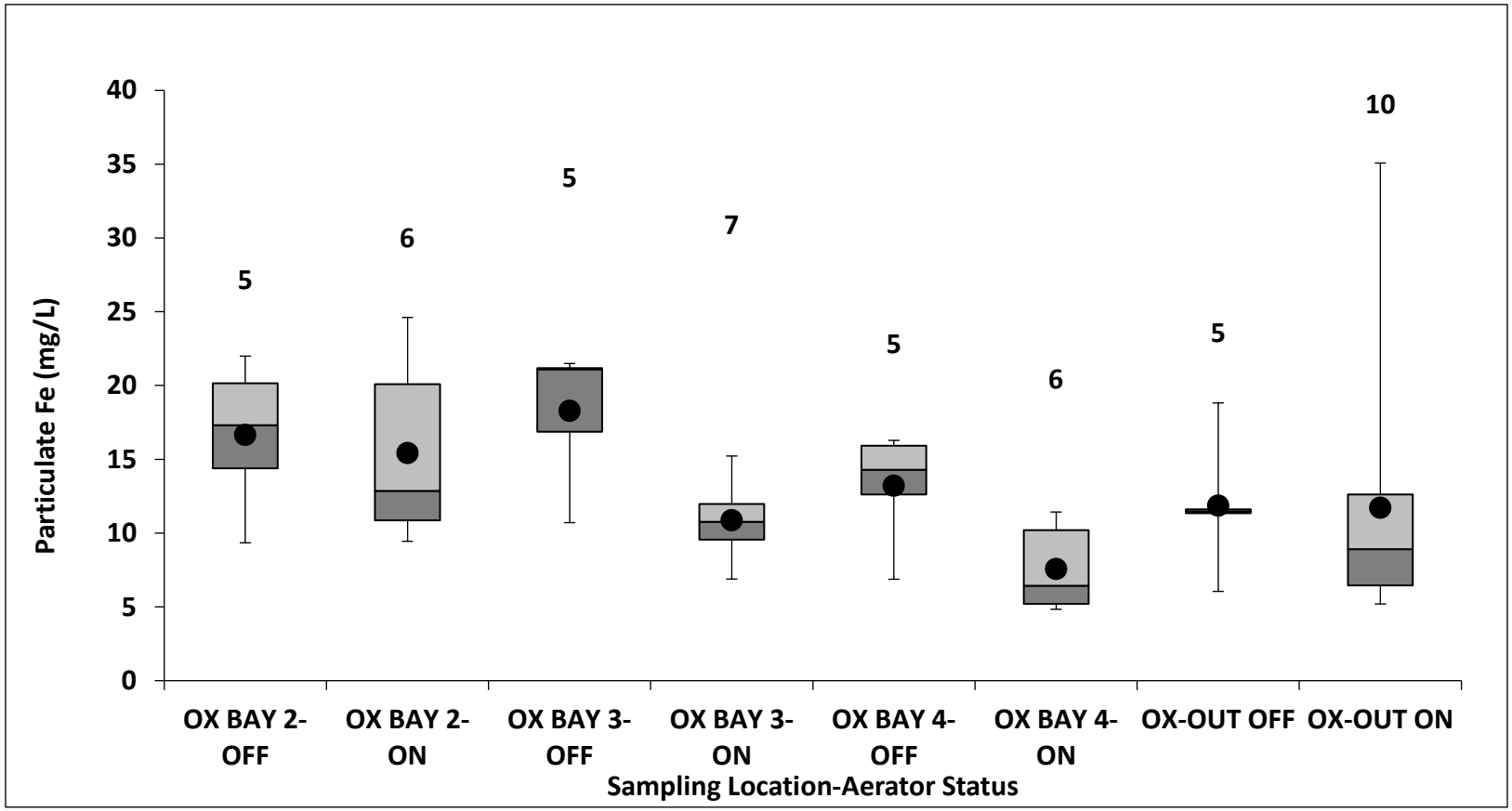

Figure 4.14 Box and whisker plot of particulate Fe concentrations at each location within the oxidation pond for the ON and OFF studies. The points represent the mean value for each data set and the numbers above the plot represent *n*, the sample size for each data set.

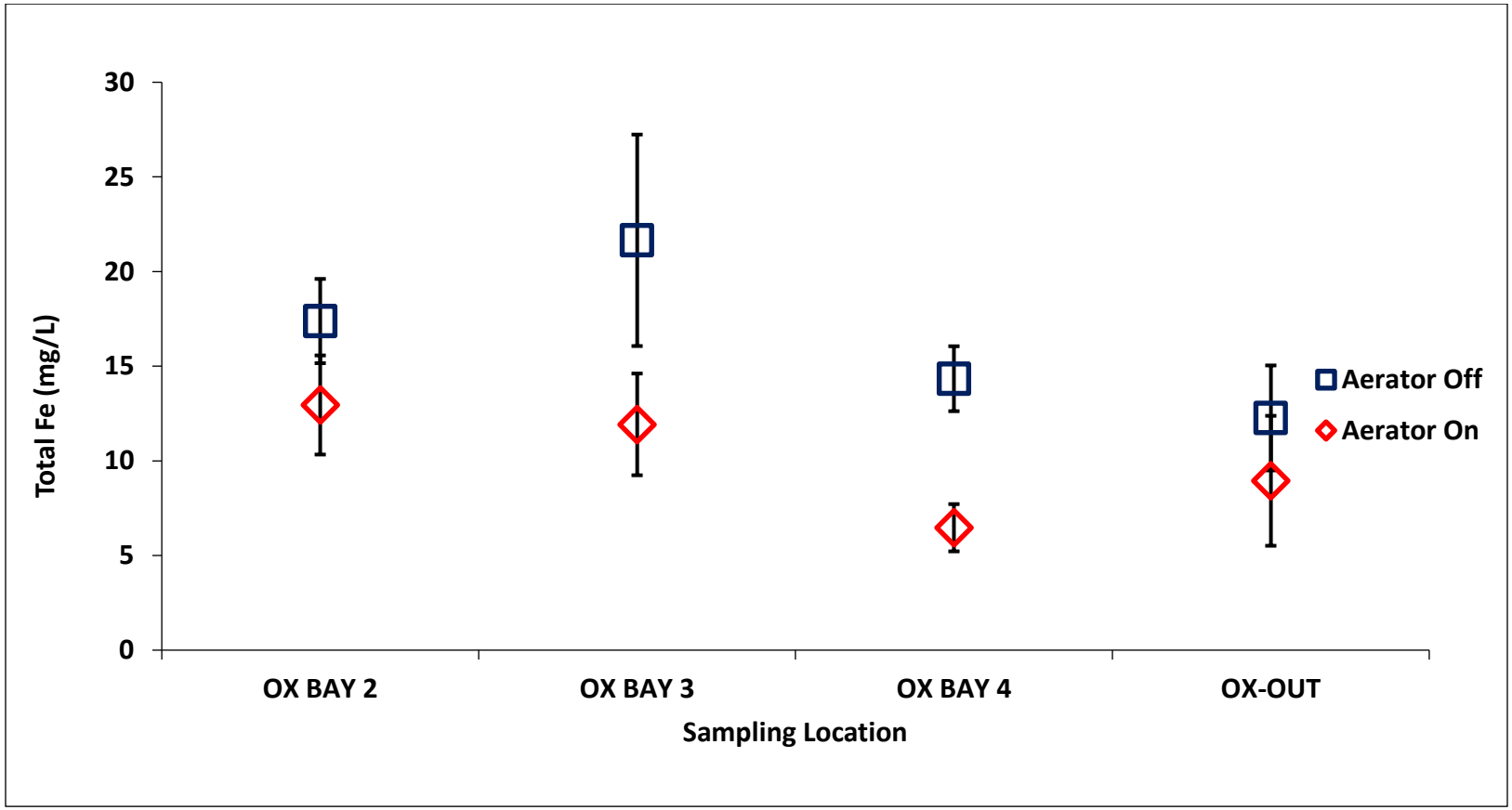

Figure 4.15 Median total Fe concentrations (mg/L) data with standard error bars for each sampling location within the oxidation pond for the ON and OFF studies.

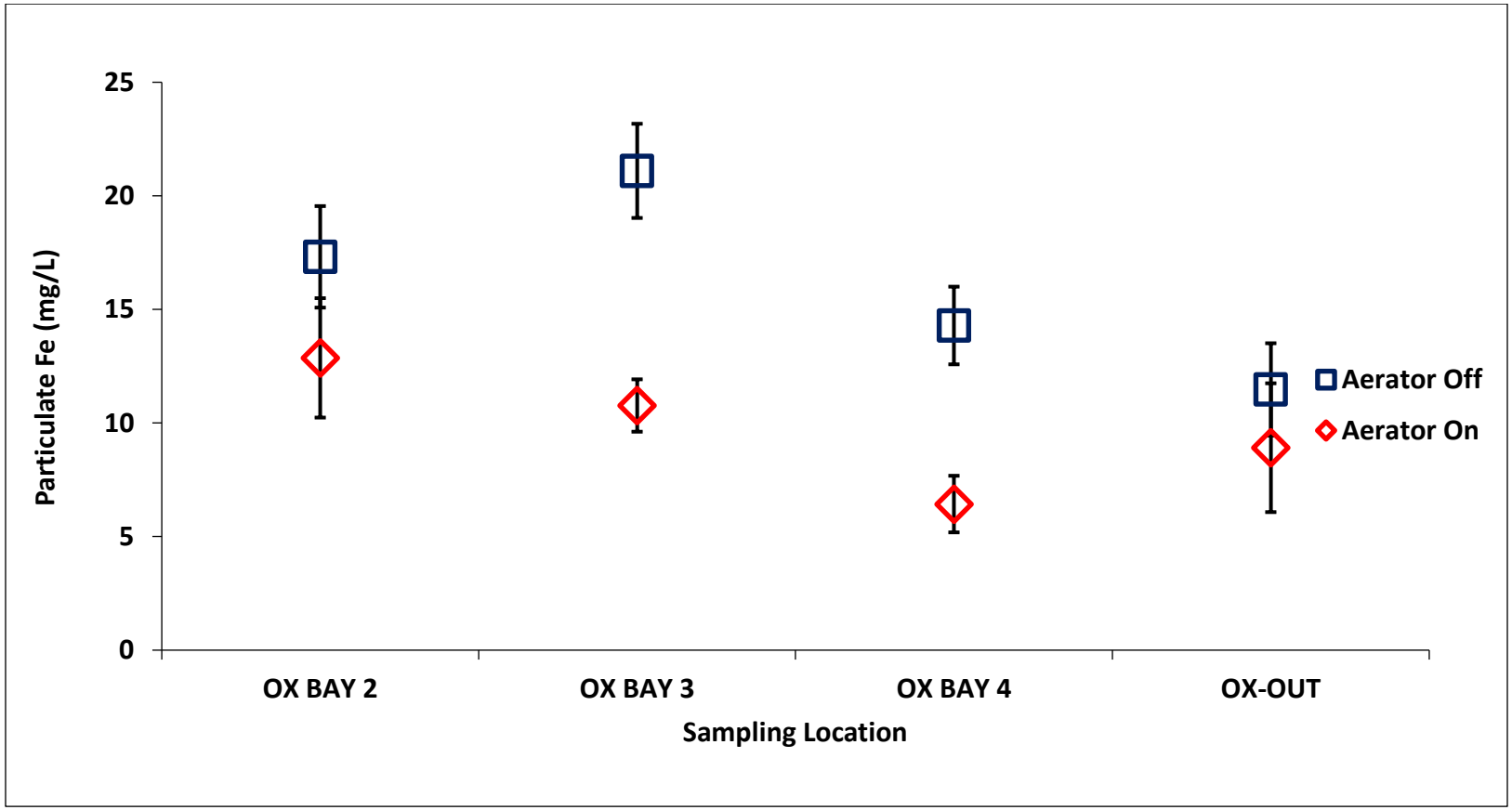

Figure 4.16 Median particulate Fe concentrations (mg/L) data with standard error bars for each sampling location within the oxidation pond for the ON and OFF studies.

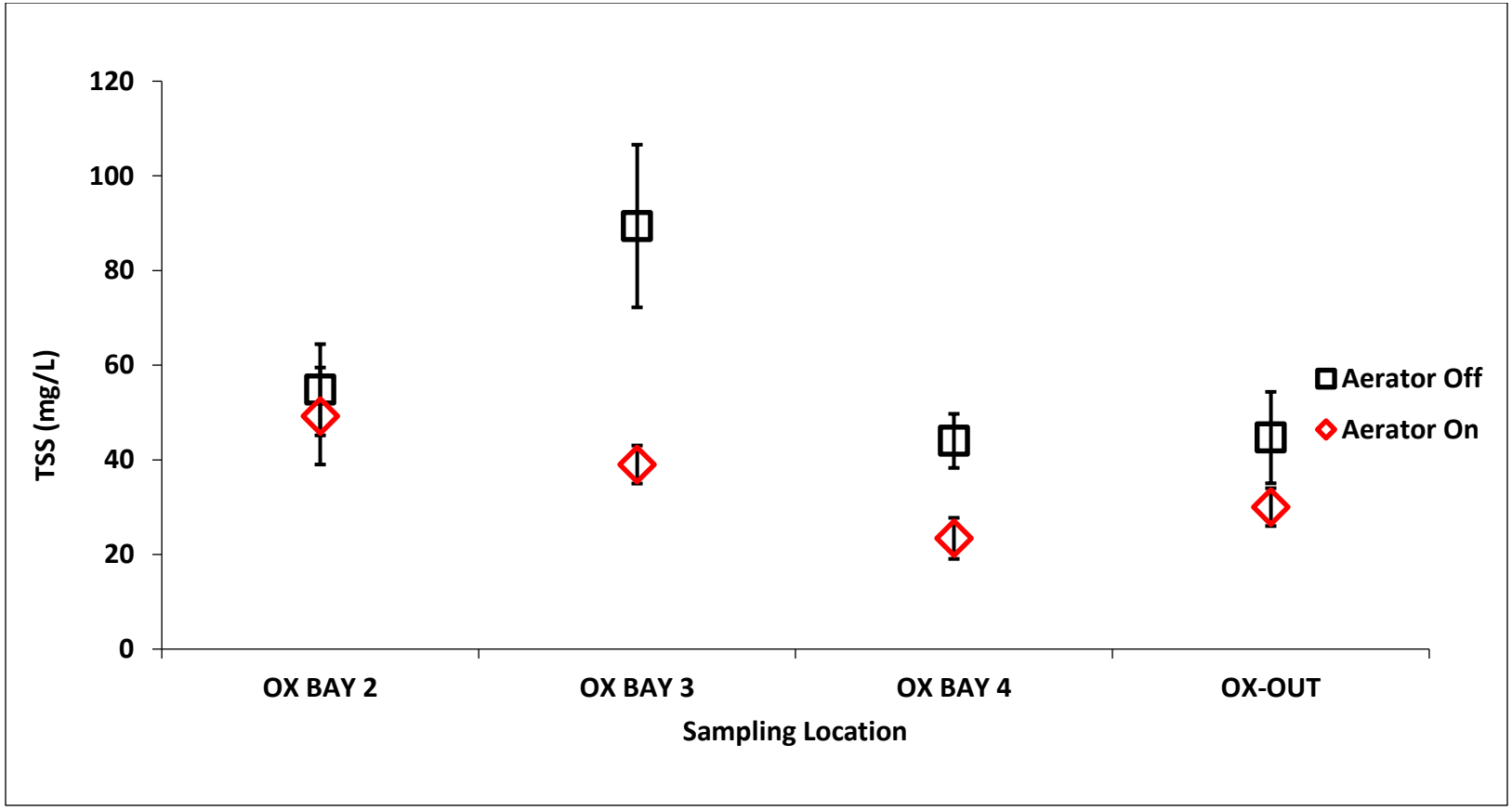

Figure 4.17 Median total suspended solids (TSS) concentrations (mg/L) data with standard error bars for each sampling location within the oxidation pond for the ON and OFF studies.

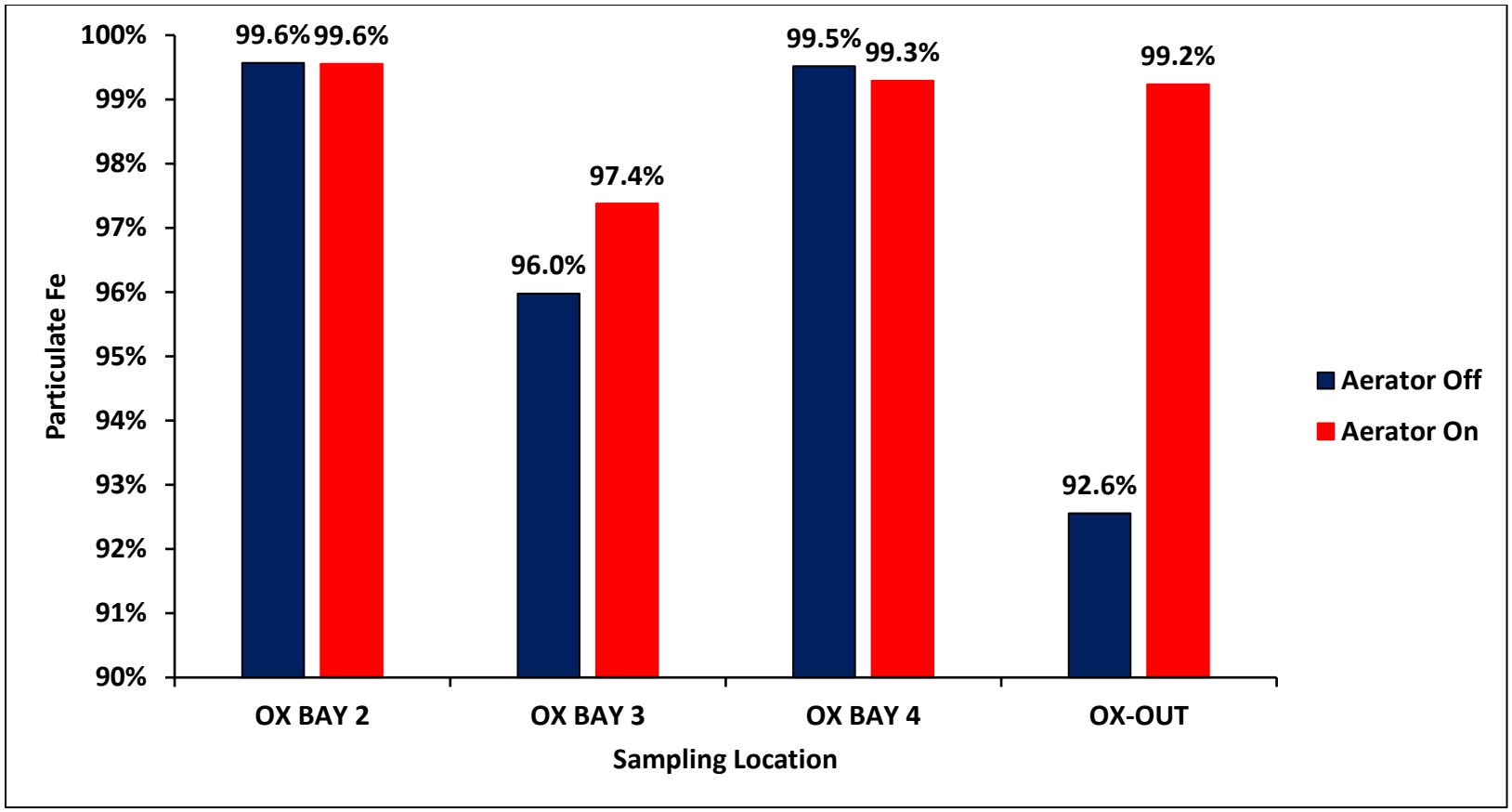

Figure 4.18 Median percentage of total Fe present as particulate Fe at each location within the oxidation pond for the ON and OFF studies.

It was hypothesized that the aerators on would increase the amount of Fe precipitated and retained within the oxidation pond. Total Fe and particulate Fe concentrations are lower at each location with the aerators on compared to with the aerators off. Similarly, as the water moves through the oxidation pond, the Fe concentrations decrease indicating that the aerators are working as hypothesized and are promoting more Fe retention and thus less total Fe is exiting the oxidation pond. Influent total Fe concentration from the three influents (Fe_{in}), total Fe concentration exiting the oxidation pond at OX-OUT (Fe_{out}), SECPTS flows measured at the VFBR outlets (Q), and the oxidation pond surface area based on its water elevation (SA) were used to determine Fe retention rates (IRR) for when the aerator was on and when the aerator was off since October 2018 (Equation 4.3).

$$IRR = \frac{(Fe_{in} - Fe_{out})Q}{SA} = \frac{g}{m^2 d} \quad (4.3)$$

Fe retention rates prior to October 2018 were not calculated since no water quality data for the UPW-IN location were collected. When VFBR flows were not taken, a daily average flow was calculated from elevation data collected from a pressure transducer deployed in the final polishing unit outlet and the v-notch weir equation. The calculated Fe retention rates are shown in Table 4.7.

Oxidation ponds are typically sized for a designed Fe removal rate of 20 g m^{-2} d^{-1} as suggested by Hedin et al. (1994). Table 4.7 shows that while the oxidation pond met the designed removal rate without active aeration, the addition of the FMAs increased the amount

of Fe retained in the oxidation pond. This is critical for the operation of the SECPTS since a decreased loading of Fe to the wetland ensures that more Fe particulates are retained, preventing them to coat the substrate in the vertical flow bioreactor, reducing its hydraulic conductivity and overall performance. An average Fe removal rate of 20 g m^{-2} d^{-1} is used to design the minimum oxidation pond size required to remove the target Fe loading. Therefore, an increased Fe removal rate suggests that less surface area is required to remove the same amount of Fe. However, an increase in Fe removal rate correlates with an increased rate of iron sludge accumulation potentially limiting the lifetime of the oxidation pond. Therefore, the capital cost of constructing a larger pond surface area should be compared to the expected cost and frequency of Fe sludge removal to determine the size of the oxidation pond.

Table 4.7 Calculated Fe retention rates statistics for given water quality and quantity conditions for the ON and OFF studies since October 2018.

Aerator Status	n	Mean	Std Dev	Min	Max
ON	16	26	3.7	21	33
OFF	5	22	2.8	19	26

4.4 Conclusions

It was hypothesized that the FMAs would increase the DO concentrations and pH and decrease pCO_2 partial pressures throughout the pond compared to wholly passive aeration. This hypothesis is partially accepted because DO saturation did increase at each location and progressively as the water travelled from the inlets to the outlet of the oxidation pond with the FMAs on. Similarly, the pCO_2 at each location was lower than average calculated influent

pressures indicating that CO_2 is readily degassed before the water reaches the sampling locations. The flow weighted average influent pCO_2 is 0.496 atm while the pCO_2 calculated at each sampling location within the pond ranged from 0.036 to 0.166 atm. The readily degassing of CO_2 as soon as the mine drainage became exposed to the atmosphere resulted in little to no change in pCO_2 or pH at each location in the pond between the ON and OFF studies. The limited change in pCO_2 and pH may be due to the high buffer capacity of the net alkaline mine drainage and due to the sampling locations' distances from the aerators. Loyless and Malone (1998) found that degassing of CO_2 was a function of flow rate and the number of air-lifts and that the airlift aerators degassed more CO_2 when located in areas with maximum CO_2 concentrations (Loyless and Malone 1998). Therefore, the effect of adding more FMAs nearer to the inlet structures should be explored to see if increasing the number of aerators can degas more carbon dioxide and have a larger effect on pH.

It was further hypothesized that the increase in DO concentrations and pH would result in more Fe retention within the oxidation pond compared to the oxidation pond being passively aerated. This hypothesis is partially accepted because, although total and particulate Fe concentrations were not always significantly different between the ON and OFF studies, the ON study did result in lower total and particulate Fe concentrations at each location. Similarly, each location had an equal or higher percentage of total Fe in the particulate form when the aerators were on compared to when the aerators were off. This is because the removal of Fe is limited by DO concentrations and thus, when the aerators increase DO, more Fe is oxidized and precipitated resulting in higher percentage of Fe in particulate form and lower overall Fe

concentrations downstream. Similarly, the decrease in particulate Fe concentrations further downstream shows that actively aerating and oxidizing Fe upstream allows the Fe particulates more time to settle and thus they are less likely to travel downstream.

Both the OFF and ON studies showed that the total influent Fe concentration decreased by more than 80% by the time it reached the OX BAY 2 location. This indicates that Fe oxidation occurs rapidly towards the start of the treatment train. Therefore, the placement of FMAs further upstream may promote even more oxidation earlier allowing more time for Fe particulates to settle before exiting the oxidation pond.

Overall, the FMAs improved the performance of the oxidation pond at the SECPTS. The increase in DO allowed for an average 17% increase in the Fe retention rate from 22 g m^{-2} d^{-1} to 26 g m^{-2} d^{-1}. FMAs appear to be a viable aeration technology for PTS treating mine drainage with elevated Fe concentrations in relatively flat landscapes. The FMAs increased DO concentrations and Fe retention rates as designed.

Chapter 5: Conclusions and Future Work

Aeration plays a vital role in treatment of mine drainage where often the removal of Fe is limited by DO concentrations (Hedin et al. 1994). Although oxygen is readily available in the atmosphere, greater Fe oxidation rates can be achieved by actively introducing oxygen into the water column (Geroni et al. 2012; Hedin 2008; Kirby et al. 2007; Leavitt 2011; Nairn et al. 2009; Nairn et al. 2018; Oh et al. 2015; Schmidt 2004). However, aeration can be challenging for passive treatment systems (PTS) located in relatively flat landscapes where cascading water to entrain oxygen is not feasible.

This study looked at the effectiveness of float-mix aerators (FMAs), also known as airlift aerators, to promote Fe oxidation to determine if this technology can be applied to PTS in sites with limited topographic relief. This aeration technology is commonly used in wastewater treatment and aquaculture settings but limited research has been performed to determine their applicability in treating mine drainage. This study analyzed the effectiveness of FMAs to increase DO concentrations, degas CO_2 and promote Fe retention in the oxidation pond of the Southeast Commerce PTS located in the Tar Creek Superfund Site in northeastern Oklahoma, USA. This research effort consisted of three major studies: 1) analysis of the effectiveness of the FMAs with respect to depth 2) analysis of the effectiveness of the FMAs with respect to distance from the aerator and 3) analysis of the overall effectiveness of FMAs to promote iron retention within an oxidation pond.

5.1 Effectiveness of FMAs with Respect to Depth

Comparison of water quality data at different depths with the FMAs off and on showed that the FMAs increased DO, degassed CO_2 and raised pH at depths shallower than 0.4m. pH was shown to be positively correlated with DO saturation and negatively correlated with pCO_2 demonstrating that aeration degassed CO_2 and raised the pH by shifting the carbonate equilibria. The increase in DO and rise in pH lowered dissolved Fe concentrations and increased percentage of the total Fe in particulate form when the FMAs were on compared to when the FMAs were off. Similarly, when the FMAs were on there were lower total Fe concentrations at shallower depths and higher total and particulate Fe concentrations with increasing depth. The increase in DO promotes faster Fe oxidation rates which in turn allows the Fe particulates formed more time to settle, improving overall Fe retention in the pond.

It was likely that the lack of influence on DO and pCO_2 at depths greater than 0.4 m was a result of the air being delivered to the FMA at a depth of 0.4 m. It would be advantageous for a future study to analyze the effect of injecting air to the FMAs at varying depths to address this hypothesis. A deeper air injection depth may promote more mixing and help aerate the water column at a deeper depth.

5.2 Effectiveness of FMAs with Respect to Spatial Distance

The FMAs had a 3-m radius of influence to degas CO_2 and raise pH but increased DO saturation at all sampling locations, with the maximum distance of 15 m from the FMA, compared to when the FMAs were off. The EFMA data showed that not only did the water have

a higher pH when the FMAs were on, but pH also increased as the water moved downstream. A decrease in DO saturation compared to the upstream DO saturation was seen because the DO downstream was utilized for the oxidation of Fe and due to the FMAs diminishing radius of influence. Overall, the FMAs promoted Fe retention by providing enough DO to oxidize and precipitate Fe as the water moved from upstream to downstream of the FMAs. With the FMAs on, total Fe concentrations decreased with increasing distance from the FMA and the percentage of total Fe present as particulates increased. It is hypothesized that significant difference in CO_2 pressures may be seen if the number of FMAs were to be increased. Although DO is related to the total air flow rate, CO_2 degassing is a function of total airflow rate and the number of aerators (Loyless and Malone 1998). Future work needs to be performed to determine if there is an optimal number of FMAs to supply enough air to increase DO concentrations and degas CO_2 in order to more efficiently raise pH to facilitate faster Fe oxidation kinetics.

5.3 FMAs Role on Oxidation Pond Performance

Analysis of historical water quality data collected at the inlets of the SECPTS and the outlet of the oxidation pond showed that the oxidation pond increased DO by over 100%, degassed approximately half of the CO_2 from the mine drainage discharges, raised pH and removed approximately 93% of the Fe loading before the water enters the next process unit. However, until this study, no research had explicitly analyzed the effect of FMAs on the performance of an oxidation pond.

This study showed that the FMAs increased DO saturation at each sampling location in the pond compared to when the aerators were off and that the DO saturation progressively increased as the water moved from the inlets to the outlet of the oxidation pond. Similarly, pCO_2 at each location were lower than the average inlet pCO_2. However, there was no statistical difference between pCO_2 and pH at most of the locations throughout the pond compared to when the FMAs were off. Despite the limited change in pCO_2 and pH between the ON and OFF studies, there was a difference in the amount of Fe retained in the system.

Aeration provided by the FMAs decreased total and dissolved Fe concentrations at each location in the oxidation pond and increased the percentage of particulate Fe. The increased particulate Fe was because the removal of Fe is limited by DO concentrations and thus, when the FMAs increase DO, more Fe is oxidized and precipitated resulting in a higher percentage of Fe in particulate form and lower overall Fe concentrations downstream. Actively aerating the system with the FMAs allowed for an average 17% increase in the Fe retention rate from 22 g m^{-2} d^{-1} to 26 g m^{-2} d^{-1}.

Both the aerator off and on studies showed that more than 80% of the Fe was removed by the time the water reached the OX BAY 2 location (Figure 5.1). This indicates that Fe oxidation and precipitation occurred quickly in the early parts of the oxidation pond. Therefore, moving the FMAs closer to the inlets and earlier in the oxidation pond may result in an overall improvement of water quality and a greater Fe removal rate.

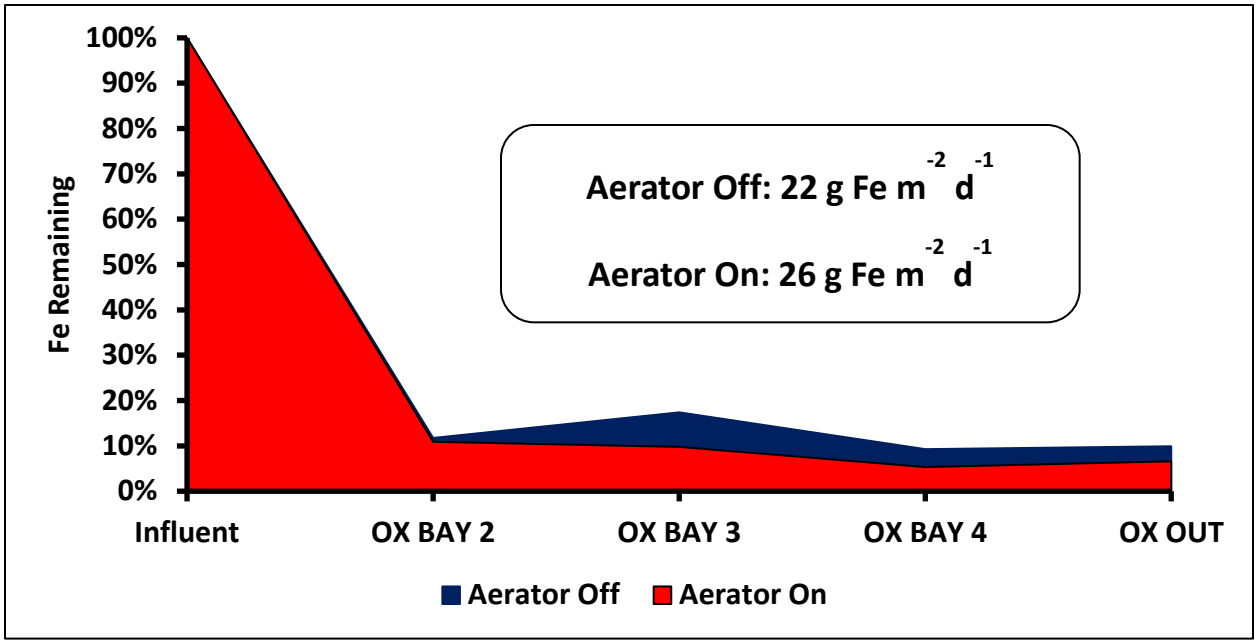

Figure 5.1 Percent of total influent iron remaining at each location within the oxidation pond compared to when the aerators are off and on.

5.4 Final Comments

This research showed that FMAs are a viable aeration technology for PTS located in relatively flat landscapes where cascade aeration and other hydraulic head driven aeration technologies are not feasible. The FMAs increased DO concentrations and facilitated Fe oxidation and increased Fe removal. Despite their ability to improve the overall Fe removal performance of the oxidation pond, the FMAs are limited to treating relatively shallow waters and within a relatively close radius. More research is needed moving forward to determine if the FMAs can be optimized to increase the depth and radius at which they have an influence. Similarly, more research needs to be performed to determine if strategic placing of the FMAs earlier in the oxidation pond, and additional FMAs, improves the Fe removal performance of the system.

References

Burris VL, McGinnis DF, Little JC (2002) Predicting oxygen transfer rate and water flow rate in airlift aerators. Water Res 36 (18): 4605-4615. doi: 10.1016/S0043-1354(02)00176-8

Chakraborti RK, Kaur J (2014) Noninvasive measurement of particle-settling velocity and comparison with stokes' law. J Environ Eng. 140(2). doi: 10.1061/(ASCE)EE .1943-7870.0000790

Danehy TP, Palmer KJ, Mahony RM, Neely CA, Guy DA, Denholm CF, Dunn MH, Leavitt BR (2016) Trompe design construction and performance. Proceedings from the 33rd Annual Meeting of the American Society of Mining and Reclamation, Spokane, WA. https://www.asmr.us/Portals/0/Documents/Meetings/2016/27-01-Danehy.pdf

Dempsey BA, Jeon B-H (2001) Characteristics of sludge produced from passive treatment of mine drainage. Geochemistry: Exploration, Environment, Analysis 1(1):89–94. doi: 10.1144/geochem.1.1.89

Dempsey BA, Roscoe HC, Ames R, Hedin RS, Jeon B-H (2001) Ferrous oxidation chemistry in passive abiotic systems for the treatment of mine drainage. Geochemistry: Exploration, Environment, Analysis 1(1):81–88. doi: 10.1144/geochem.1.1.81

Dietz JM, Dempsey BA (2017) Heterogeneous oxidation of Fe (II) in AMD. Appl Geochem 81 (June): 90-97. doi: 10.1016/j.apgeochem.2017.04.003

Eschar M, Mozes N, Fediuk M (2003) Carbon dioxide removal rate by aeration devices in marine fish tanks. Israeli J. Aquaculture-Bamidgeh 55(2): 79-85

Geroni JN, Cravotta CA, Sapsford DJ (2012) Evolution of the chemistry of Fe bearing waters during CO_2 degassing. Appl Geochem 21 (12): 2335-2347. doi: 10.1016/j.apgeochem.2012.07.017

Hedin RS (2008) Iron removal by a passive system treating alkaline coal mine drainage. Mine Water Environ 27 (4): 200-209. doi: 10.1007/s10230-008-0041-9

Hedin RS, Nairn RW, Kleinmann RLP (1994) Passive treatment of coal mine drainage. U.S. Bureau of Mines Information Circular 9389. 37 pp.

Hogsden KL, Harding JS (2012) Consequences of acid mine drainage for the structure and function of benthic stream communities: a review. Freshwater Science 31(1):108–120. doi: 10.1899/11-091.1

Jennings SR, Neuman DR, Blicker PS (2008) Acid mine drainage and effects on fish health and ecology: a review. Reclamation Research Group Publication, Bozeman, MT

Jensen JN (2003) A Problem-Solving Approach to Aquatic Chemistry. John Wiley & Sons, Hoboken, NJ

Johnson DB, Hallberg KB (2005) Acid mine drainage remediation options: A review. Sci. Total Environ. 338 (1-2):3–14. doi: 10.1016/j.scitotenv.2004.09.00

Kirby CS, Cravotta CA (2005) Net alkalinity and net acidity 1: theoretical considerations. Appl Geochem 20 (10):1920–1940. doi: 10.1016/j.apgeochem.2005.07.002

Kirby CS, Dennis A, Kahler AK (2007) Aeration to degas CO_2, increase pH and iron oxidation rates, and decrease treatment pond size in treatment of net alkaline mine drainage. J Am Soc of Min and Rec (1): 373-381. doi: 10.21000/JASMR07010373

Kirby CS, Thomas HM, Southam G, Donald R (1999) Relative contributions of abiotic and biological factors in Fe (II) oxidation in mine drainage. Appl Geochem 14 (4): 511-530. doi: 10.1016/S0883-2927(98)00071-7

Leavitt BR (2011) Aeration of mine drainage using a TROMPE. Proceedings from the 2011 West Virginia Surface Mine Drainage Task Force Symposium, Morgantown, WV

Limerick PN, Ryan JN, Brown TR, Comp TA (2005) Cleaning up abandoned hardrock mines in the west: prospecting for a better future. Center of the American West, University of Colorado at Boulder

Loyless JC, Malone RF (1998) Evaluation of air-lift pump capabilities for water delivery, aeration, and degasification for application to recirculating aquaculture systems. Aquacult Eng 18: 117-133. doi: 10.1016/S0144-8609(98)00025-9

Moran D (2010) Carbon dioxide degassing in fresh and saline water I: Degassing performance of a cascade column. Aquacult Eng 43:29-36. doi: 10.1016/j.aquaeng.2010.05.001

Moran D (2010) Carbon dioxide degassing in fresh and saline water II: Degassing performance of an air-lift. Aquacult Eng 43:120-127. doi: 10.1016/j.aquaeng.2010.09.001

Nairn RW (2013) Carbon dioxide impacts both passive treatment system effectiveness and carbon footprint. Reliable Mine Water Technology: Proceedings International Mine Water Association, Golden, CO, USA, 6 pp.

Nairn RW, Beisel T, Thomas RC, LaBar JA, Strevett KA, Fuller D, Strosnider WH, Andrews WJ, Bays J, Knox RC (2009) Challenges in design and construction of a large multi-cell passive treatment system for ferruginous lead-zinc mine waters. Proceedings from the 2009 National Meeting of the American Society of Mining and Reclamation, Billings, MT. doi: 10.21000/JASMR09010871

Nairn RW, O'Sullivan AD, Coffey J (2002) Iron oxidation in net alkaline CO_2-rich mine waters. J Am Soc of Min and Rec 2002 (1): 1133-1137. doi: 10.21000/JASMR02011133

Nairn RW, Shepherd NL, Danehy T, Neely C (2018) Aeration via renewable energies improves passive treatment system performance. In: Wolkersdorfer C, Sartz L., Weber A, Burgess J Tremblay G (eds)Mine Water – Risk to Opportunity (Vol I). Pretoria, South Africa (Tshwane University of Technology), p. 151 – 157.

Oh C, Ji S, Yu C, Cheong Y, Yim G, Song H, Hong J, Ji S (2015) Efficiency assessment of cascade aerator in a passive treatment system for Fe (II) oxidation in ferruginous mine drainage of net alkaline. Environ Earth Sci 73(9): 5363-5373. doi:10.1007/s12665-014-3791-7

Oxenford LD (2016) Iron transport and removal dynamics in the oxidative units of a passive treatment system. PhD Diss, University of Oklahoma

Parker NC, Suttle MA (1987) Design of airlift pumps for water circulation and aeration in aquaculture. Aquacult Eng.6 (2): 97-110. doi: /10.1016/0144-8609(87)90008-2

Perkins MG, Effler SW, Peng F, Pierson D, Smith DG, Agrawal YC (2007) Particle characterization and settling velocities for a water supply reservoir during a turbidity event. J Environ Eng 133 (8): 800-808. doi: 10.1061/(ASCE)0733-9372(2007)133:8(800)

Schmidt TW (2004) Evaluation of aeration techniques for mine water treatment in passive systems. J Am Soc of Min and Rec 2004 (1): 1619-1626. doi: 10.21000/JASMR04011619

Shammas NK (2007) Fine pore aeration of water and wastewater. In: Wang LK, Hung YT, Shammas NK (eds) Physicochemical Treatment Technologies. Hummana Press, Totowa, NJ, p 391-448.

Singer PC, Stumm W (1970) The rate-determining step in the production of acidic mine wastes. Science 167 (3921): 1121-1123.

Skousen J, Zipper CE, Rose A, Ziemkiewicz PF, Nairn RW, McDonald LM, Kleinmann RL (2017) Review of passive treatment systems for acid mine drainage treatment. Mine Water Environ 36: 133-153. doi: 10.1007/s10230-016-0417-1

Taylor J, Pape S, Murphy N (2005) A summary of passive and active treatment technologies for acid and metalliferous drainage (AMD). Proceedings from the Fifth Australian Workshop on Acid Drainage.

United States Environmental Protection Agency (1984) EPA superfund record of decision: Tar Creek (Ottawa County) operable unit 1. EPA/ROD/R06-84/004

United States Environmental Protection Agency (1994) Five-year review report for the Tar Creek superfund site, Ottawa County, OK
United States Environmental Protection Agency (2018) USEPA: Site Information for Tar Creek (Ottawa Co) https://cumulis.epa.gov/supercpad/cursites/csitinfo.cfm?id=0601269 Accessed 2019-08-21

Watzlaf GR, Schroeder KT, Kleinmann RLP, Kairies CL, Nairn RW, Street WB (2004) The passive treatment of coal mine drainage.: 1-72. DOE/NETL-2004/1202

Younger PL, Banwart SA, Hedin RS (2002) Mine Water: Hydrology, Pollution, Remediation. Vol 5. Springer, Alloway.

Yu SL, Hamrick JM, Lee D (1984) Wind effects on air-water oxygen transfer in a lake. In: Brutsaert W, Jirka GH (eds) Gas Transfer at Water Surfaces. Water Science and technology Library, Vol 2. Springer, Dordrecht, 357-367.

Zhang DD, Peart M, Zhang YJ, Zhu A, Cheng Z (2000) Natural water softening processes by waterfall effects in karst areas. Desalination 129 (3): 247-259. doi: 10.1016/S0011-9164(00)00065-5